THE STRUCTURE AND CONSTITUTION OF ARCHAEOLOGICAL FERROUS PROCESS SLAGS

Volume 2 of 2 : Tables, Figures and Appendices

Stephanie Fells

Ph.D.

University of Aston in Birmingham

April 1983

CONTENTS

Figure 2.1

Photograph of Wellingborough Middle Quarry, Finedon, showing the Northampton Sand Ironstone in situ. This quarry is located south of the Lincolnshire Limestone's margin, hence the Grantham Formation and Lincolnshire Limestone are absent, the ironstone being directly overlain by the Rutland Formation.

Figure 2.2

Idealised stratigraphic column for North-east Northamptonshire

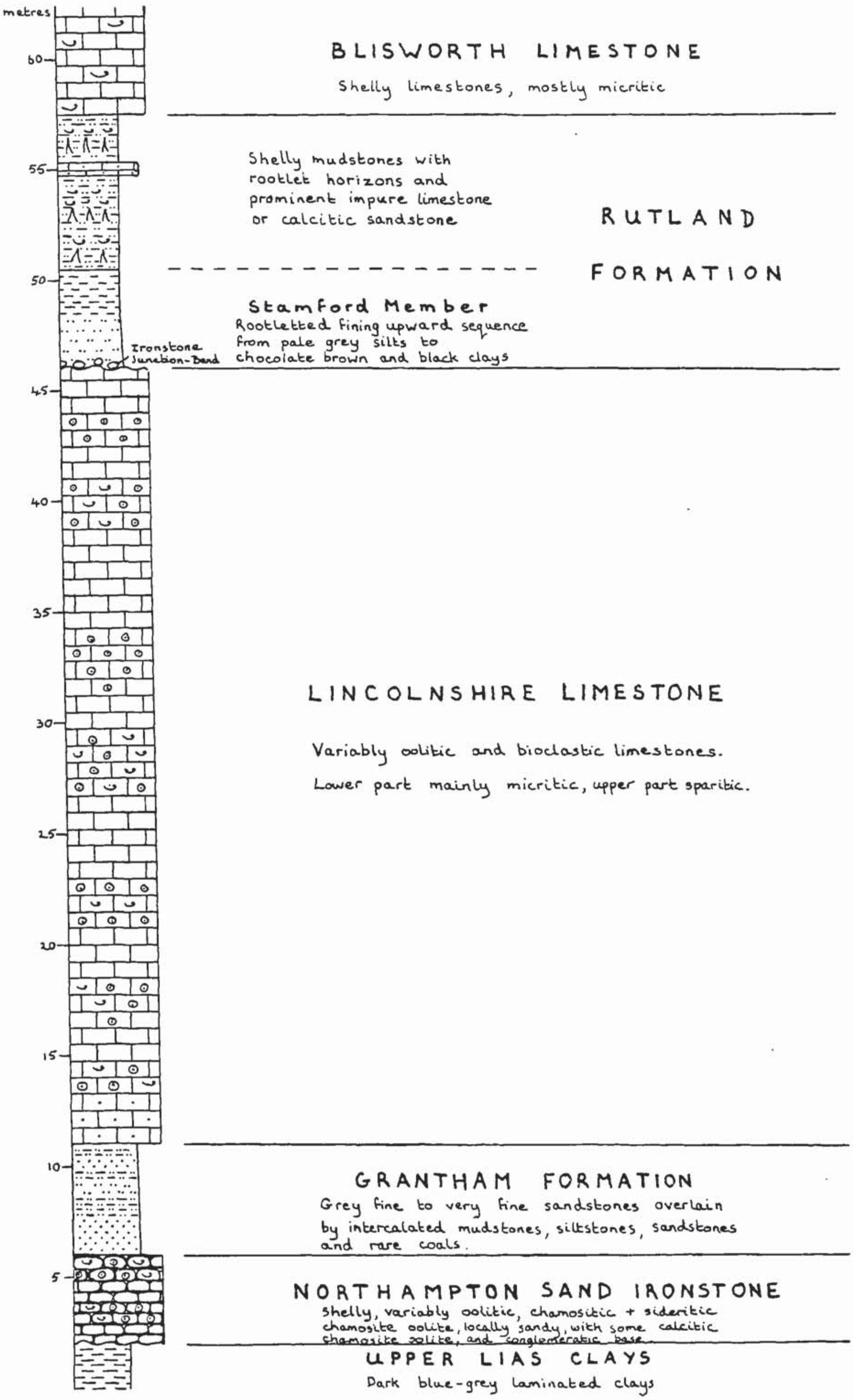

BLISWORTH LIMESTONE

Shelly limestones, mostly micritic

RUTLAND FORMATION

Shelly mudstones with rootlet horizons and prominent impure limestone or calcitic sandstone

Stamford Member

Rootletted fining upward sequence from pale grey silts to chocolate brown and black clays

LINCOLNSHIRE LIMESTONE

Variably oolitic and bioclastic limestones.

Lower part mainly micritic, upper part sparitic.

GRANTHAM FORMATION

Grey fine to very fine sandstones overlain by intercalated mudstones, siltstones, sandstones and rare coals.

NORTHAMPTON SAND IRONSTONE

Shelly, variably oolitic, chamositic + sideritic chamosite oolite, locally sandy, with some calcitic chamosite oolite, and conglomeratic base.

UPPER LIAS CLAYS

Dark blue-grey laminated clays

Figure 2.3

Map of the 'Northamptonshire area', comprising North-east Northamptonshire with parts of Leicestershire and Lincolnshire. The distribution of the outcrops of the Northampton Sand Ironstone are shown in orange and those of the Ironstone Junction-Band are shown in black. Localities from which ironstone samples were obtained are shown by a cross, whilst the archaeological sites from which slags were obtained are circled.

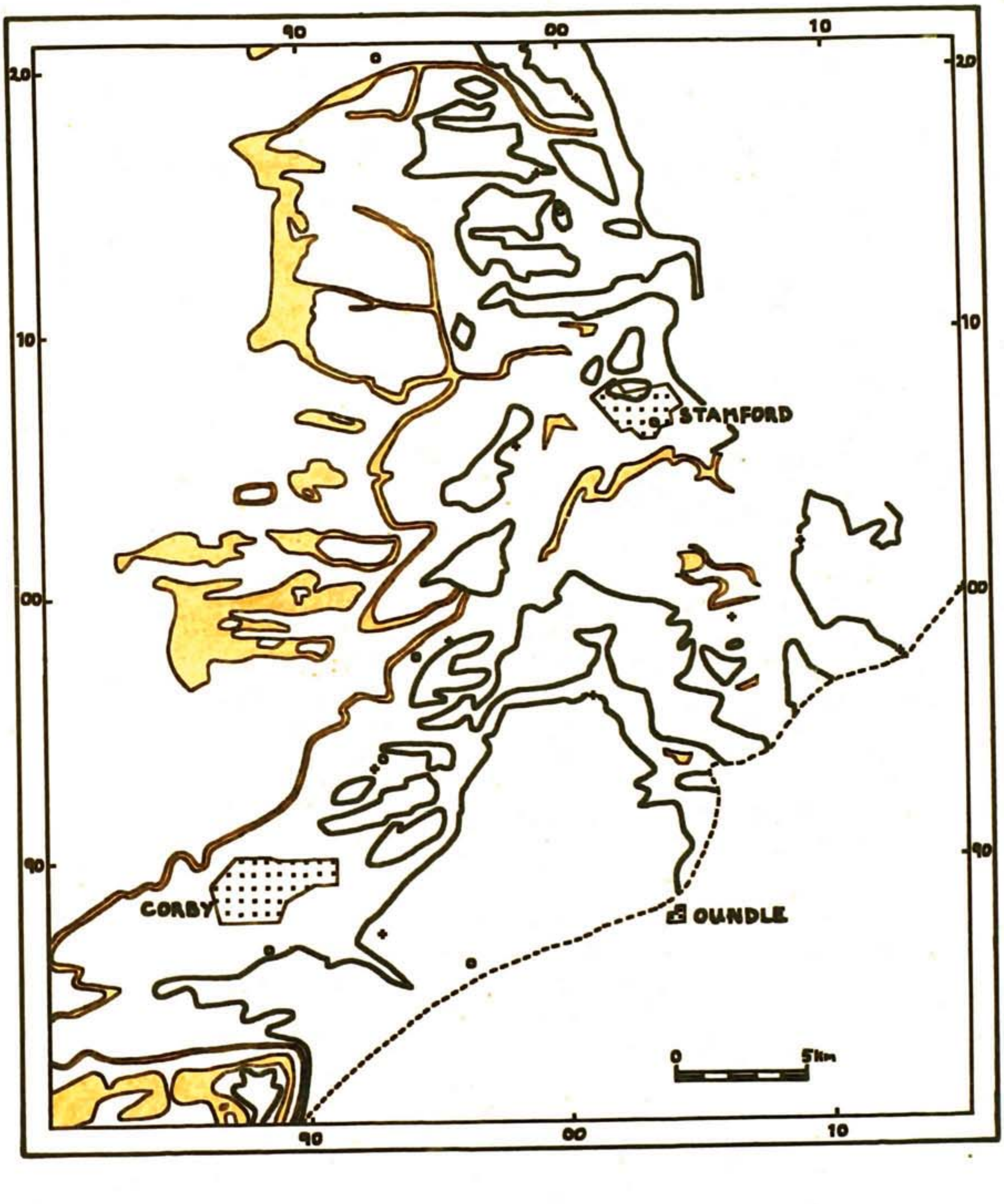
90
00
10
20
10
00
90
STAMFORD
CORBY
OUNDLE
0
5km

Figure 2.4

Photograph of an Ironstone Junction-Band nodule *in situ*.

Figure 2.5

Sample of Ironstone Junction-Band from the Wakerley site showing a spherulitic texture. Spheruliths are 1-2 mm across. Transmitted light, plane polarized.

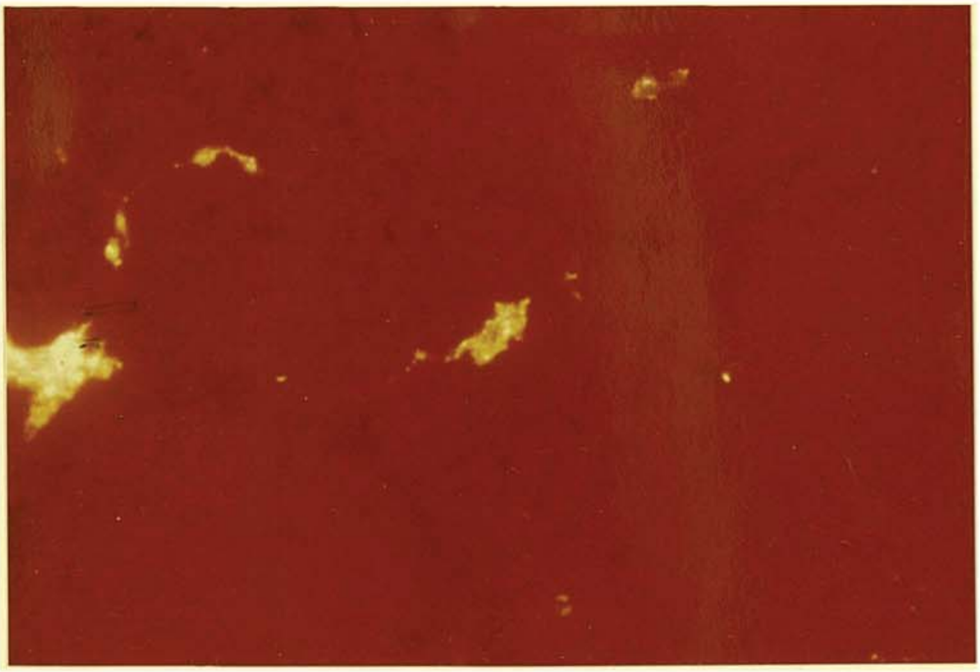

Figure 2.6

Map showing detailed geology of the area around Wakerley and Bulwick. The investigated sites are shown as circled crosses and other known or probable ironworking sites (see Jackson[32]) are shown by crosses.

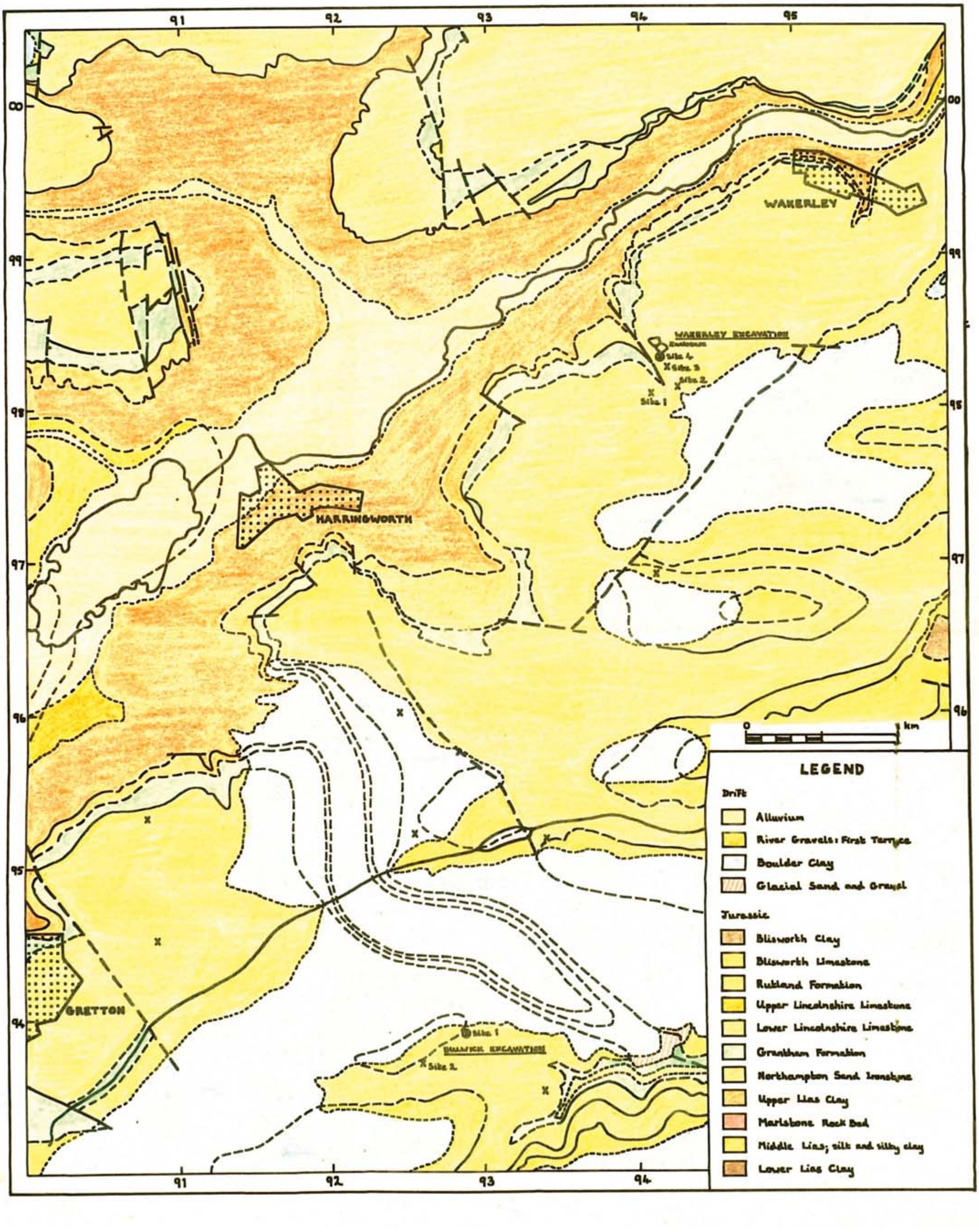
91
92
93
94
95
00
99
98
97
96
95
94
WAKERLEY
WAKERLEY EXCAVATION
Site 4
Site 3
Site 2
Site 1
HARRINGWORTH
GRETTON
BULWICK EXCAVATION
Site 1
Site 2.
0
1 km
LEGEND
Drift
Alluvium
River Gravels: First Terrace
Boulder Clay
Glacial Sand and Gravel
Jurassic
Blisworth Clay
Blisworth Limestone
Rutland Formation
Upper Lincolnshire Limestone
Lower Lincolnshire Limestone
Grantham Formation
Northampton Sand Ironstone
Upper Lias Clay
Marlstone Rock Bed
Middle Lias; silt and silty clay
Lower Lias Clay

Figure 2.7

Map of Wakerley site, adapted from Jackson and Ambrose.[31]

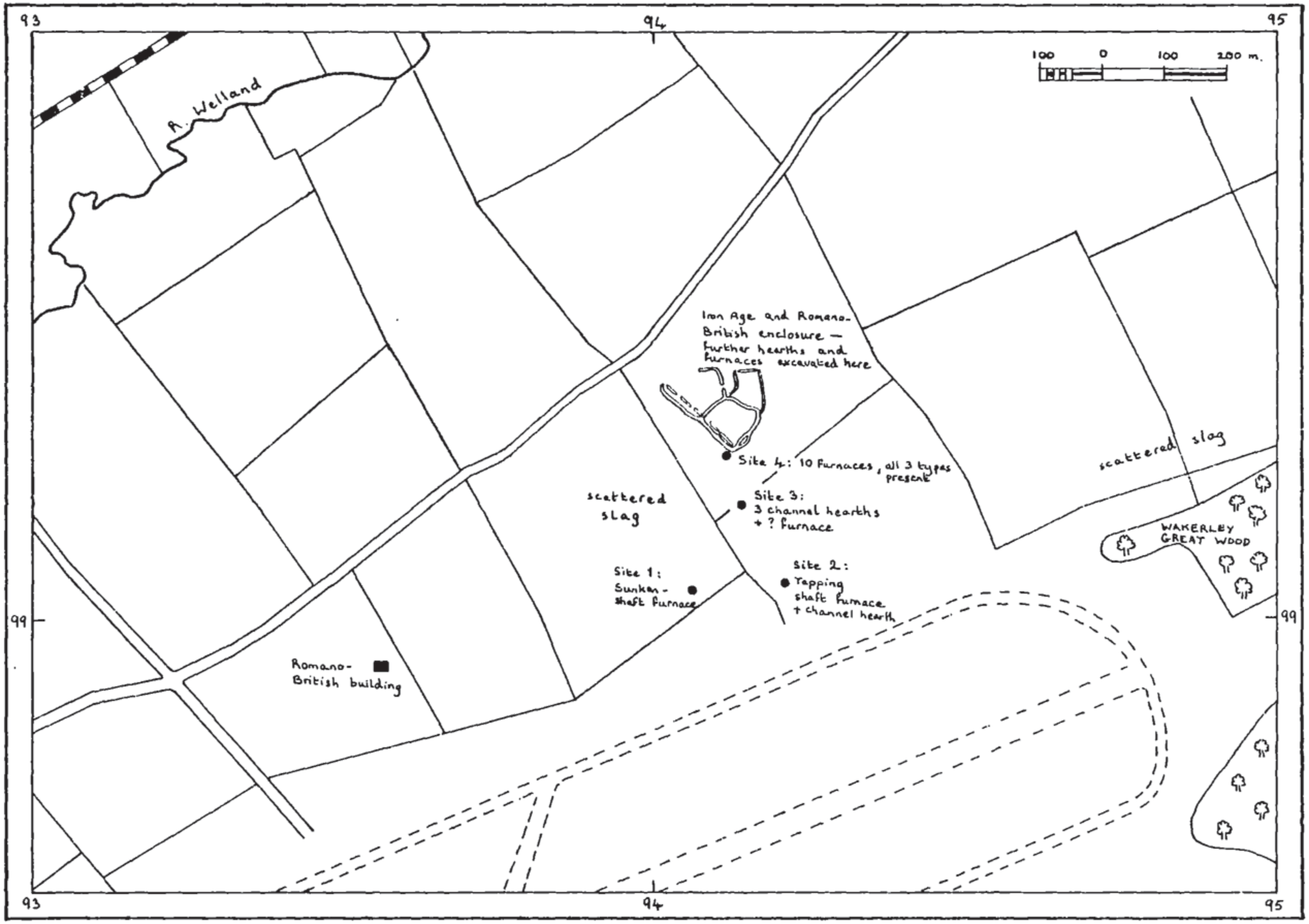
93
94
95
99
100
0
100
200 m.
R. Welland
Iron Age and Romano-British enclosure — further hearths and furnaces excavated here
Site 4: 10 furnaces, all 3 types present
Site 3: 3 channel hearths + ? furnace
Site 2: Tapping shaft furnace + channel hearth
Site 1: Sunken-shaft furnace
scattered slag
scattered slag
WAKERLEY GREAT WOOD
Romano-British building
93
94
95
99

Figure 2.8

Map of the Stamford district showing the outcrops of Northampton Sand Ironstone (coloured orange) and Ironstone Junction-Band (coloured red). Adapted from Mahany et al.[37]

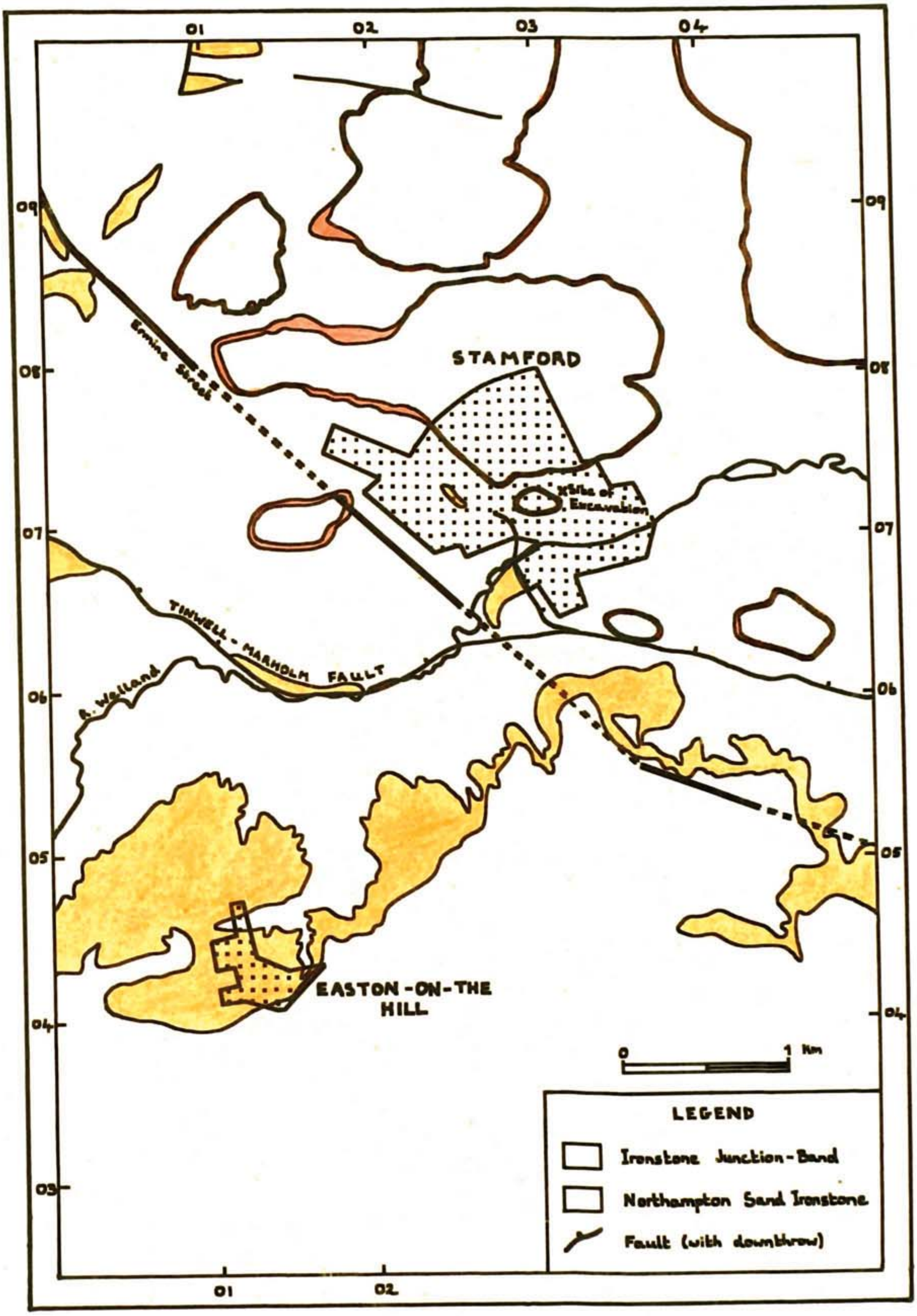
01
02
03
04
09
08
07
06
05
04
03
Ermine Street
STAMFORD
Site of Excavation
TINWELL - MARHOLM FAULT
R. Welland
EASTON - ON - THE HILL
0
1 Km
LEGEND
Ironstone Junction - Band
Northampton Sand Ironstone
Fault (with downthrow)

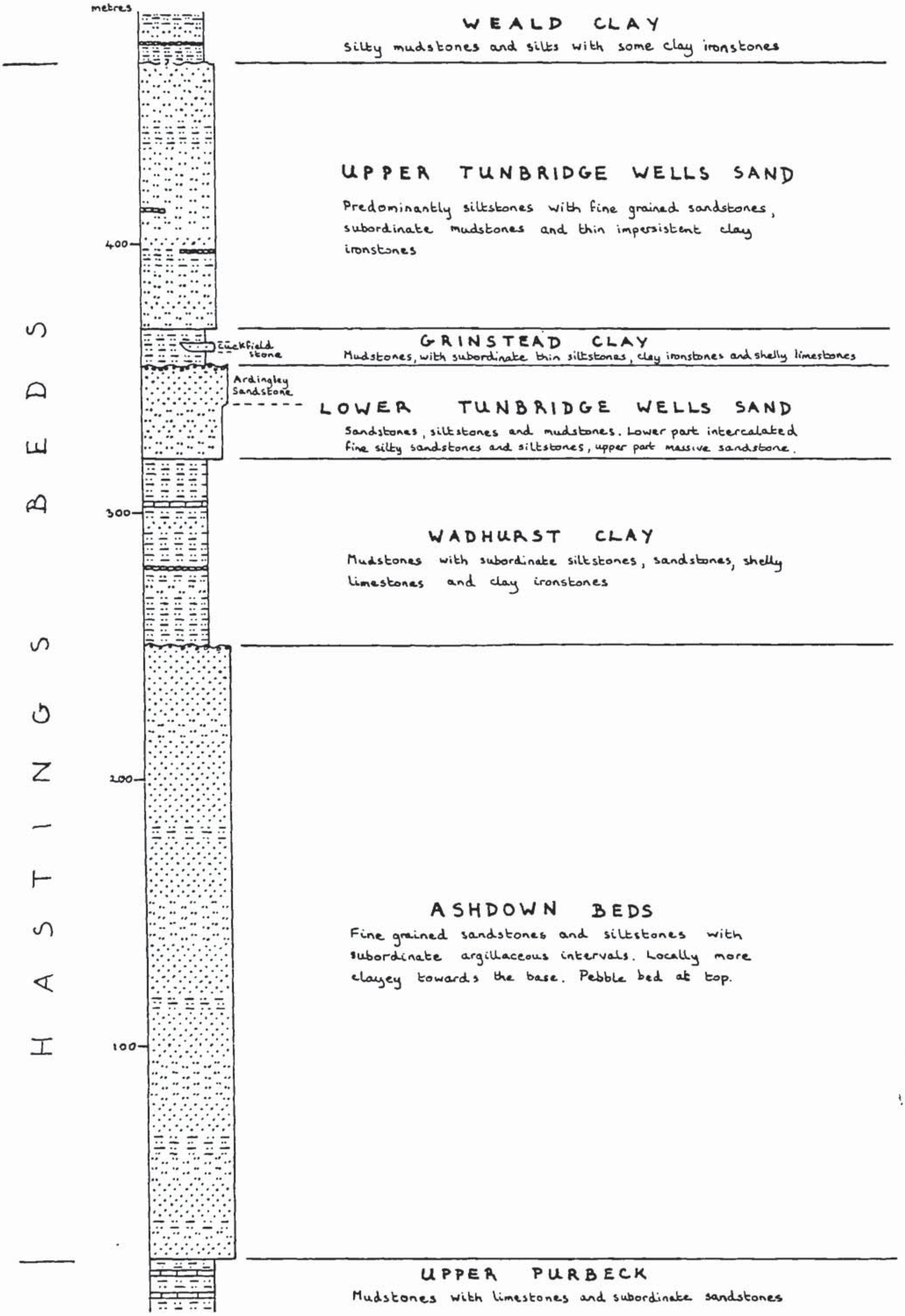

WEALD CLAY

Silty mudstones and silts with some clay ironstones

UPPER TUNBRIDGE WELLS SAND

Predominantly siltstones with fine grained sandstones, subordinate mudstones and thin impersistent clay ironstones

GRINSTEAD CLAY

Mudstones, with subordinate thin siltstones, clay ironstones and shelly limestones

LOWER TUNBRIDGE WELLS SAND

Sandstones, siltstones and mudstones. Lower part intercalated fine silty sandstones and siltstones, upper part massive sandstone.

WADHURST CLAY

Mudstones with subordinate siltstones, sandstones, shelly limestones and clay ironstones

ASHDOWN BEDS

Fine grained sandstones and siltstones with subordinate argillaceous intervals. Locally more clayey towards the base. Pebble bed at top.

UPPER PURBECK

Mudstones with limestones and subordinate sandstones

Figure 2.9

Idealised stratigraphic column for the western part of the High Weald.

Figure 2.10

(a) Photograph of Wadhurst Clay Ironstone *in situ*, Sharpthorne Brickworks, near West Hoathly. By courtesy of C.F. Tebbutt. Pole is 2 m long.

(b) Photograph of section through an old minepit exposed in the quarry face of Sharpthorne Brickworks, near West Hoathly. By courtesy of C.F. Tebbutt. Pole is 2 m long.

Figure 2.11

Map showing detailed geology of the area around the Garden Hill and Millbrook sites.

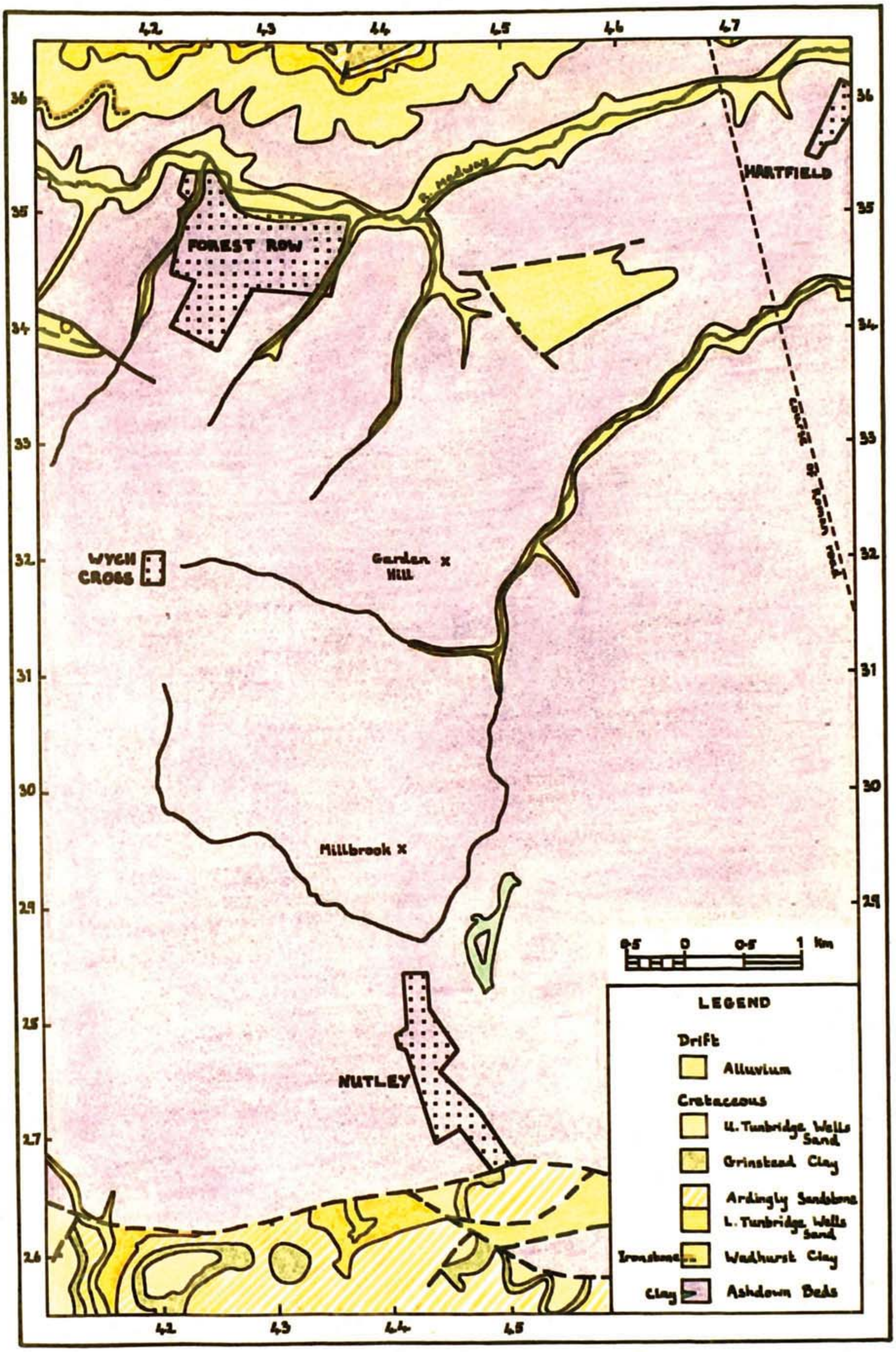
42
43
44
45
46
47
36
35
34
33
32
31
30
29
28
27
26
R. Medway
HARTFIELD
FOREST ROW
Course of Roman road
WYCH CROSS
Garden x Hill
Millbrook x
NUTLEY
0·5
0
0·5
1 km
LEGEND
Drift
Alluvium
Cretaceous
U. Tunbridge Wells Sand
Grinstead Clay
Ardingly Sandstone
L. Tunbridge Wells Sand
Ironstone
Wadhurst Clay
Clay
Ashdown Beds

Figure 2.12

Photograph of shaft furnace reconstruction built by R. Adams. By courtesy of M. Darby.

Figure 2.13

Map showing detailed geology of the Ramsbury district

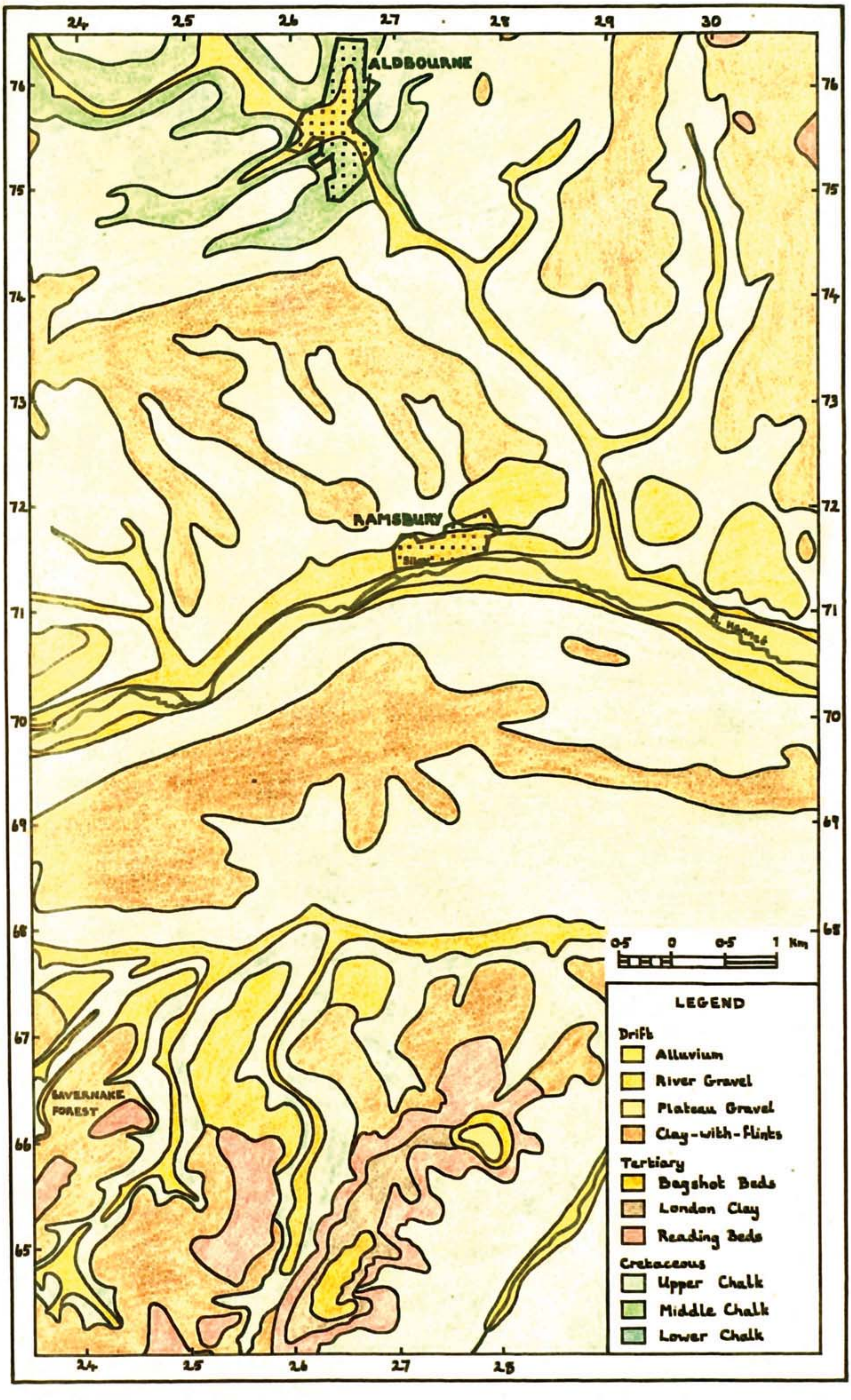
24
25
26
27
28
29
30
76
75
74
73
72
71
70
69
68
67
66
65
ALDBOURNE
RAMSBURY
R. Kennet
SAVERNAKE FOREST
0·5
0
0·5
1 Km
LEGEND
Drift
Alluvium
River Gravel
Plateau Gravel
Clay-with-flints
Tertiary
Bagshot Beds
London Clay
Reading Beds
Cretaceous
Upper Chalk
Middle Chalk
Lower Chalk

Figure 2.14

Map showing detailed geology of the Bulbourne Valley

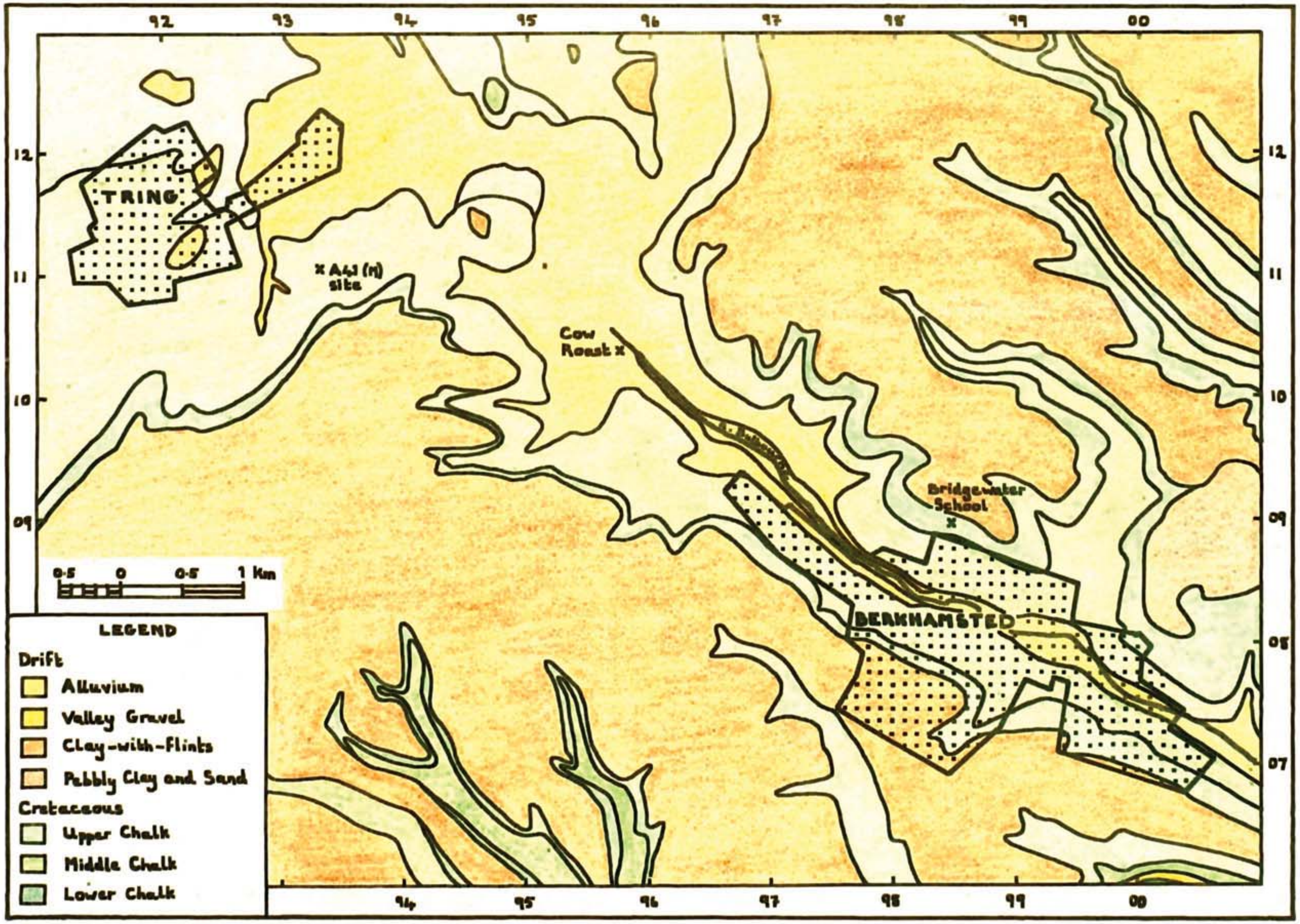
92
93
94
95
96
97
98
99
00
12
11
10
09
08
07
TRING
x A41 (M) site
Cow Roast x
Bridgewater School x
BERKHAMSTED
0·5 0 0·5 1 Km
LEGEND
Drift
Alluvium
Valley Gravel
Clay-with-Flints
Pebbly Clay and Sand
Cretaceous
Upper Chalk
Middle Chalk
Lower Chalk

Figure 3.1

Sketch of the Catalan furnace showing the different zones designated by Francois.

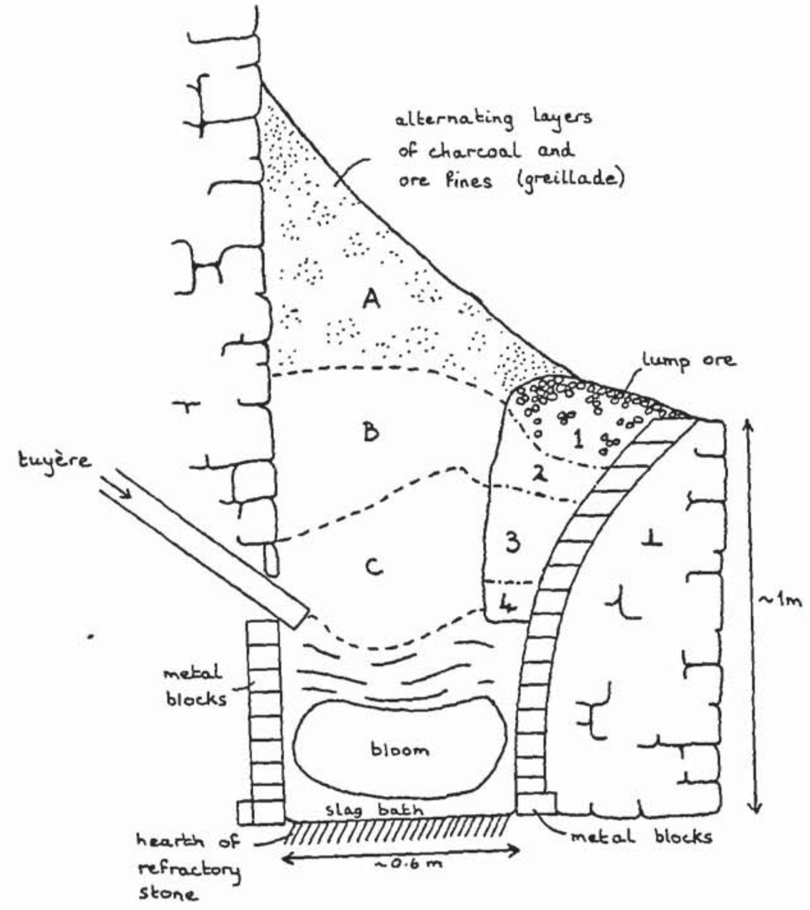
alternating layers of charcoal and ore fines (greillade)
A
B
C
lump ore
1
2
3
4
tuyère
metal blocks
bloom
slag bath
hearth of refractory stone
~0.6 m
metal blocks
~1m

Figure 3.2

Wakerley slag WK-AV in reflected light showing branching grains of metallic iron. Field of view is 0.36 mm wide.

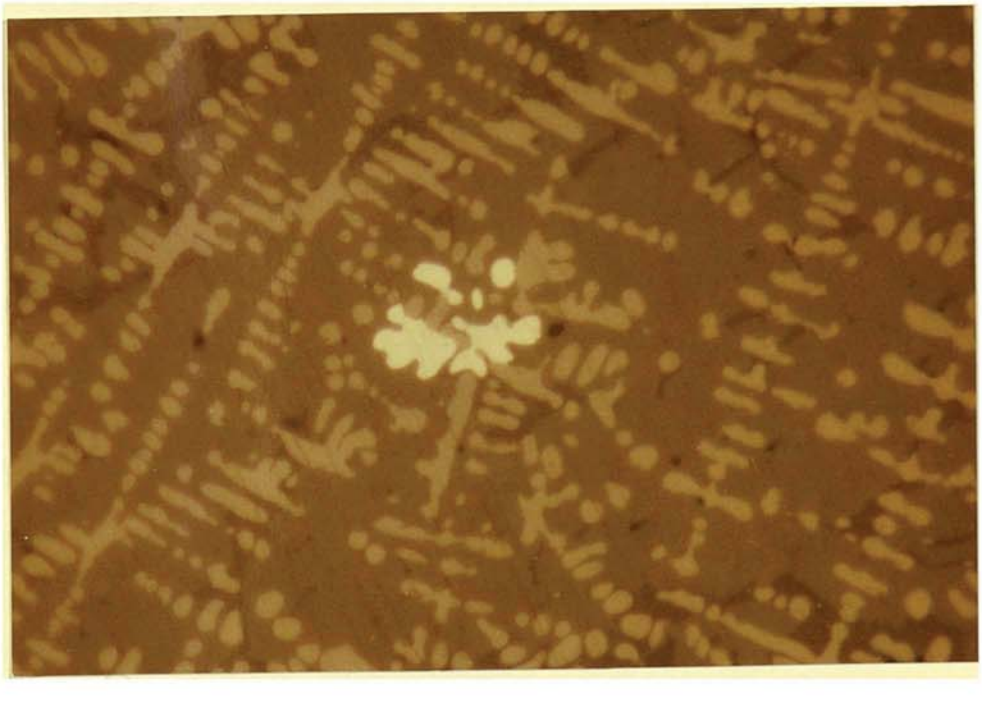

Figure 3.3

Bowl furnace reconstruction slag RR2 in reflected light showing metallic iron at the boundary between slag and charcoal, indicating the reduction of slag by solid carbon. Field of view is 0.725 mm wide.

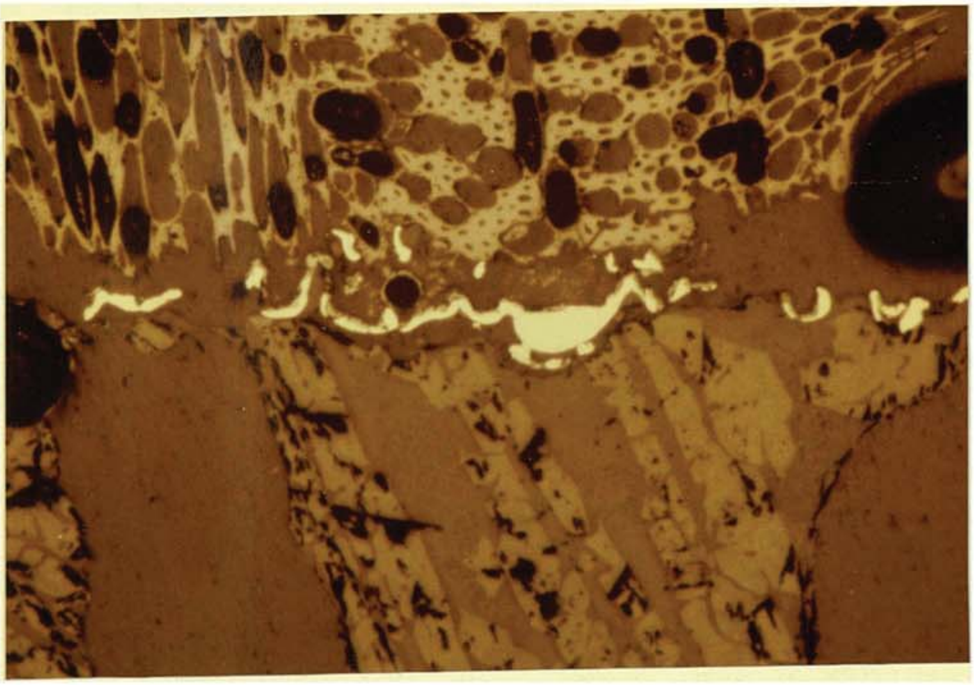

Table 4.1

Brief descriptions of slag petrography

Samples	Fayalite	Wustite	Hercynite	Leucite	Others	Glass
Great Oakley						
GO3	70% massive, wust. exsoln	15% short dendrites	5-7% euhedral + intergrowths	5% rounded patches	-	3%
GO4	60% massive wust. exsoln	20% dendrites	5-10% euhedral + intergrowths	7% irregular patches	-	3% + crystallites
GO 792017	60% skeletal laths	20% dendrites + film at C.S.	2% euhedral + intergrowths	2%	metallic iron grains, magnetite at C.S.	15% + minute crystallites
Wakerley						
WAK	50-55% laths skeletal to massive	35% fine dendrites + films at C.S.	5% euhedral + intergrowths	-	metallic iron magnetite + Fe-rich spinel	5%
WAK 48A	60% laths, some wustite exsolution	15-20% long dendrites	10-15% large euhedral	1% rounded patches	metallic iron grains	1-2% + crystallites
WK-AV	50% laths	40% v. long fine dendrites + film at C.S.	3% intergrowths	-	metallic iron magnetic + Fe-rich spinel	5%
WK K 4	60% laths to equant, some wust. exsoln	15% short dendrites + film at C.S.	10% intergrowths	7% patches + intergrowths	magnetite, Fe-rich spinel + Ca-p phase	2% + crystallites
WK K 4 2	60% ring laths	rare tiny dendrites	-	-	some metallic iron grains	40% + crystallites
WGW	60% laths to massive	35% dendrites + film at C.S.	2-3% euhedral + intergrowths	1-2% patches near C.S.	metallic iron grains	2% + crystallites
Garden Hill						
GH1	40% laths some equant	50% dendrites long to short	1% localized euthedral + intergrowths	1% localized patches	Iron grains + furnace wall inclusion	7.5% + crystallites
GH2	55% skeletal laths + some equant	30% dendrites	-	-	metallic iron grains	15% + crystallites
GH671	75% laths wust exsoln	2% dendrites	3-5% intergrowths	7-10% irreg patches	iron growths ca-p phase	5%
GH653	45% skeletal laths	35% dendrites to globular	-	2% intergrowths	iron grains ca-p phase	15-20% + crystallites
GH 6536	50% laths to equant	20% dendrites	1-2% euhedral + intergrowths	2-3% patches + intergrowths	iron grains	25% + crystallites
GHE1	60-65% massive	1% mostly globular	15% euthdral + intergrowths	10% patches + intergrowths	localised magnetite	2-5%

Table 4.1 continued

Brief descriptions of slag petrography

Sample	Fayalite	Wustite	Hercynite	Leucite	Others	Glass
Bulbourne Valley						
BCR1	65-70% laths some wustite exsolution	15% dendrites + films at chilled surfs	2% fine intergrowths	7% near chilled surfs	-	7% + some crystallites
BCR 2	90% long laths, much wust. exsoln	3% dendrites + film at C.S.	-	-	euhedral magnetite at C.S.	7% + crystallites
BCR 3	70% mostly massive, wust. exsolution	20% long dendrites	5% intergrowths	1-3% mostly intergrowths	inclusions of lining and charcoal	1-3% abundant crystallites
BBS	85% laths some skeletal	1-2% tiny dendrites + films at C.S.	-	-	magnetic + Fe-rich spinel	12-15% crystallites
NOR 1	70-75% laths most skeletal	-	-	-	5% magnetic	20-25% crystallites
NOR 2	85% laths sust. exsoln	1-2% dendrites films at C.S.	-	-	iron grains magnetite	7-10% + some crystallites
Brigstock	40% laths to massive	30% dendritic to globular	10-15% large euhedral	5-7% inter-growths	-	5%
Bulwich	80% laths most skeletal wust exsoln	5% small dendrites + films at C.S.	10% euthdral + inter-growths	-	Fe-rich spinel near C.S.	5%
Caerwent						
697096	55-60% laths to equant most skeleted	35% dendrite to globular + films at C.S.	-	-	-	5-10% + some crystallites
697275B	45% skeletal laths, some wust. exsoln	30% dendrites	-	-	some metallic iron grains	20-25% + some crystallites
Blind Eye Quarry						
BEQ1	80-85% laths wust. exsoln	Few primary dendrites + films at C.S.	5-10% inter-growths	-	some magnetite at C.S.	5% and few crystallites
BEQ2	70-75% laths wust. exsoln	5-7% dendrites films at C.S.	5-7% mostly euhedral	A little near chilled surfs	-	10%

Table 4.1 continued

Sample	Fayalite	Wustite	Hercynite	Leucite	Others	Glass
Ramsbury						
RAM	55-60% laths to massive	10% dendrites	2-3% mostly euhedral	15% patches + intergrowths	Ca-p phase	10% + crystallites
RAM 5	55% laths to massive some wust exsoln	15-20% mostly dendrites	2-3% euhedral + intergrowths	10% patches + intergrowths	some metallic iron grains	7-10% + crystallites
RAM 6	55% laths to equant mostly skeletal	25% fine dendrites + film at C.S.	5% fine intergrowth	5% in glass	iron grains + magnetite at skilled surf	10% + crystallites
Millbrook						
D	55% laths to equant	3-5% tiny dendrites	7% some euhedral	-	-	30-35% + crystallites
E	30%	50% dendritic to globular	15% intergrowths	3% in glass	-	2%
E_2	30%	60%	5% intergrowths	3%	magnetite in leucite	2%
F	35%	40% dendritic to globular	15% intergrowths	-	iron grains	10%
C	40% mostly equant	25% fine dendrites	-	-	-	35% + many crystallites
Stamford						
700128	55-60% laths most skeletal some wust ex.	15-20% fine dendrites + films at C.S.	-	-	some metallic iron grains	25%
700130	50% skeletal laths	25% fine dendrites + films at C.S.	3-5% intergrowths	some patches near C.S.	iron grains Fe-rich spinel	15% + some crystallites
630532	50-55% laths to massive	20% dendritic to globular + films at C.S.	10-15% mostly intergrowths	some patches near C.S.	iron grains magnetite + Fe-rich spinel	7% + some crystallites
S. Witham	75% laths part skeletal	15% fine dendrites + films at C.S.	5% mostly euhedral	some patches near C.S.	iron grains Fe-rich spinel + magnetite	2-5% + crystallites

Table 4.1 continued

Sample	Fayalite	Wustite	Hercynite	Leucite	Others	Glass
Reconstructions						
GHR 1	50% skeletal laths	-	-	-	10% skeletal magnetite	40% + crystallites
GHR4	45% skeletal laths to equant	-	tiny crystals in glass	-	15% skeletal magnetite + iron grains	40% + crystallites
GHR 10	50% large skeletal laths	v. rare tiny dendrites	tiny crystals in glass	-	15% skeletal magnetite + iron sponge	35% + some crystallites
RR1	60% long skeletal laths	-	-	some 'arcs' + intergrowths	5-10% mag. skeletal + film at CS Fe-rich spinel + iron grains	30-35%
RR2	45% skeletal laths	-	-	5% euhedral + patches	15% magnetite euhedral + films at C.S. iron sponge	35%

Table 4.2

Results of X-ray diffraction analyses of slags

Sample		Fayalite	Wüstite	Magnetite	Hercynite
Great Oakley	GO4	++	+		?
	GO7	++	++		
Wakerley	WAK 48A	++	++		+
	WK/AV	++	++		?
	WK K4	++	++		
	WGW	++	+		
Garden Hill	GH1	++	++		
	GH2	++	++		
Bulbourne Valley	NOR 1*	++		+	
	NOR 2	++	+		
Blind Eye Quarry	BEQ1	++	+		
	BEQ2	++	**		+
Bulwick	BUL	++	+		?
Brigstock	BRIG	++	++		+
Caerwent	CAER	++	++		
Ramsbury	RAM 5	++	+		
Millbrook	Bulk	++	++	+	
	D	++	+		
	E*	++	++	?	?
Stamford	700130	++	+		?
	630532	++	+		?
Reconstructions	RR1	++			
	RR2	++			
	GHR1	++		+	
	GHR4	++			
	GHR10	++			
	GHR11	++			

++ major constituent, + minor constituent, ? possibly present

* quartz also detected; NOR 1 contained pockets of quartz sand and Millbrook E probably contained inclusions of flint

Table 4.3

Miller Indices	d-spacing (Å)			
	Magnetite	Spinel in WAK 48A	Spinel in Brigstock	Hercynite
311	2.532_{100}	2.47_{100}	2.467	2.45_{100}
400	2.099_{20}	2.045	n.d.	2.02_{80}
440	1.485_{50}	1.447	1.445	1.43_{80}
220	2.967_{30}	2.89	2.89	2.87_{60}
511	1.616_{30}	n.d.	1.570	1.56_{40}

n.d. = not detected

subscripts indicate relative intensities published in powder difraction file

Table 4.4

Comparison of the proportions of hercynite and leucite in slags with the Al_2O_3 and K_2O contents of the ores

Site	% hercynite	% leucite	Average Al_2O_3 in slag wt %	Average Al_2O_3 in ore wt %	Average K_2O in slag wt %	Average K_2O in ore wt %	Average 'Fe_2O_3 in ore wt %
Wakerley	2-15	0-7	6.14	2.63	0.56	0.08	73.3
Bulwick	10	-	6.49	2.66	0.49	0.08	71.3
Great Oakley	2-10	2-7	4.05	3.07	0.42	0.06	76.4
Stamford	0-15	0-1	6.38	3.92	0.94	0.53	69.6
Ramsbury	2-5	5-15	5.51	2.07	1.74	0.27	89*
Garden Hill	0-5	0-10	4.90	3.54	0.68	0.56	52.3
Reconstruction, shaft	0-0.5	-	5.91	3.54	1.05	0.56	52.3
Reconstruction, bowl	0[+]	1-5	7.2	3.54	2.1	0.56	52.3

* Average 'Fe_2O_3' in roasted ore

[+] Spinel is a titaniferous magnetite

Table 4.5

Calculation of late liquid compositions

Example A : Slag RAM 5

Estimated Volume of Minerals	(%)	Specific gravity of phases	Weight % Minerals*	Idealised Formula	Molecular Weight	Moles
Fayalite	55	4.4	56	$2FeO.SiO_2$	203.8	0.275
Wüstite	20	5.7	27	FeO	71.85	0.376
Hercynite	3	4.4	3	$FeO.Al_2O_3$	173.8	0.017
Leucite	12	2.5	7	$K_2O.Al_2O_3.4SiO_2$	436.5	0.016
	100		100			

If all fayalite, wüstite and hercynite is assumed to have crystallised, total number of moles used

$FeO = 2 \times 0.275 + 0.376 + 0.017 = 0.943 = 67.8$ wt %

$SiO_2 = 0.275 = 16.5$ wt %

$Al_2O_3 = 0.017 = 1.7$ wt %

XRF analysis:

FeO	SiO_2	Al_2O_3	CaO	MnO	MgO	TiO_2	V_2O_5	P_2O_5	K_2O
58.9	26.0	5.51	2.23	1.58	1.08	0.30	0.06	0.95	1.74

Total FeO already accounted for apparently exceeds that actually present, but this is because other oxides substitute for FeO in the phases. If it is assumed that MnO, MgO and some CaO substitutes for FeO in fayalite and TiO_2 and V_2O_5 substitute in hercynite, probable liquid composition after crystallization of fayalite, wüstite and hercynite can be calculated as below

	Oxides remaining (%)	Liquid composition (%)
FeO	2	10
SiO_2	9.5	49
Al_2O_3	3.8	19
CaO	1.5	8
P_2O_5	0.95	5
K_2O	1.74	9
	19.49	100

(continued)

Table 4.5 (continued)

$$* \text{ wt \% of a mineral } i = \frac{\text{Vol \%}_i \times \text{S.G.}_i}{{}_{i-j}(\text{Vol \%}_i \times \text{S.G.}_i)} \times 100\ \%$$

Example B : Slag G04

Estimated Volume of Minerals	(%)	Specific gravity of phases	Weight % Minerals	Moles
Fayalite	60	4.4	59	0.290
Wüstite	20	5.7	26	0.362
Hercynite	7	4.4	7	0.040
Leucite	10	2.5	6	0.014
Glass	3	3.0	2	-
	100		100	

If all fayalite, wüstite and hercynite is assumed to have crystallised, total number of moles used

$$\text{FeO} = 2 \times 0.290 + 0.362 + 0.04 = 0.982 = 70.5 \text{ wt \%}$$

$$\text{SiO}_2 = 0.290 = 17.4 \text{ wt \%}$$

$$\text{Al}_2\text{O}_3 = 0.040 = 4.1 \text{ wt \%}$$

XRF analysis:

FeO	SiO_2	Al_2O_3	CaO	MnO	MgO	TiO_2	V_2O_5	P_2O_5	K_2O
63.7	22.3	4.16	0.78	0.47	0.25	0.27	0.05	0.42	0.65

Following similar arguments to those used for Example A,

	Oxides remaining (%)	Liquid composition (%)
FeO	2	22
SiO_2	4.9	54
Al_2O_3	0.5	6
CaO	0.5	6
K_2O	0.42	5
P_2O_5	0.65	7
	8.97	100

Table 4.6

Minor oxide content of fayalite and probable ores, averages and variation

	Mean, $\bar{x}$	Sample std deviation, $_{n-1}$	Number of analyses, n
MgO in fayalite	1.12	1.02	62
MgO in fayalite, Weald*	1.48	1.06	32
MgO in fayalite, Northamptonshire*	0.49	0.30	17
MgO in Wealden ores*	1.04	0.68	6
MgO in Northamptonshire ores*	0.12	0.07	20
MnO in fayalite	2.09	1.20	62
MnO in fayalite, Weald	2.95	0.83	32
MnO in fayalite, Northamptonshire	1.16	0.61	17
MnO in Wealden Ores	2.41	0.29	6
MnO in Northamptonshire ores	0.55	0.42	20
CaO in fayalite	0.97	1.06	62
CaO in fayalite, Weald	1.24	1.34	32
CaO in fayalite, Northamptonshire	0.71	0.62	17
CaO in Wealden ores	2.19	1.22	6
CaO in Northamptonshire ores	1.17	1.84	20

* For the purposes of this comparison, the Wealden ores are represented entirely by analyses of Wadhurst Clay Ironstone and the Wealden slags are all those, including material from present-day furnace reconstructions, which are known to have been or were probably produced from the smelting of Wadhurst Clay Ironstone. The Northamptonshire ores are represented by analyses of the Ironstone Junction-Band only and the slags are from the Wakerley, Great Oakley and Bulwick sites where there is good evidence that the above ironstone was used (see Section 4).

Table 4.7

Calculation of chemical formulae from spinel analyses

Example 1 : spinel in G04

	wt % oxides	molecular proportions of oxides	atomic props. of oxygen from each mol.	Nos. of anions on basis of 32 (0)	Nos. of ions in formula		
MnO	0.38	0.005	0.005	0.076	0.1	0.1	
MgO	-	-	-	-	-	-	8.0
FeO	51.23	0.713	0.713	10.793	10.8	7.9 2.9	
Al_2O_3	45.87	0.450	1.350	20.435	13.6	13.6	
SiO_2	0.35	0.006	0.012	0.182	0.1	0.1	17.1
TiO_2	0.94	0.012	0.024	0.363	0.4	0.4	
V_2O_5	0.40	0.002	0.010	0.151	0.1	0.1	
			2.114				

Example 2 : spinel in RR2 (columns as above)

MnO	1.26	0.018	0.018	0.33	0.3	0.3	
MgO	0.22	0.005	0.005	0.09	0.1	0.1	8.0
FeO	72.52	1.009	1.009	18.43	18.4	7.6 10.8	
Al_2O_3	11.80	0.116	0.348	6.36	4.2	4.2	
SiO_2	1.00	0.017	0.034	0.62	0.3	0.3	18.3
TiO_2	11.50	0.144	0.288	5.26	2.6	2.6	
V_2O_5	1.76	0.010	0.050	0.91	0.4	0.4	
			1.752				

Each spinel should contain 8 di-valent and 16 tri-valent cations, the slight discrepancies are a result of having to assume initially that all iron is in the di-valent state.

Figure 4.1

Phase relations in the system $FeO-SiO_2$, after Bowen and Schairer. The system is not a true binary. The range in composition of the slags investigated is cross-hatched.

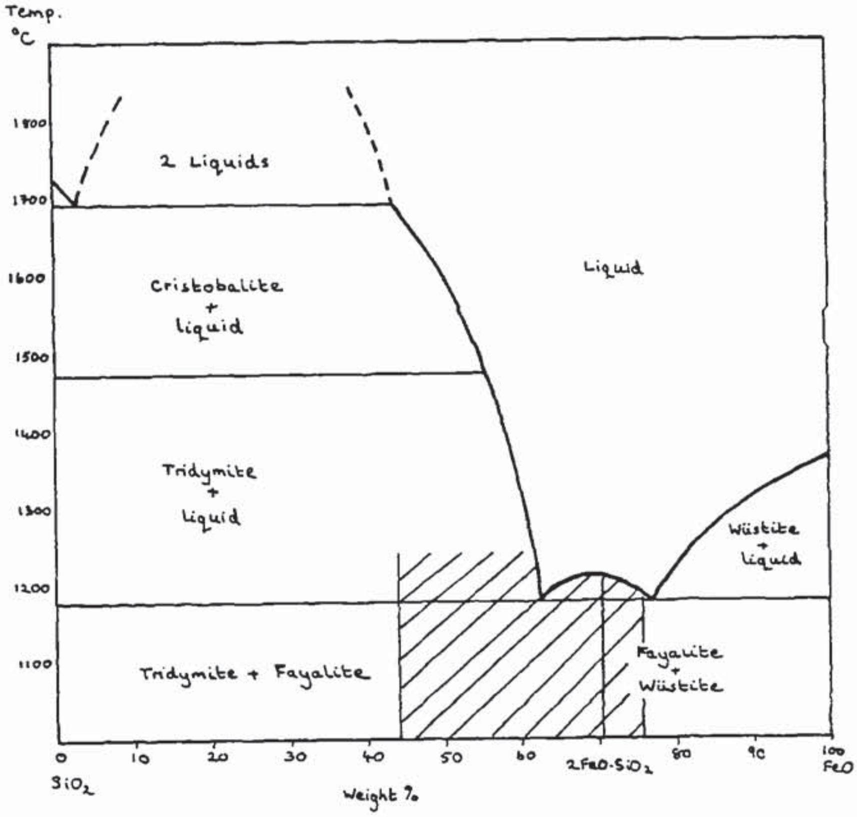
Temp.
°C
1800
1700
1600
1500
1400
1300
1200
1100
2 Liquids
Cristobalite + liquid
Liquid
Tridymite + Liquid
Wüstite + liquid
Tridymite + Fayalite
Fayalite + Wüstite
0
10
20
30
40
50
60
$2FeO \cdot SiO_2$
80
90
100
SiO_2
FeO
Weight %

Figure 4.2

Projection of the liquidus surface of the system $FeO-Fe_2O_3-SiO_2$, after Muan and Osborn.[97] Fine dashed lines are oxygen isobars.

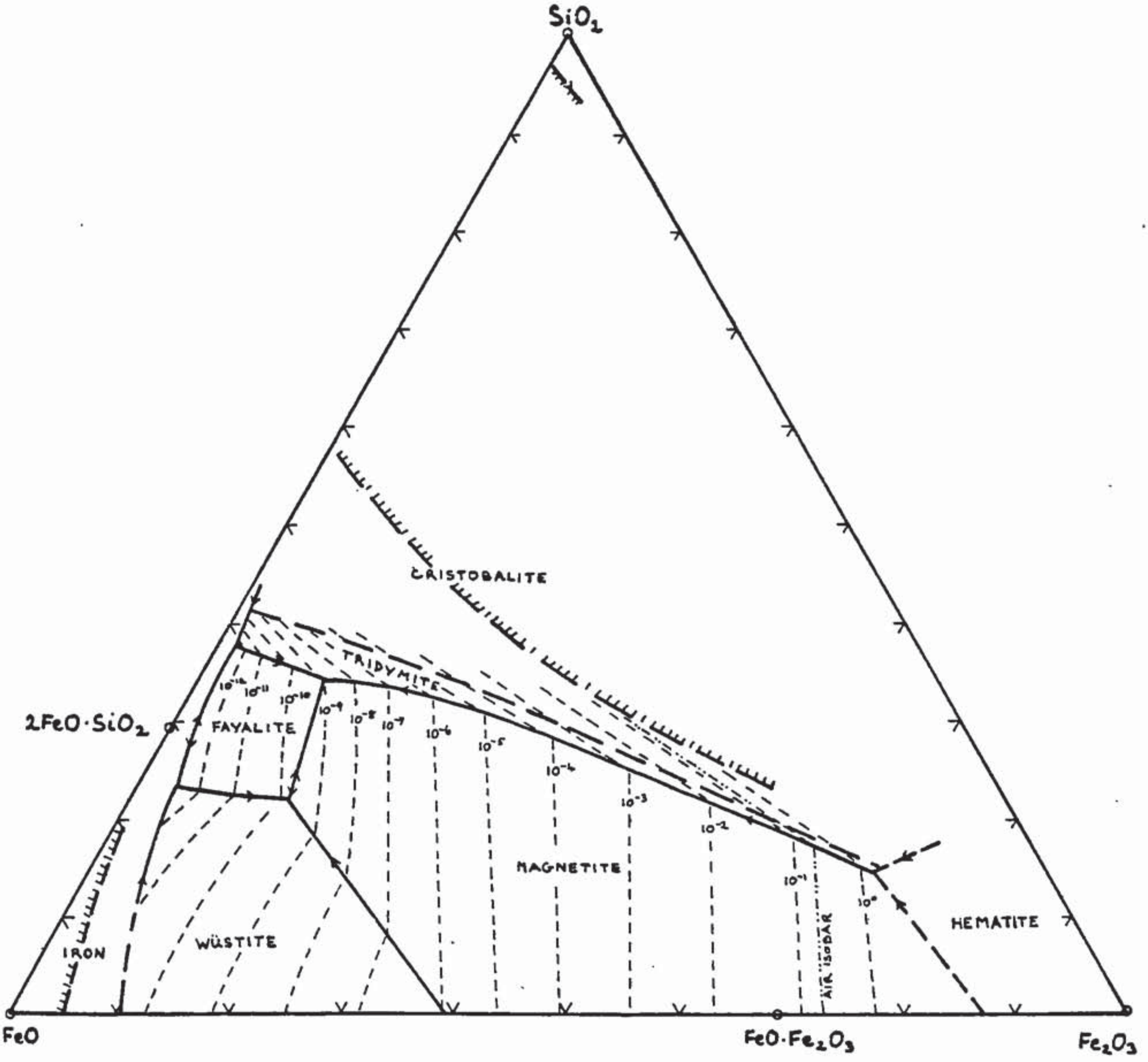
SiO_2
CRISTOBALITE
TRIDYMITE
$2FeO \cdot SiO_2$
FAYALITE
10^{-12}
10^{-11}
10^{-10}
10^{-9}
10^{-8}
10^{-7}
10^{-6}
10^{-5}
10^{-4}
10^{-3}
10^{-2}
10^{-1}
10^{0}
AIR ISOBAR
MAGNETITE
HEMATITE
WÜSTITE
IRON
FeO
$FeO \cdot Fe_2O_3$
Fe_2O_3

Figure 4.3

Perspective drawing of tetrahedron representing the system $FeO-Fe_2O_3-Al_2O_3-SiO_2$, showing phase relations at liquidus temperatures. After Muan and Osborn.[97]

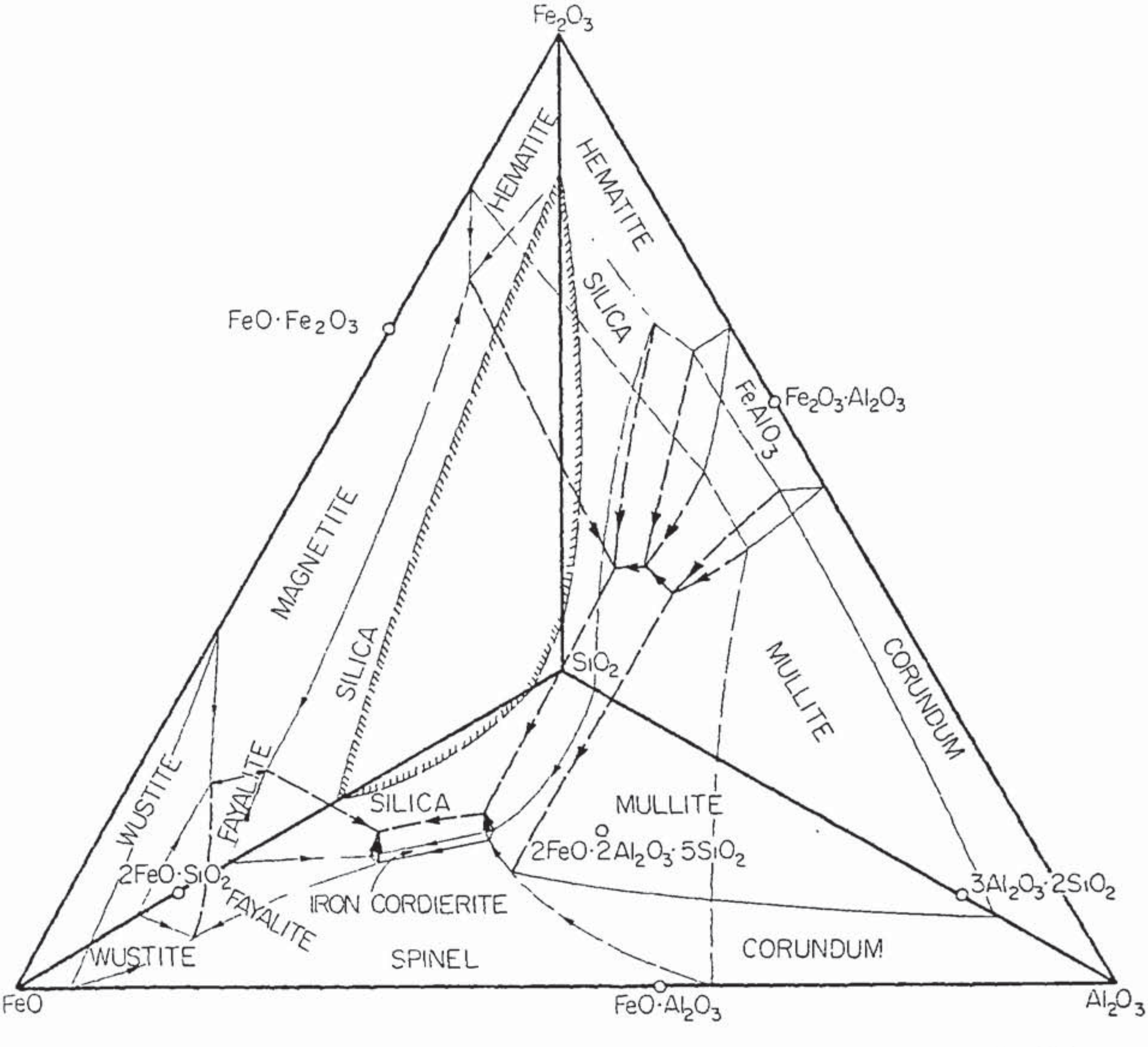

Fig. 97. Perspective drawing of tetrahedron representing the system FeO-Fe_2O_3-Al_2O_3-SiO_2 and showing phase relations at liquidus temperatures, after Muan.(279)

Figure 4.4

Phase relations in the system $FeO-Al_2O_3-SiO_2$ in contact with metallic iron, after Muan and Osborn.[97] The system is not a true ternary. (Compositions of condensed phases have been projected along oxygen reaction lines onto the plane $FeO-Al_2O_3-SiO_2$.) In order to include minor oxides, molar proportions of CaO, MgO, MnO, TiO_2 were added to FeO and molar proportions of P_2O_5 were added to SiO_2 before rounding to 100 wt %.

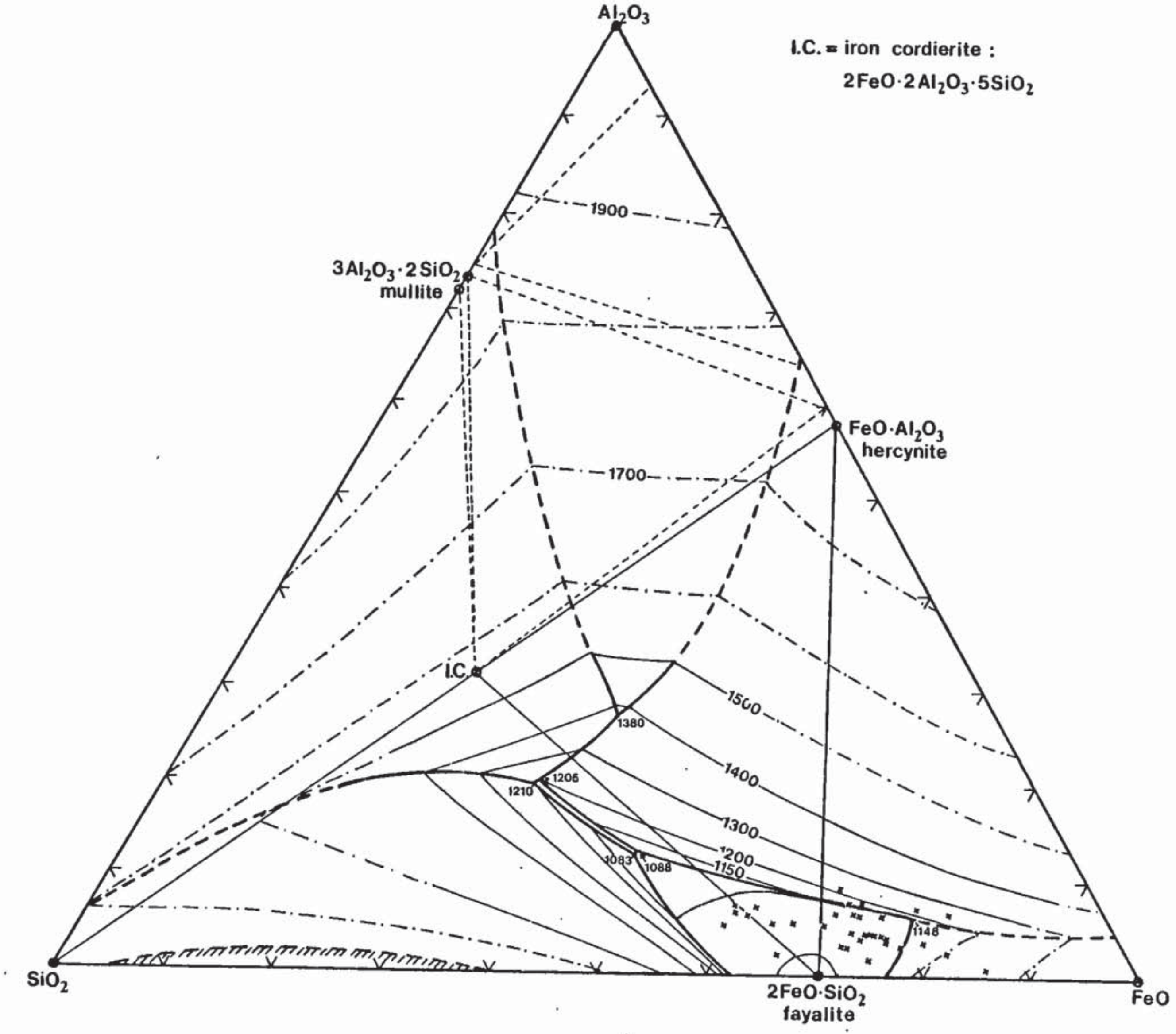

I.C. = iron cordierite :
$2FeO \cdot 2Al_2O_3 \cdot 5SiO_2$

Figure 4.5

FeO apex of $FeO-Al_2O_3-SiO_2$ system, showing the liquid paths of slags 19, 31 and 62 in equilibrium conditions. 19 and 62 both crystallize fayalite initially and their liquid compositions move directly away from the fayalite composition. 19 precipitates only a very small amount of fayalite (62 precipitates a much larger proportion) before the cotectic (boundary curve) is reached, when wüstite and fayalite crystallize together and the liquid composition moves down the cotectic with falling temperature towards the ternary eutectic of fayalite + hercynite + wüstite. At 1148°C the eutectic is reached and the remaining liquid crystallizes to a mixture of these three phases. Slag 31 precipitates wüstite initially, then on reaching the wüstite-fayalite cotectic, the crystallization sequence is as above. The presence of glass in these three slags indicates that the liquid solidified before the ternary eutectic was reached.

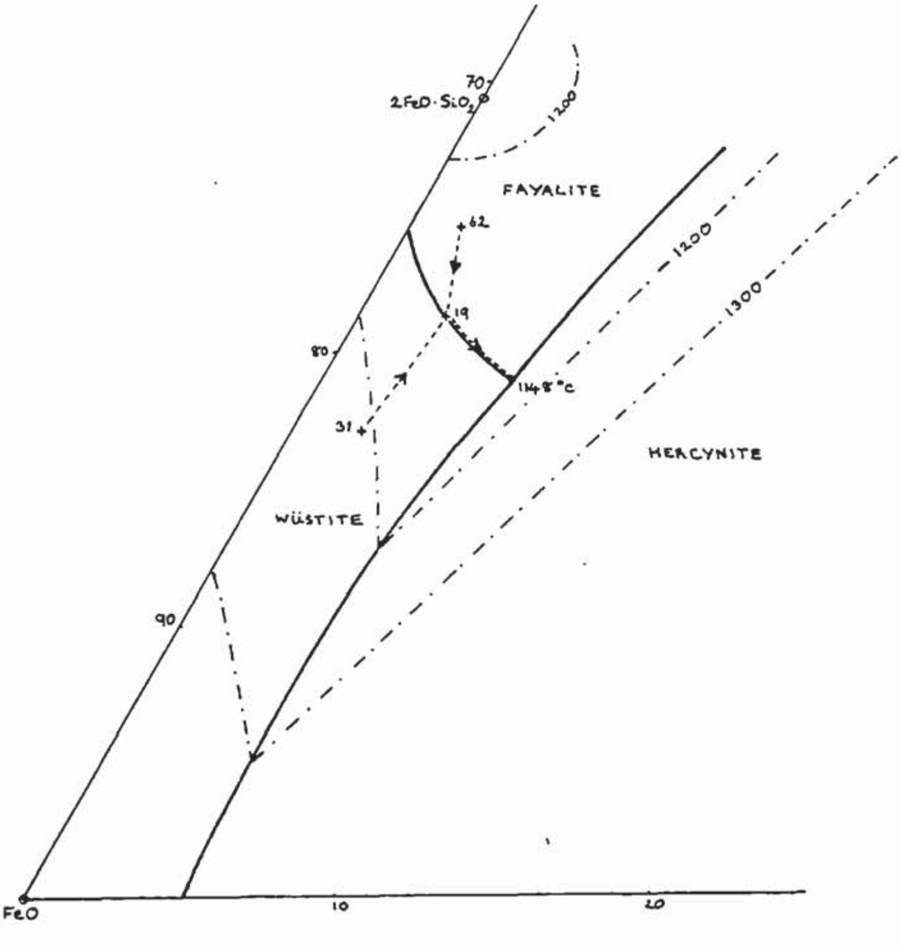
70
2FeO·SiO$_2$
1200
FAYALITE
62
19
80
31
1148°C
1200
1300
HERCYNITE
WÜSTITE
90
FeO
10
20

Figure 4.6

Phase relations in the system CaO-FeO-SiO_2 in contact with metallic iron, after Muan and Osborn.[97] The system is not a true ternary. The slags of this investigation have been plotted after the method of Sperl.[85]

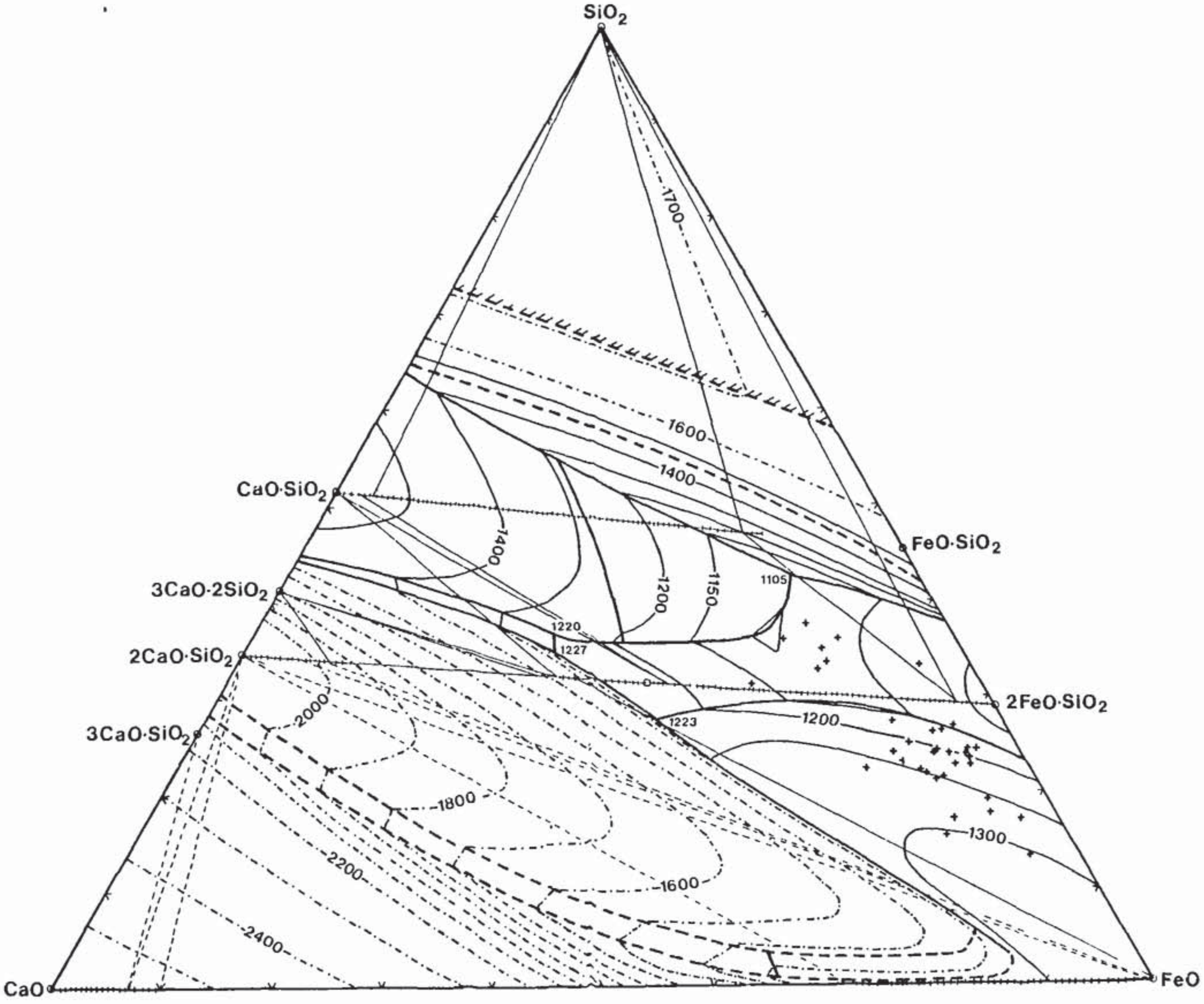
SiO₂
1700
1600
1400
CaO·SiO₂
FeO·SiO₂
1400
1200
1150
1105
3CaO·2SiO₂
1220
1227
2CaO·SiO₂
2FeO·SiO₂
2000
1223
1200
3CaO·SiO₂
1800
1300
2200
1600
2400
CaO
FeO

Figure 4.7

Phase relations in the system Anorthite ($CaO.Al_2O_3.2SiO_2$)-SiO_2-FeO.

The slags of this investigation have been plotted after the method of Morton and Wingrove.[4]

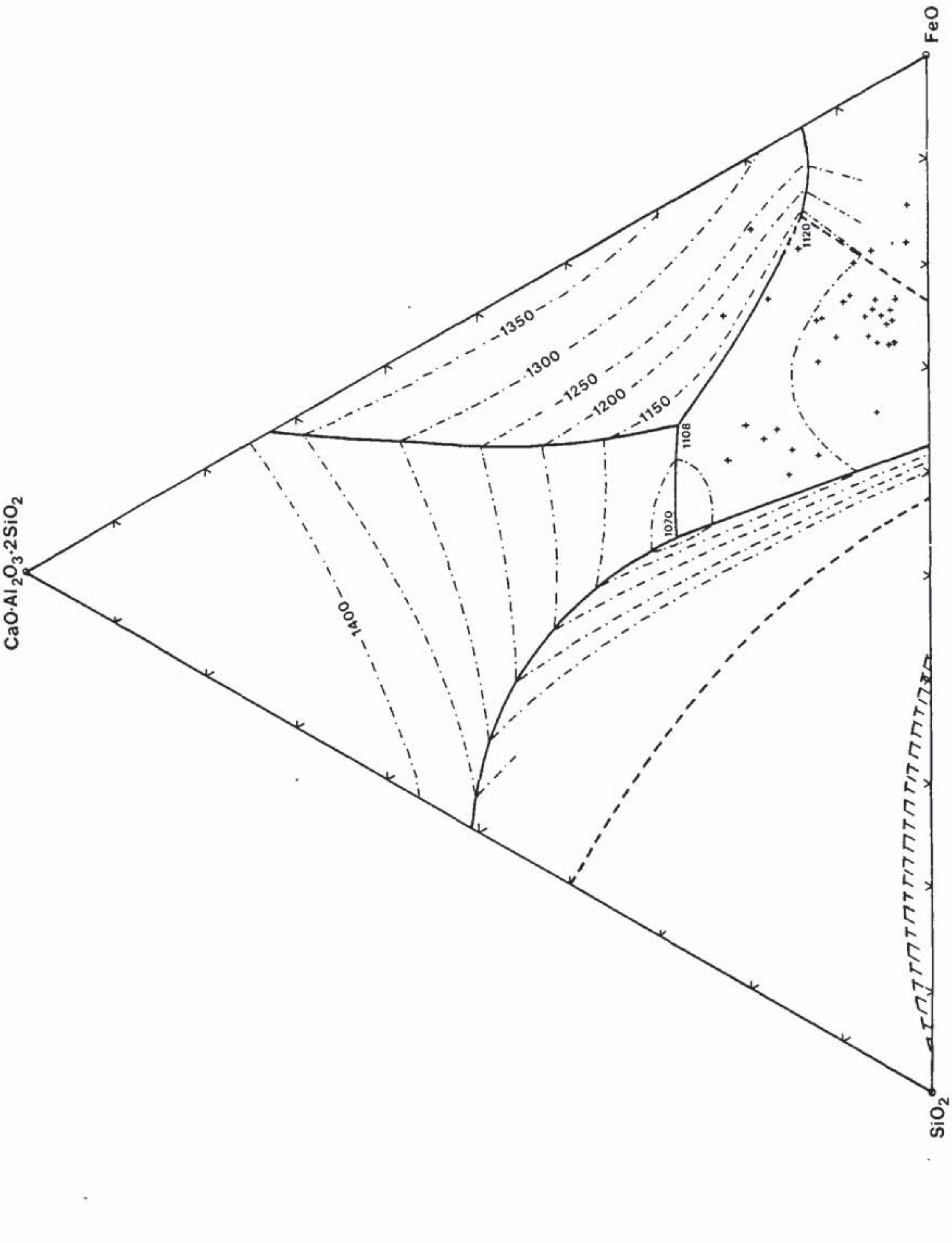
CaO·Al$_2$O$_3$·2SiO$_2$
FeO
SiO$_2$
1400
1350
1300
1250
1200
1150
1108
1070
1120

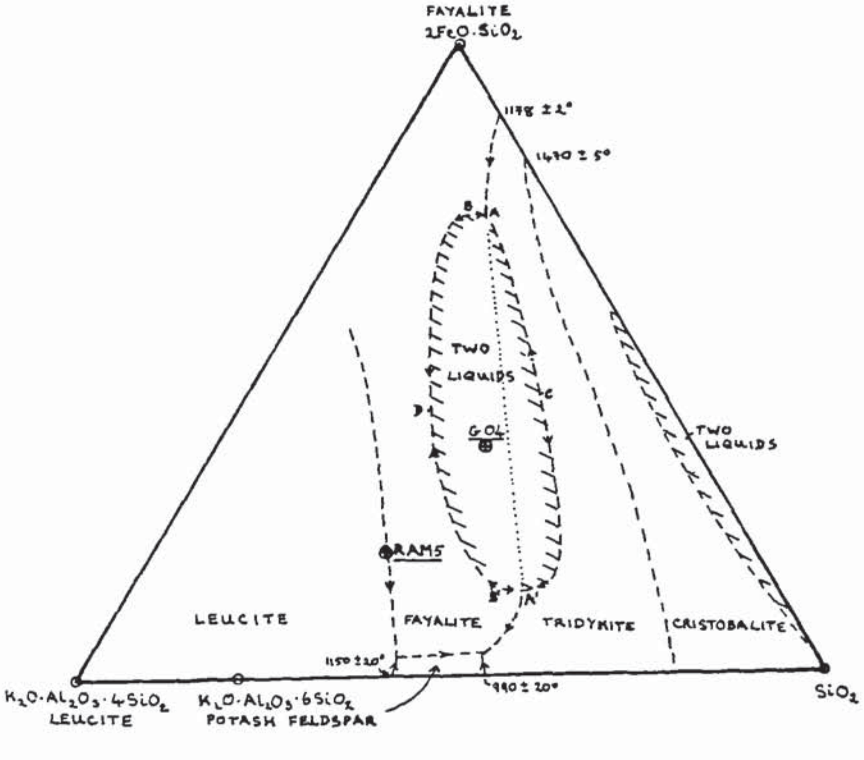

AA' 1153 ± 2°C

BB' ~1155°C

C ~1270°C

D < 1100°C

Figure 4.8

Approximate phase relations in the system leucite ($K_2O,Al_2O_3.4SiO_2$)-fayalite ($2FeO.SiO_2$)-SiO_2, in contact with metallic iron, after Roedder.[87]
The calculated compositions of late liquids in RAM 5 and G04 (see Table 4.5) are plotted.

Figure 4.9(a)

Phase relations in the system CaO-P_2O_5-FeO in contact with metallic iron, after Muan and Osborn.[97] The system is not a true ternary. The calculated compositions of late liquids in RAM 5 and GO4 (see Table 4.5) are plotted.


P₂O₅
2CaO·P₂O₅
3CaO·P₂O₅
4CaO·P₂O₅
2FeO·P₂O₅
3FeO·P₂O₅
1700
1300
1200
RAM 5
GO4
1400
1500
1600
1600
1500
1400
2000
1900
1800
1700
1600
2100
2200
2300
2400
2500
1400
1500
1400
1300
CaO
FeO

Figure 4.9(b)

Sketch showing estimated effect of SiO_2 on the liquid immiscibility field of the system $CaO-P_2O_5-FeO$ in contact with metallic iron, after Oelsen and Maetz.[98]

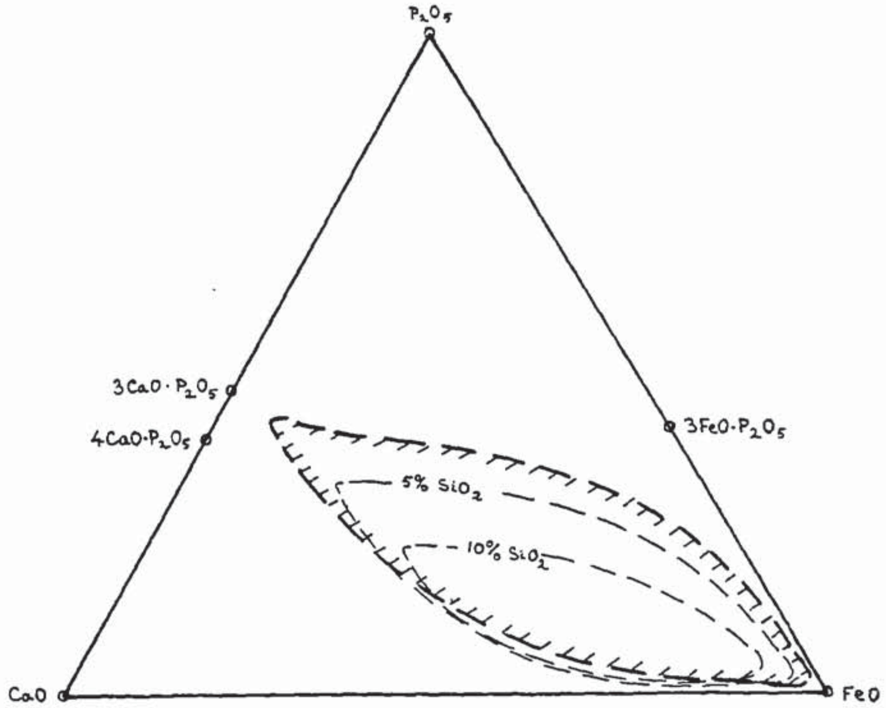
P_2O_5
$3CaO \cdot P_2O_5$
$4CaO \cdot P_2O_5$
$3FeO \cdot P_2O_5$
5% SiO_2
10% SiO_2
CaO
FeO

Figure 4.10

Equilibrium diagram of the system Ca_2SiO_4-Fe_2SiO_4, after Bowen *et al*.

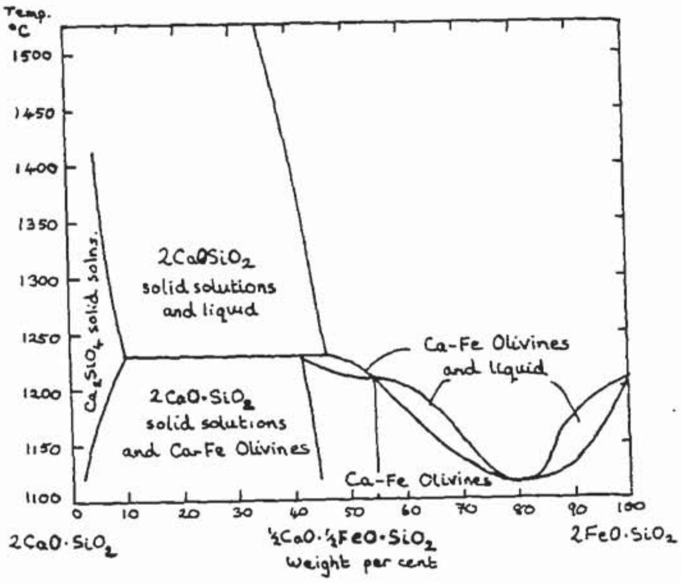
Temp. °C
1500
1450
1400
1350
1300
1250
1200
1150
1100
Ca2SiO4 solid solns.
2CaO·SiO2 solid solutions and liquid
2CaO·SiO2 solid solutions and Ca-Fe Olivines
Ca-Fe Olivines and liquid
Ca-Fe Olivines
0
10
20
30
40
50
60
70
80
90
100
2CaO·SiO2
½CaO·½FeO·SiO2
2FeO·SiO2
Weight per cent

Figure 4.11

SEM photograph of GH 653a with Kevex traces to show changing composition of the large fayalite crystal and the composition of the crystallites in the glass. The paler, rounded phase is wüstite. Note how the crystallites have nucleated on the wüstite.

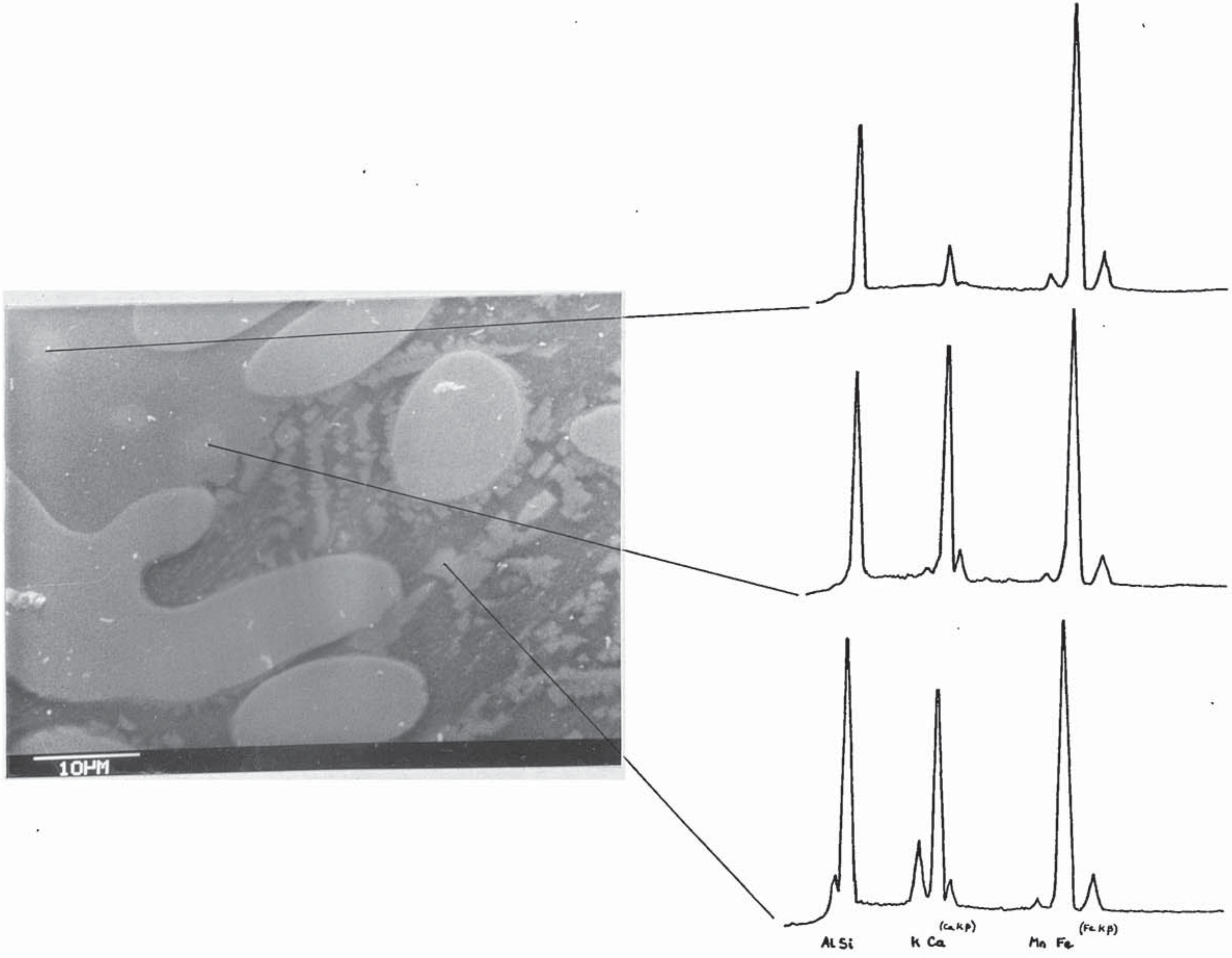
10µM
Al Si
K Ca
(Ca Kβ)
Mn Fe
(Fe Kβ)

Figure 4.12

Kevex traces comparing the compositions of large, primary olivines and olivine-type crystallites in the glass. Because of the small size of the crystallites, the beam has in some cases penetrated through into the surrounding glass resulting in anomalous peaks (e.g. for K). The large fayalite crystal in GH2 appears highly calcic, but this analysis was probably made towards the edge, rather than at the centre.

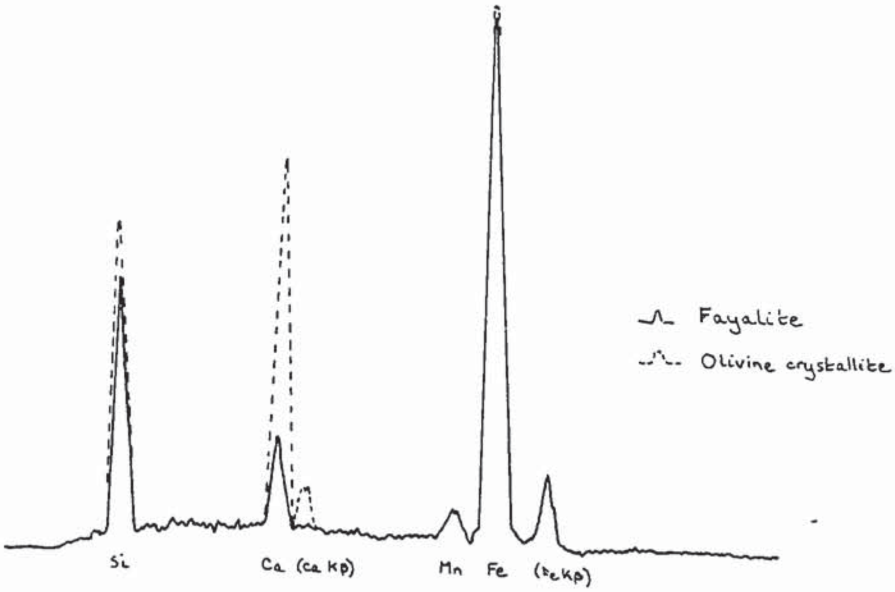

GH 653a

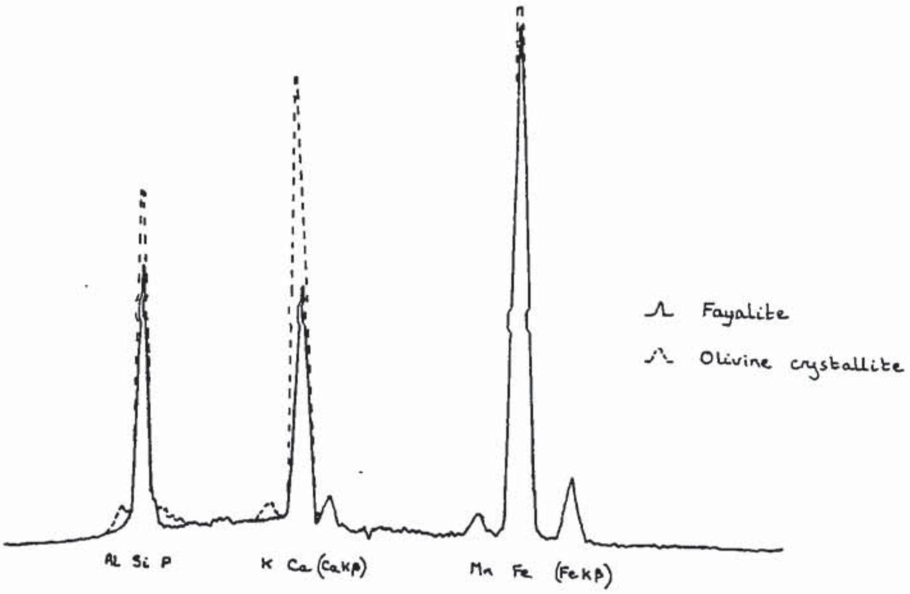

GH2

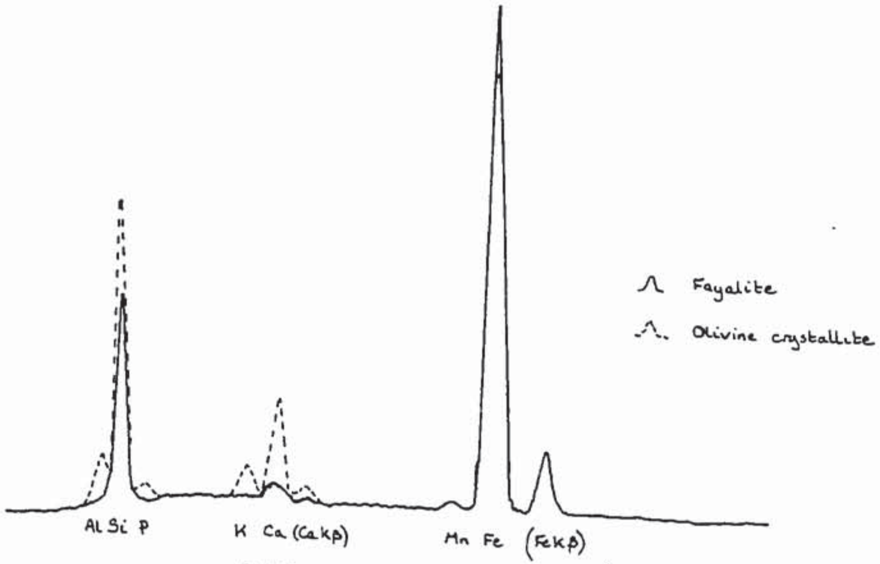

GH1

Figure 4.13(a)

SEM photograph of fayalite laths (medium grey) in NOR 2 showing wüstite exsolution.

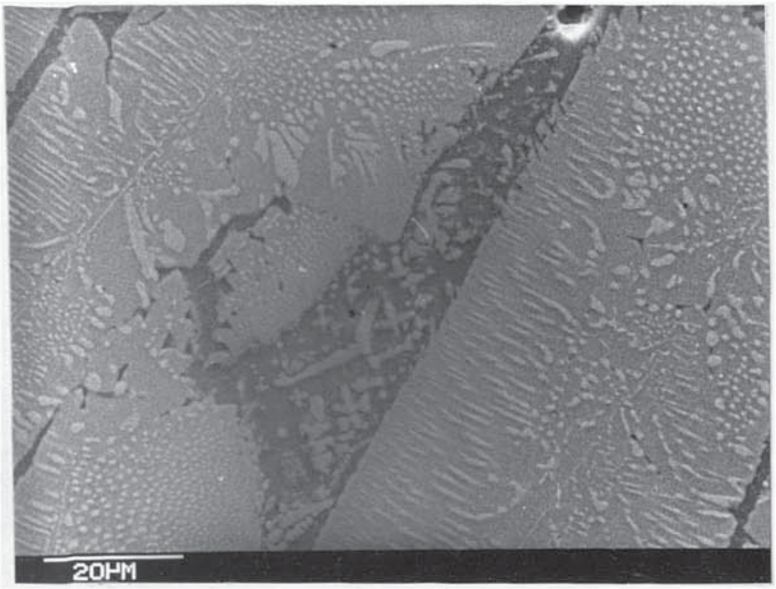
20HM

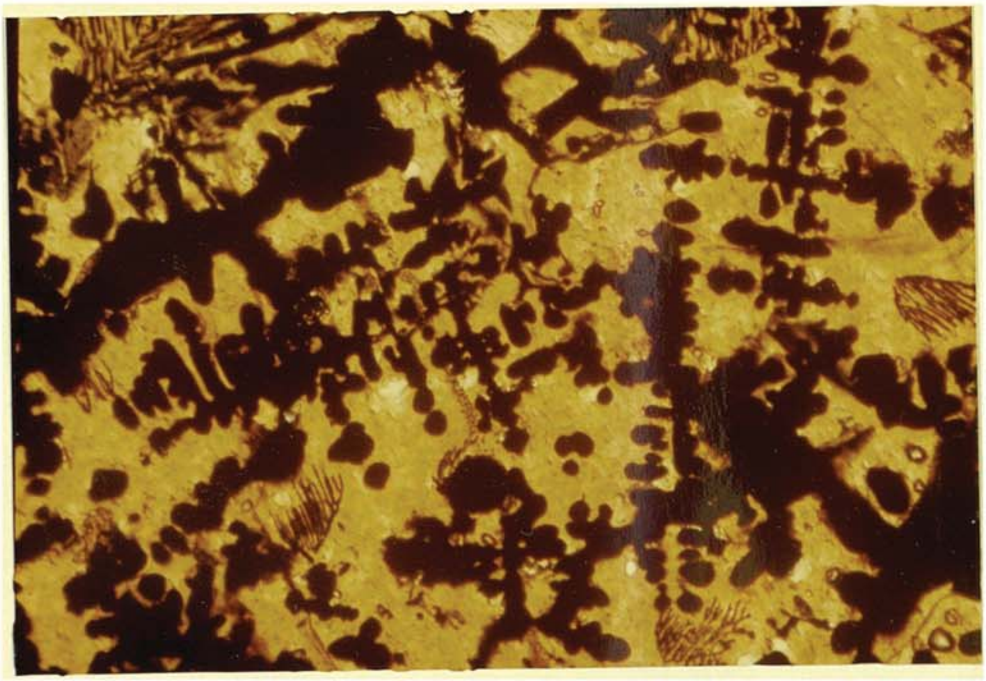

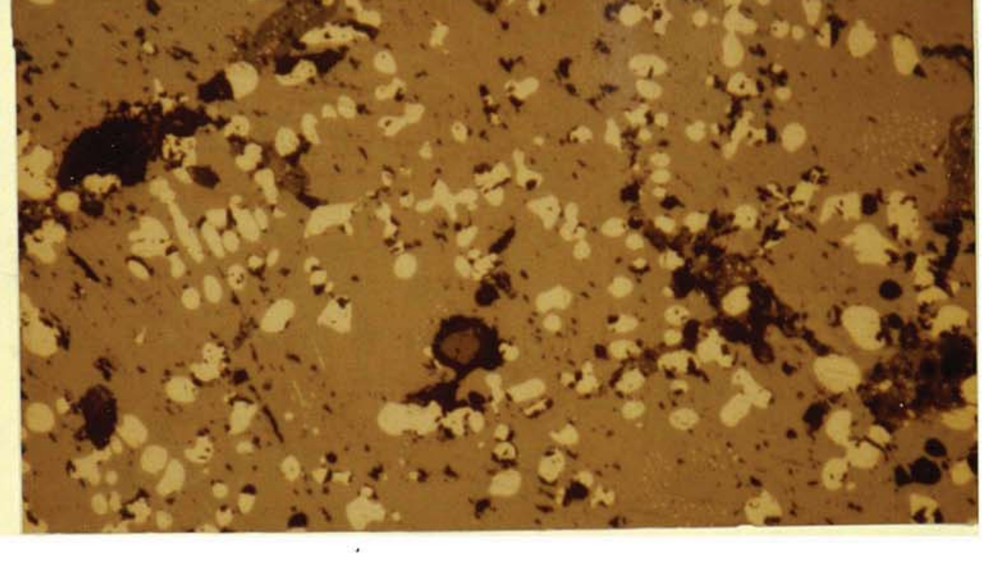

Figure 4.13(b)

(i) G03 in transmitted light showing comb-like form of wüstite. Crossed polars. Field of view 0.89 mm wide.

(ii) Same area in reflected light.

Figure 4.14

(a) SEM photograph of slag from Bulwick showing wüstite exsolution along central part of fayalite lath.

(b) SEM photograph of slag from Bulwick showing some additional wüstite exsolution in areas of fayalite/hercynite intergrowth.

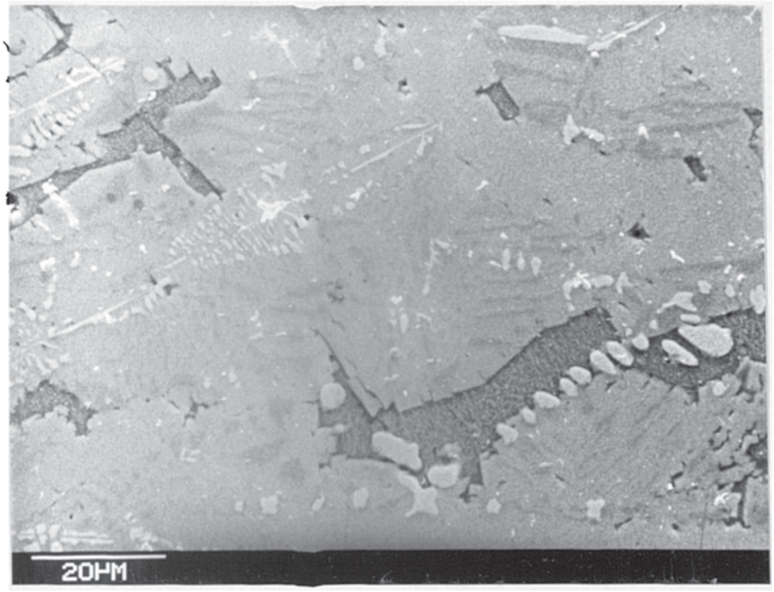
20µM

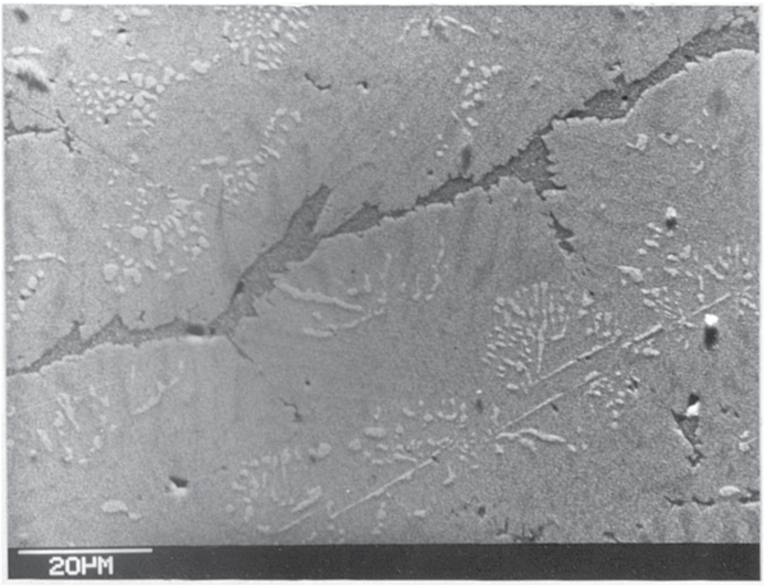
20µM

Figure 4.15

Phase relations in the system FeO-Fe_2O_3, after Muan and Osborn.[97] Fine dashed lines are oxygen isobars.

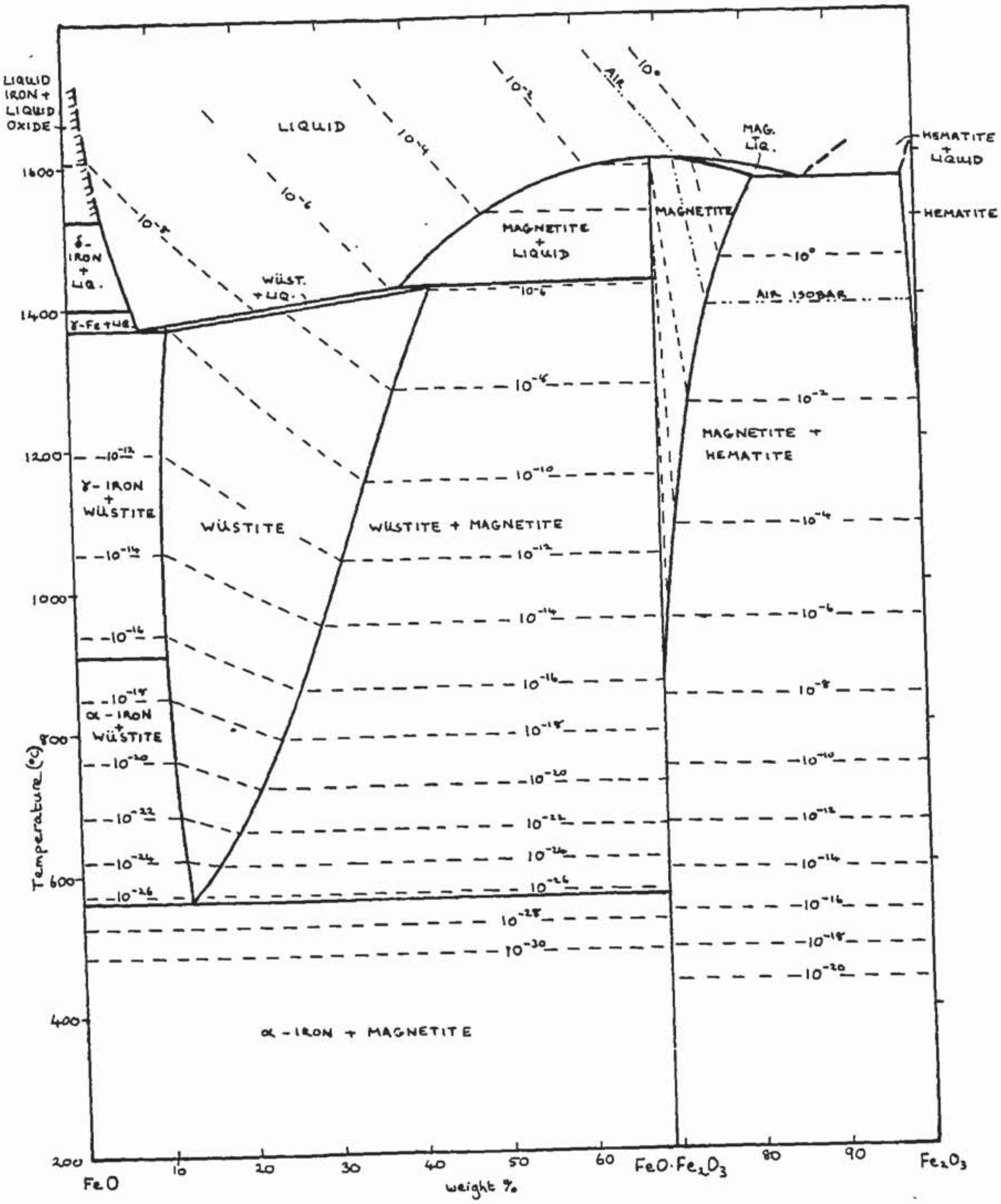
LIQUID IRON + LIQUID OXIDE
LIQUID
10-4
10-2
AIR
10°
MAG. + LIQ.
HEMATITE + LIQUID
HEMATITE
10-6
10-8
δ-IRON + LIQ.
γ-Fe + LIQ.
WÜST. + LIQ.
MAGNETITE + LIQUID
MAGNETITE
10°
AIR ISOBAR
10-6
10-8
10-2
MAGNETITE + HEMATITE
10-12
γ-IRON + WÜSTITE
WÜSTITE
10-10
WÜSTITE + MAGNETITE
10-4
10-14
10-12
10-14
10-6
10-16
10-16
10-18
α-IRON + WÜSTITE
10-8
10-18
10-20
10-20
10-10
10-22
10-22
10-12
10-24
10-24
10-14
10-26
10-26
10-16
10-28
10-18
10-30
10-20
α-IRON + MAGNETITE
Temperature (°C)
1600
1400
1200
1000
800
600
400
200
FeO
10
20
30
40
50
60
FeO·Fe2O3
80
90
Fe2O3
weight %

Figure 4.16

Stamford slag 630532 in reflected light showing compositionally zoned spinels. The paler bands are richer in iron. Field of view 0.30 mm wide.

Figure 4.17

SEM photograph of WAK 48A showing typical habit of leucite. Example shows abundant exsolution of wüstite rods. Also present are hercynite (mid grey, angular), fayalite (pale grey) and primary wüstite dendrites. X-ray maps show distribution of main constituent oxides.

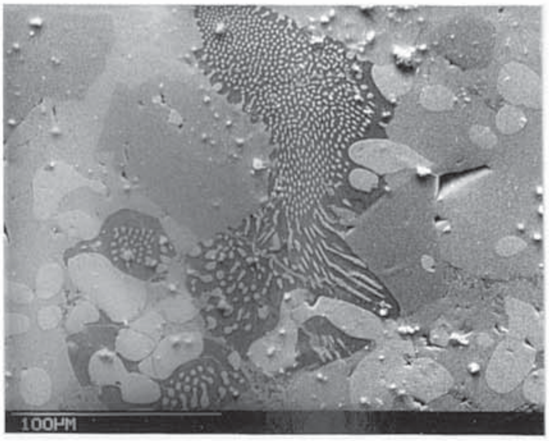

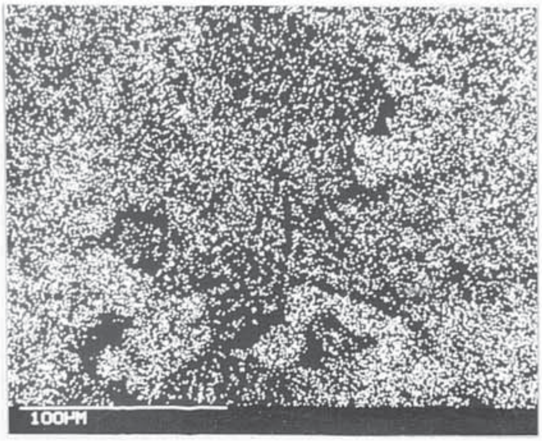

Fe

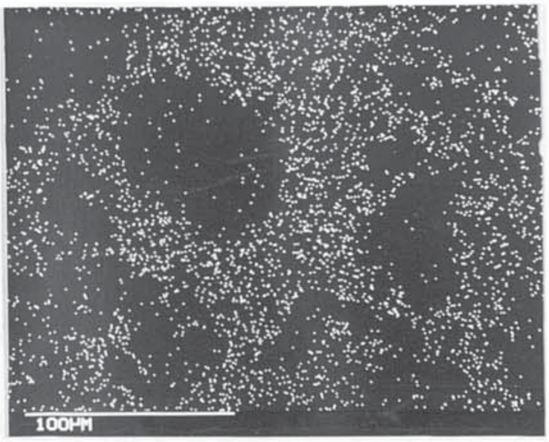

Si

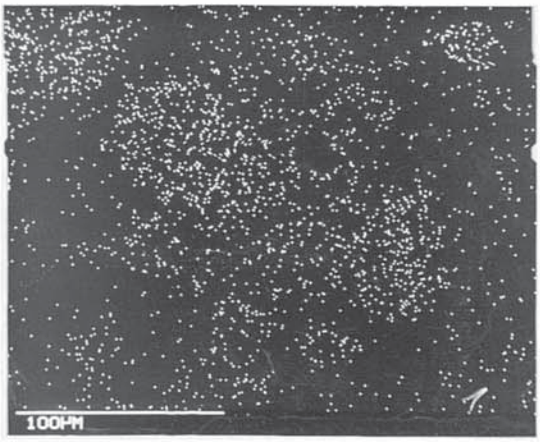

Al

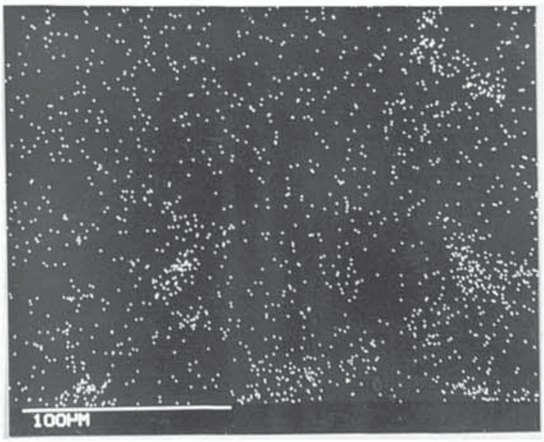

Ca

K

Figure 4.18

Kevex trace of crystallite in GH 631

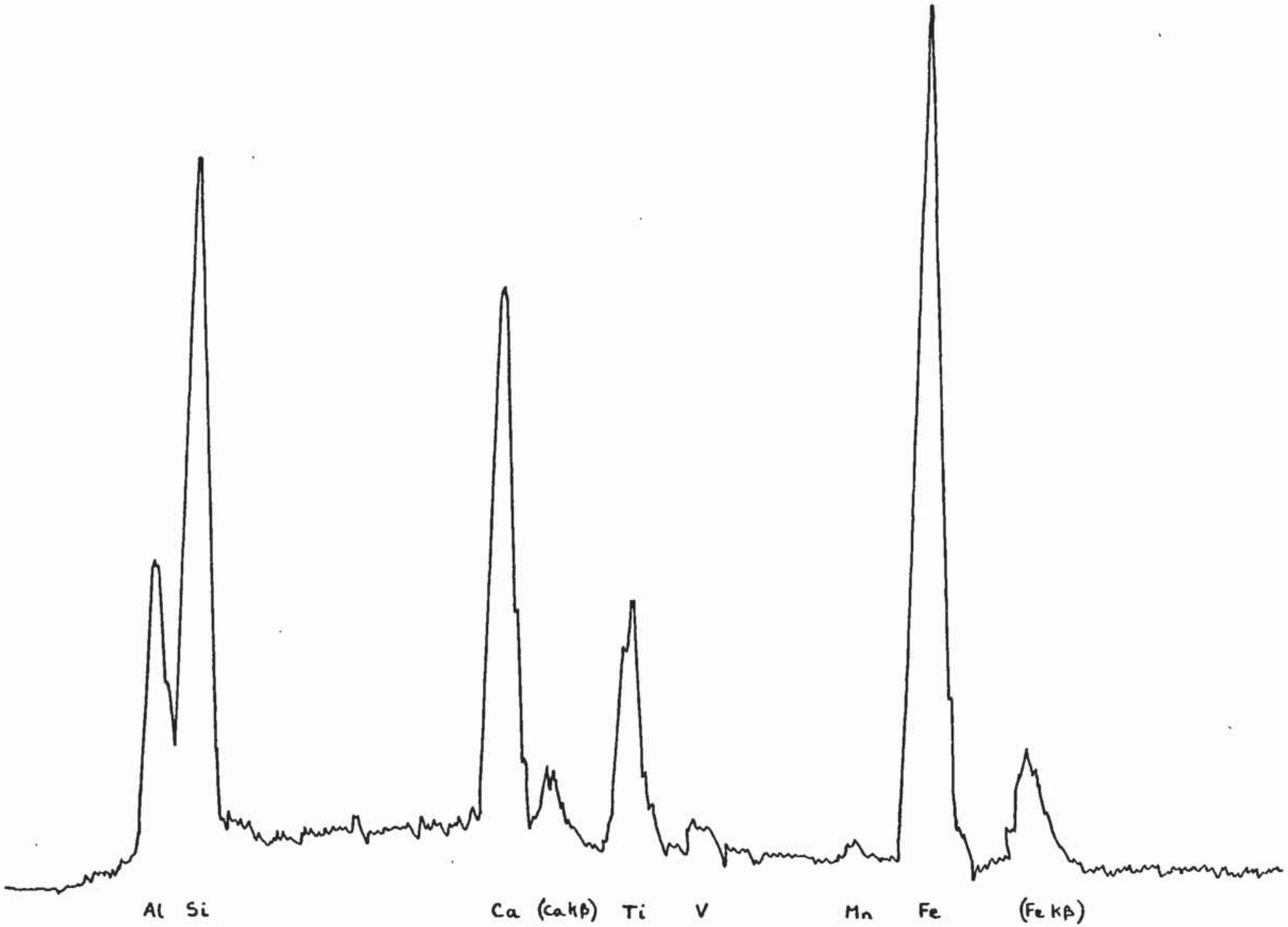
Al
Si
Ca
(Ca kβ)
Ti
V
Mn
Fe
(Fe kβ)

Figure 4.19(a) and (b)

SEM photographs of crystallites in RR1, (a) normal image, (b) backscattered electron image. In both cases pale grey phase is fayalite and glass is medium grey. In (b), the dark arc-like area is leucite.

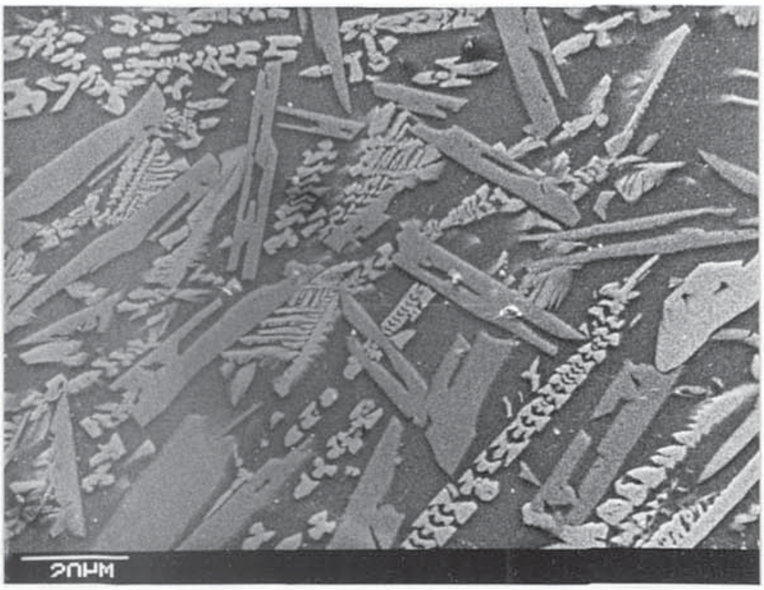
20µM

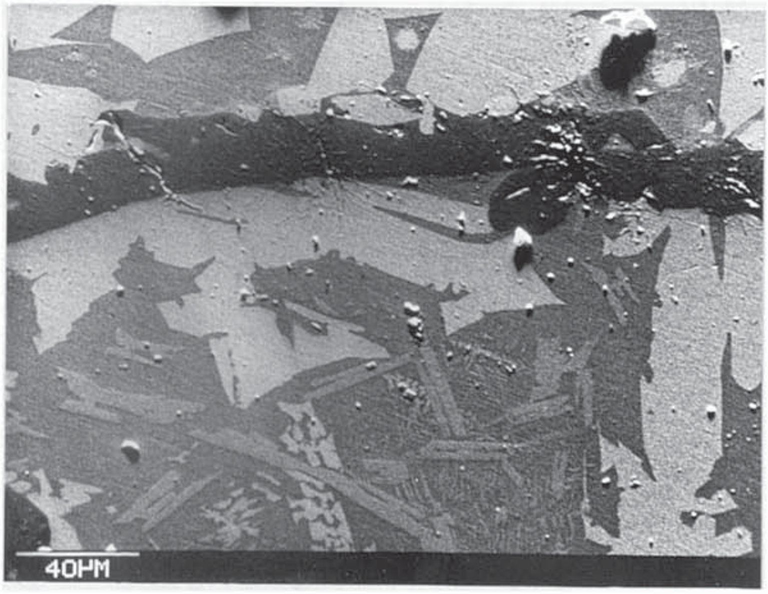
40µM

Figure 4.20

SEM photograph of GH 671 showing patch of leucite (dark grey) containing tiny crystals of a calcium phosphate phase (arrowed). Accompanying Kevex trace shows the phase's composition.

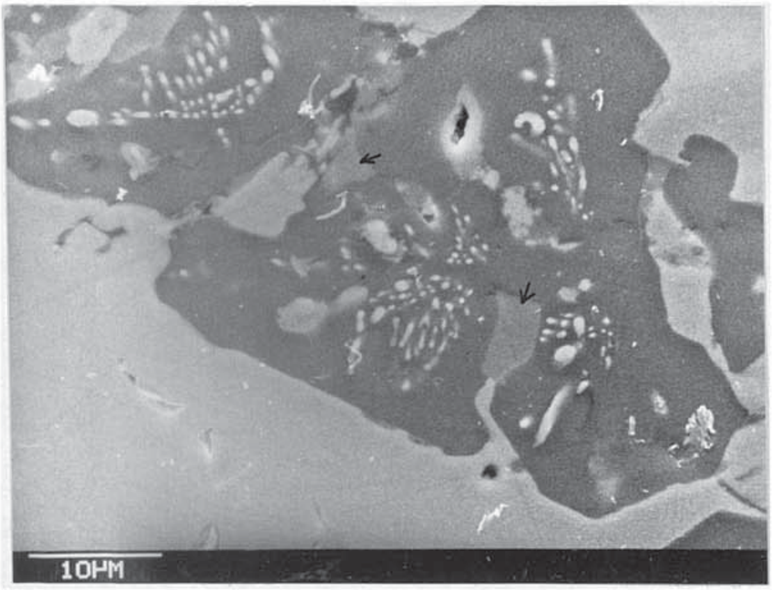
10µM

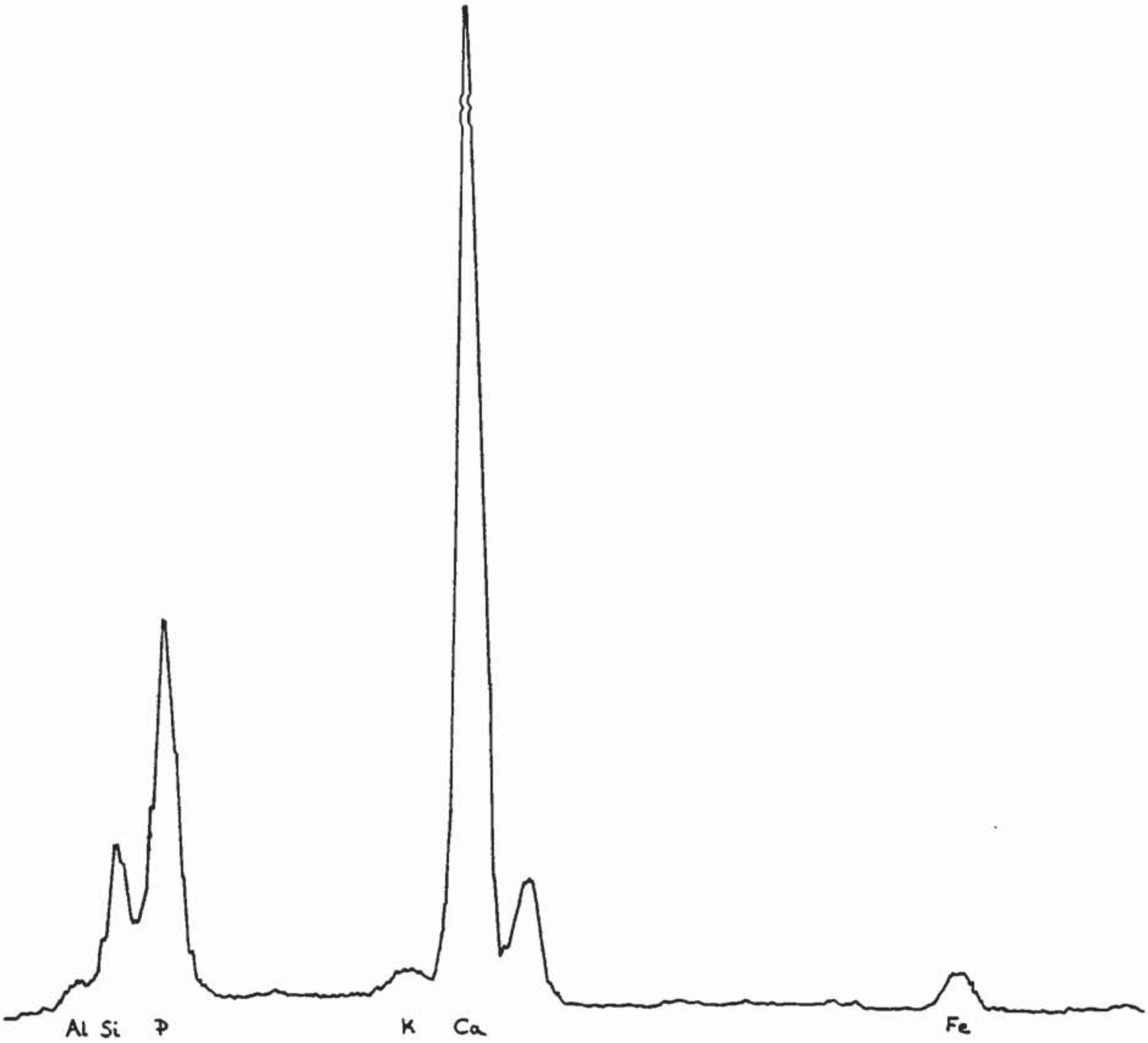
Al
Si
P
K
Ca
Fe

Figure 4.21

Slag WK-AV in reflected light showing metallic iron enclosing wüstite, indicating that the iron was molten when crystallization commenced.

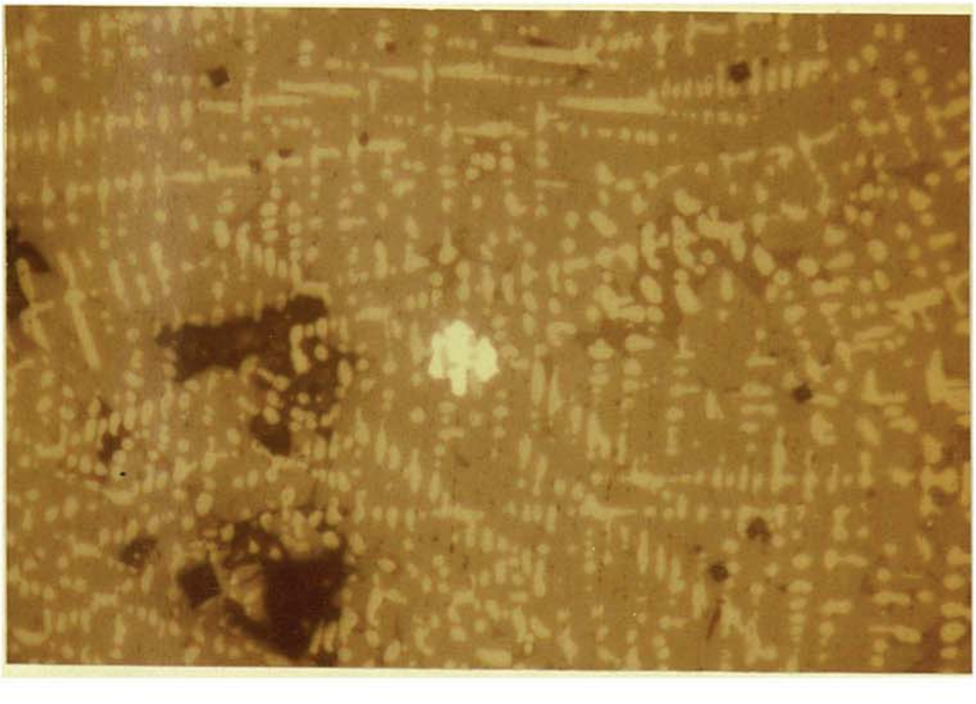

Figure 4.22

(a) Caerwent slag 697096 in transmitted light showing skeletal equant fayalite. Crossed polars. Field of view is 3.4 mm wide.

(b) Bowl furnace reconstruction slag RR2 in reflected light showing skeletal fayalite laths. Note also the tiny angular dendrites of magnetite. Field of view is 2.4 mm wide.

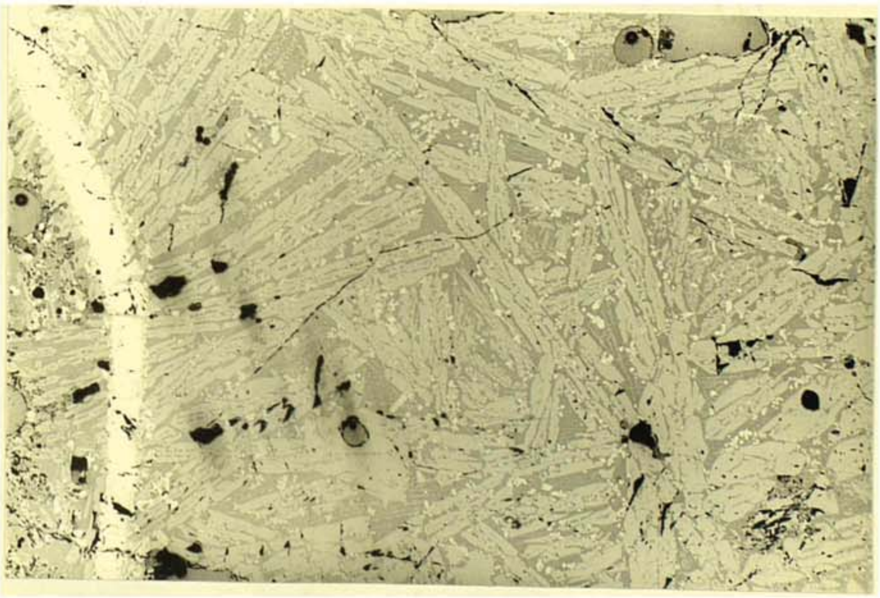

Figure 4.23

(a) Stamford slag 700128 in reflected light showing parallel oriented skeletal fayalite laths. Field of view is 1.2 mm wide.

(b) Bowl furnace reconstruction slag RR1 in reflected light showing large randomly oriented skeletal fayalite laths with smaller laths arranged parallel to them. Field of view is 3.9 mm wide.

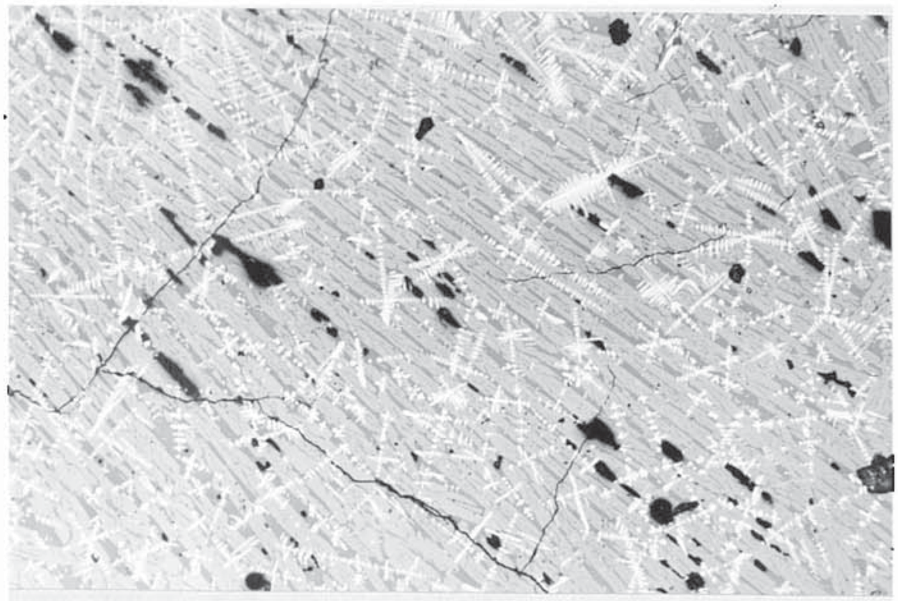

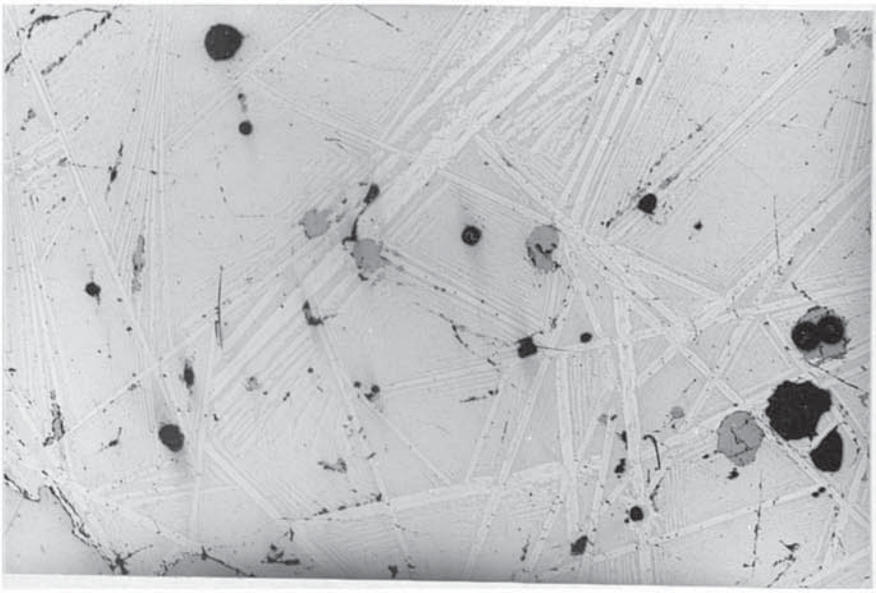

Figure 4.24

Great Oakley slag GO4 in reflected light showing massive fayalite. The distribution of the exsolved wüstite indicates the positions of the first-formed fayalite laths which subsequently grew widthways and coalesced. Field of view 1.125 mm wide.

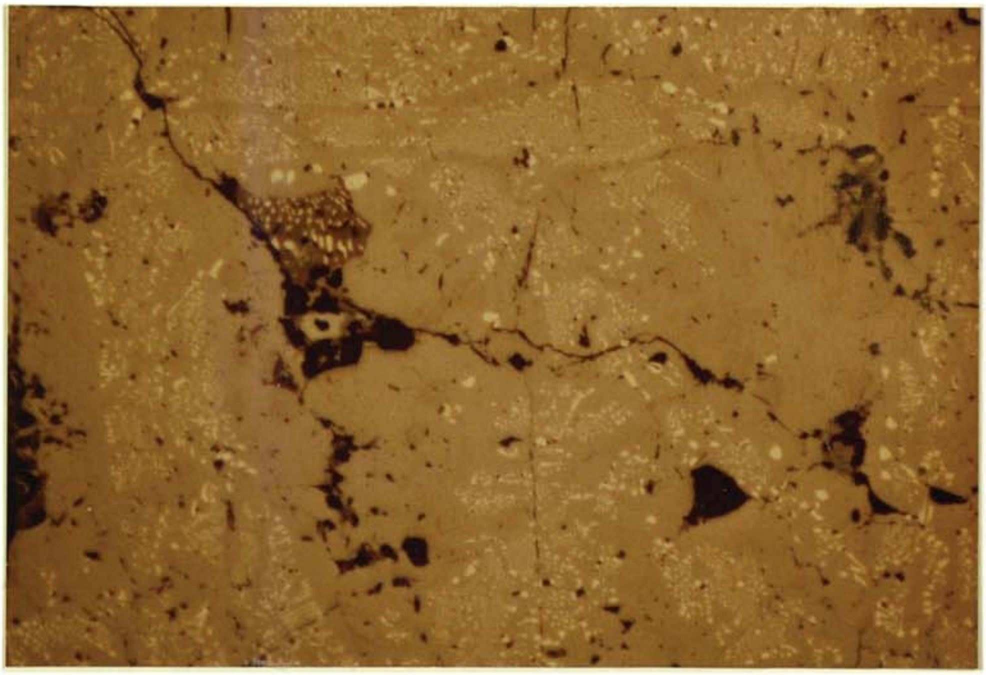

Figure 4.25

(a) Great Oakley slag GO3 in reflected light showing massive fayalite. Field of view is 2.22 mm wide.

(b) Same area in transmitted light illustrating anhedral nature of fayalite. Crossed polars. Field of view is 3.4 mm wide.

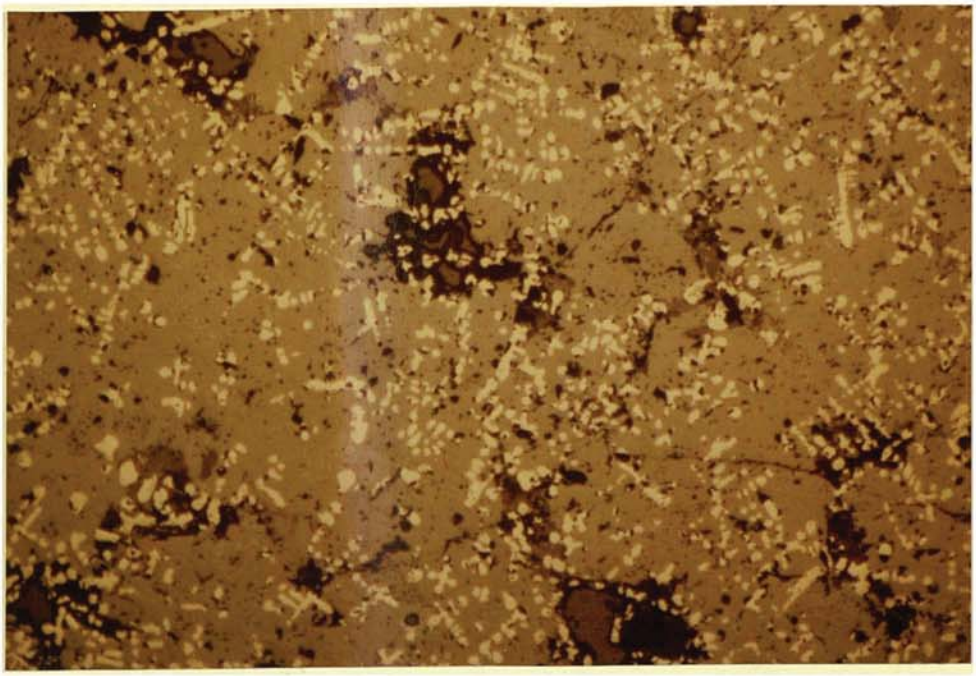

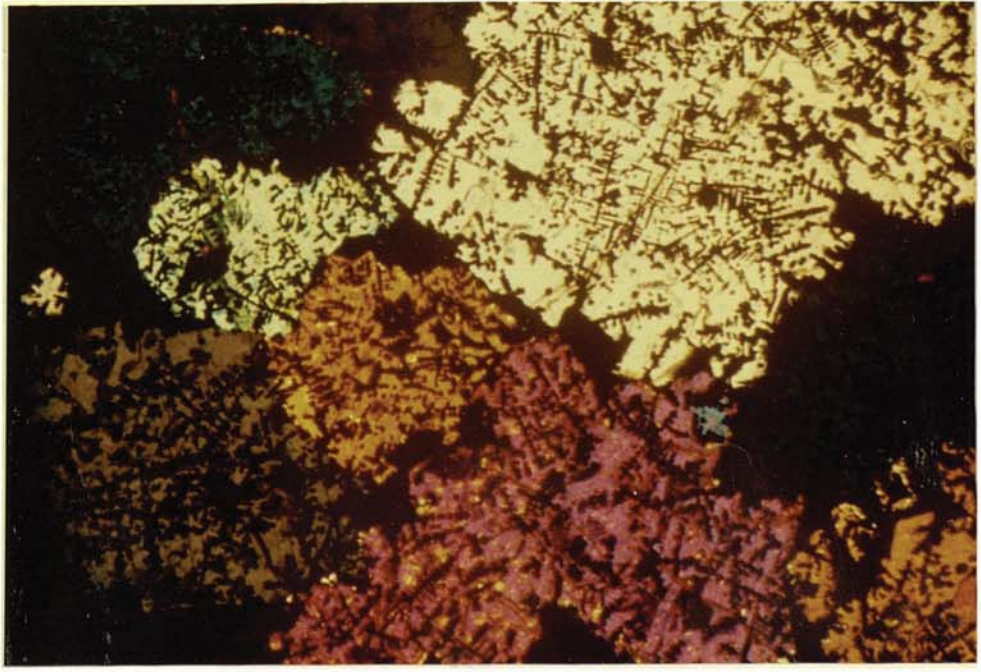

Figure 4.26

Garden Hill slag GH 653a in reflected light showing a typical texture with randomly oriented wüstite dendrites cross-cutting the fayalite, which here is in the form of skeletal laths. Field of view is 1.9 mm wide.

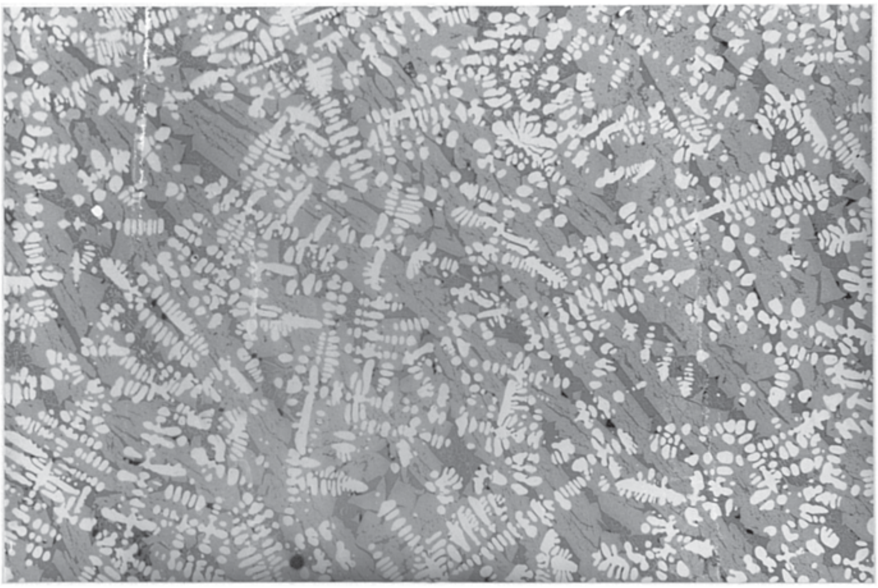

Figure 4.27

SEM photograph of slag from Santa Eulalia de Boveda, Spain, showing fayalite which neucleated on the first-formed wüstite dendrites and now surrounds them.

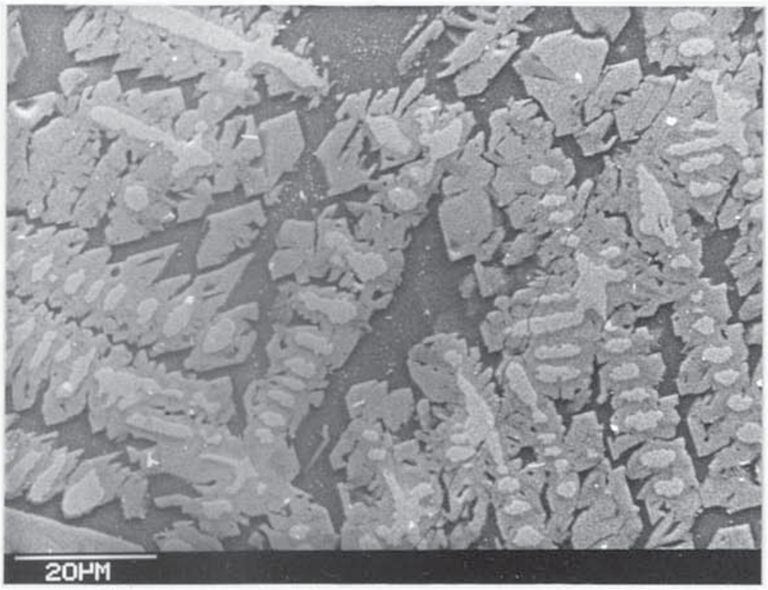
20µM

Figure 4.28

(a) Stamford slag 700130 in reflected light showing tiny angular dendrites of skeletal magnetite beneath a chilled surface (marked by densely-packed layer of wüstite globules), giving way to rounded dendrites of wüstite in lower third of photograph. Note also the larger compositionally zoned spinels and leucite (dark grey) in an unusual dendritic habit. Field of view is 3.1 mm high.

(b) Stamford slag 630532 in reflected light showing oxidation of wüstite layer at chilled surface to magnetite (white). Also present are wüstite and euhedral spinel (both pale grey), skeletal fayalite laths and glass (speckled). Field of view is 0.24 mm wide.

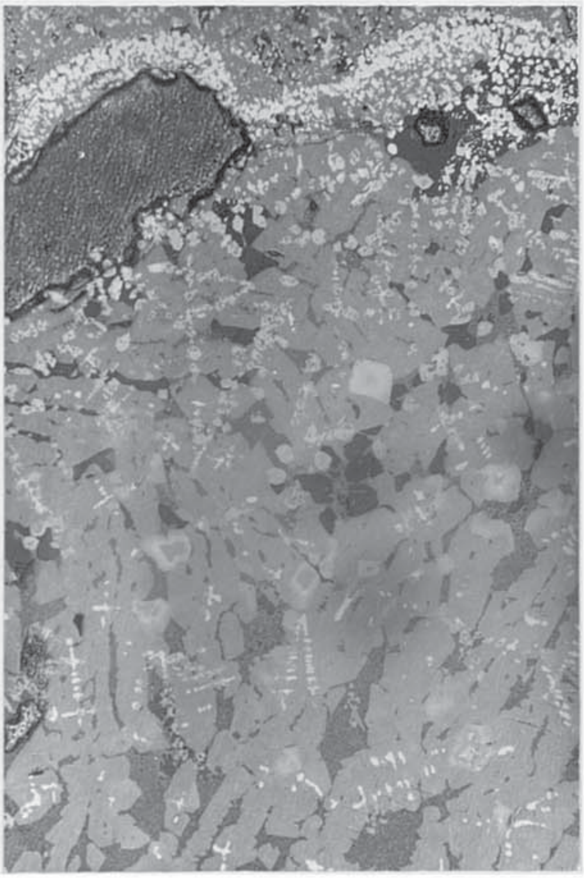

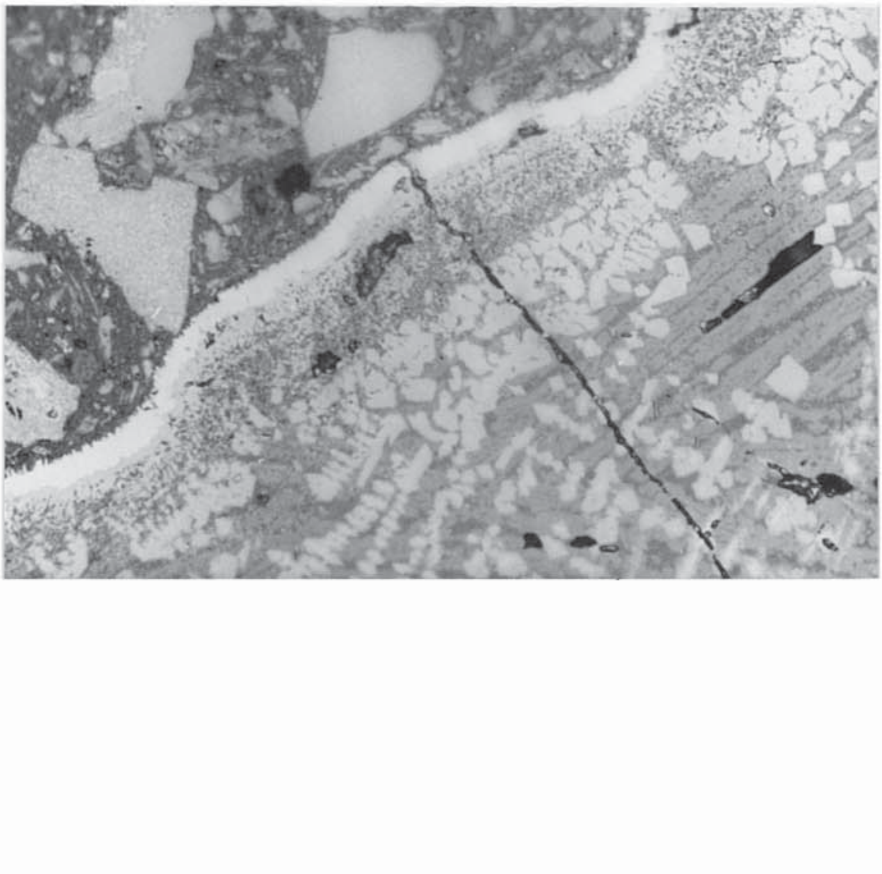

Figure 4.29

(a) SEM photograph of Wakerley slag WK K4 showing a tiny globule of wüstite with an area of magnetite (darker) at the top right.

(b) Different area of same slag showing magnetite 'veins' in the lobes of wüstite dendrites. Larger patches of magnetite also occur at the edges of the lobes and this is particularly clearly seen in the top right of the photograph.

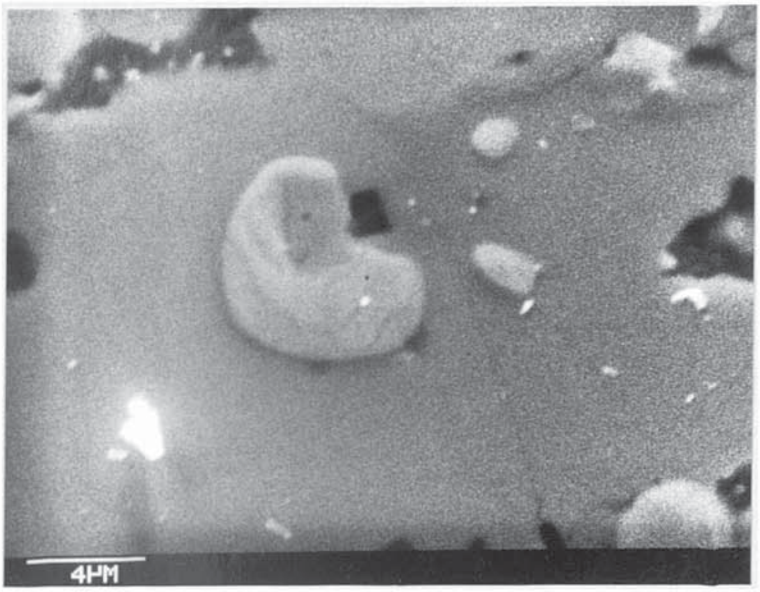
4µM

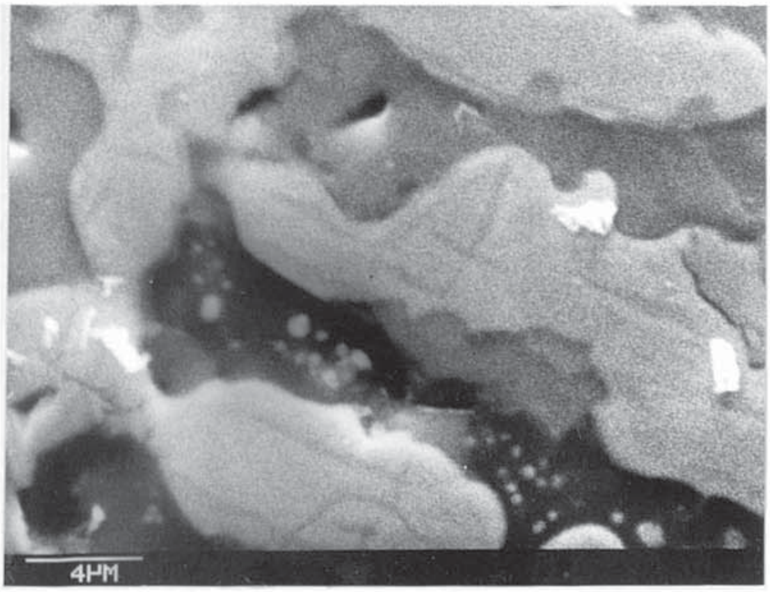
4µM

Figure 4.30

(a) SEM photograph of shaft furnace reconstruction slag GHR 4 showing skeletal magnetite.

(b) SEM photograph of bowl furnace reconstruction slag RR1 showing tiny euhedral cyrstals (cubic) of titaniferous magnetite.

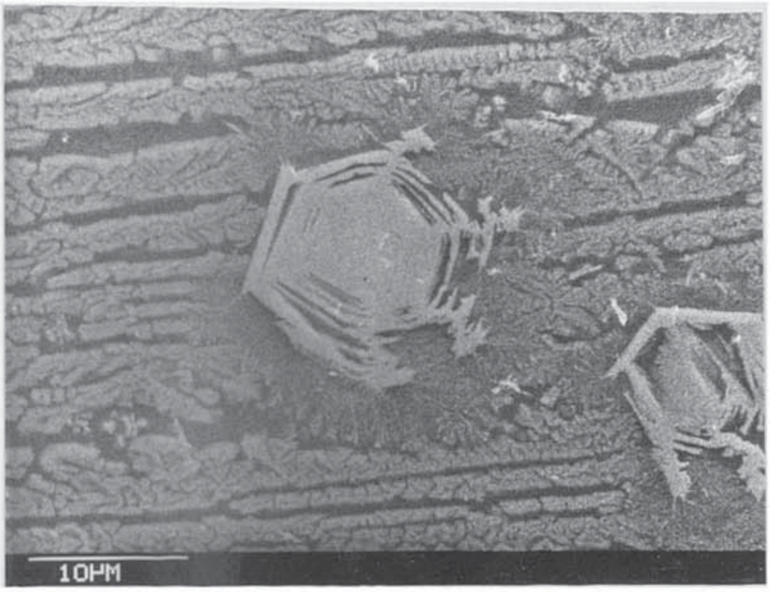
10µM

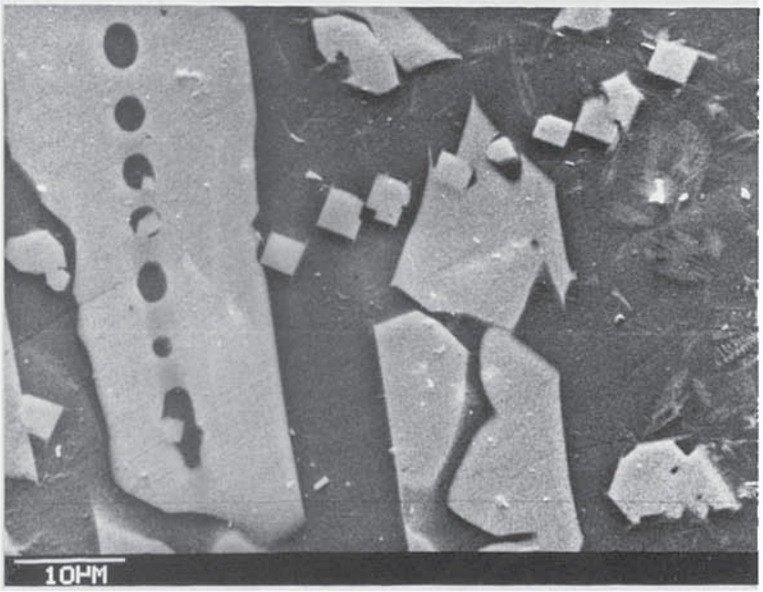
10µM

Figure 4.31

Stamford slag 700130 in reflected light showing skeletal fayalite laths with lobe-like projections consisting of fayalite/hercynite intergrowth (example arrowed). Field of view 7.5 mm wide.

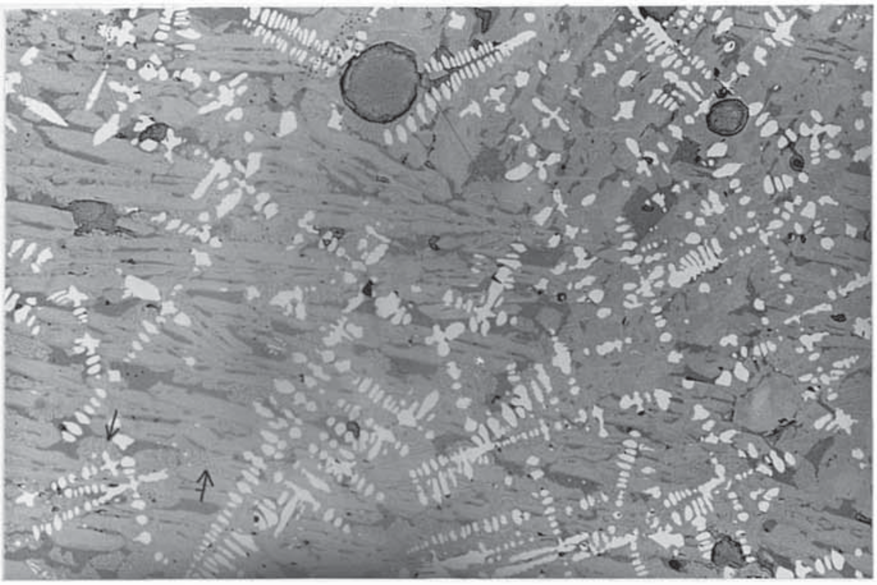

Figure 4.32

(a) Ramsbury slag RAM 5 in reflected light showing skeletal fayalite laths with rounded patches of leucite or leucite/fayalite intergrowths between. Leucite also fills the holes in the fayalite 'skeleton'. Some hercynite (paler grey, angular) is also present. Field of view is 0.24 mm wide.

(b) Ramsbury slag RAM 5 in reflected light showing areas between fayalite crystals occupied by large rounded patches of leucite, with abundant wüstite exsolution, and by fine leucite/fayalite intergrowths. Field of view is 0.37 mm wide.

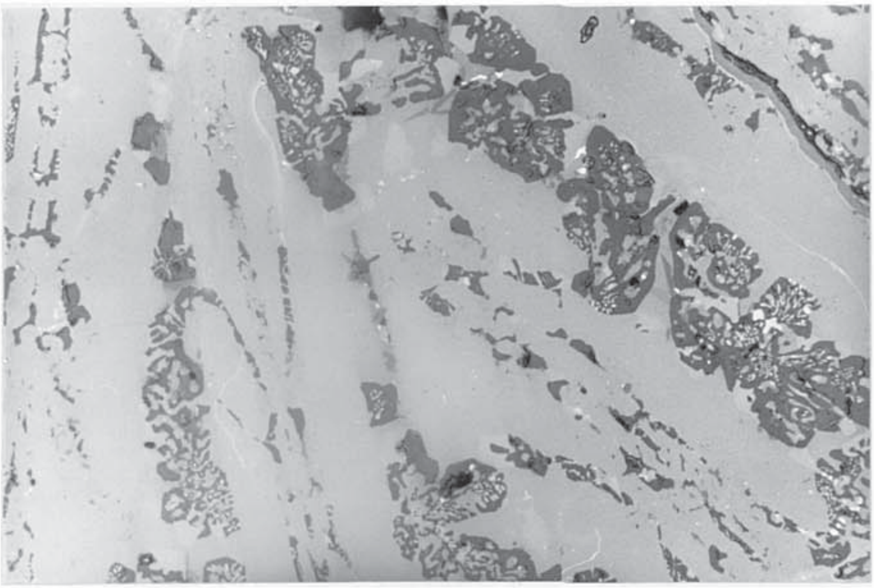

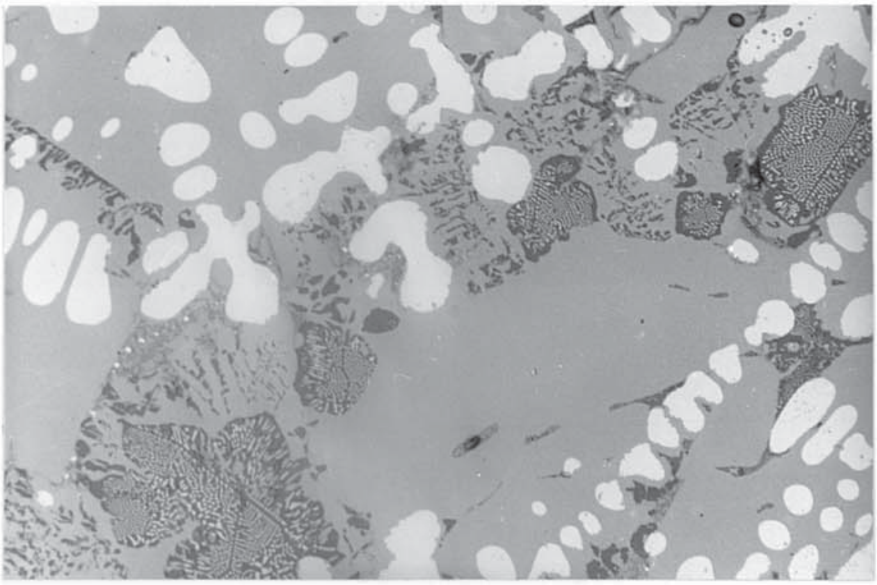

Figure 4.33

(a) Garden Hill slag GH 653b in reflected light showing rounded patches of leucite (dark grey) in glass, which here contains abundant fayalite cyrstallites. Field of view is 0.37 mm wide.

(b) SEM photograph of Garden Hill slag GH 671 showing leucite between fayalite laths. The concave edges of the fayalite crystals result from the interference during growth by the leucite, which must have been crystallizing at the same time.

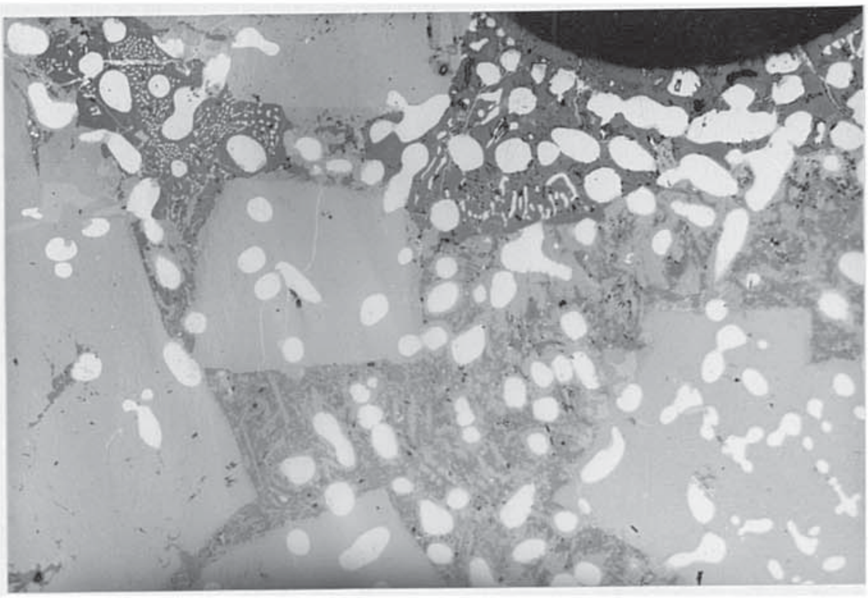

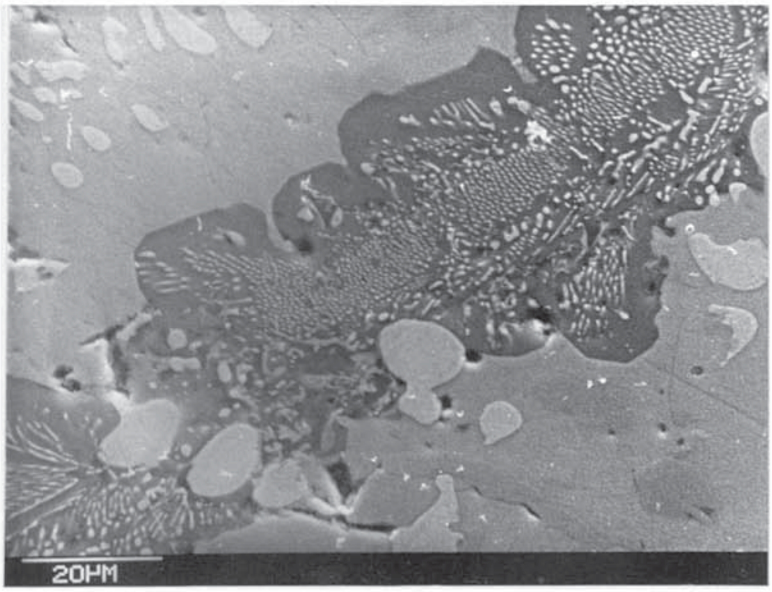
20µM

Figure 4.34

Ramsbury slag RAM 5 in reflected light showing transition from normal glass to interstitial leucite.

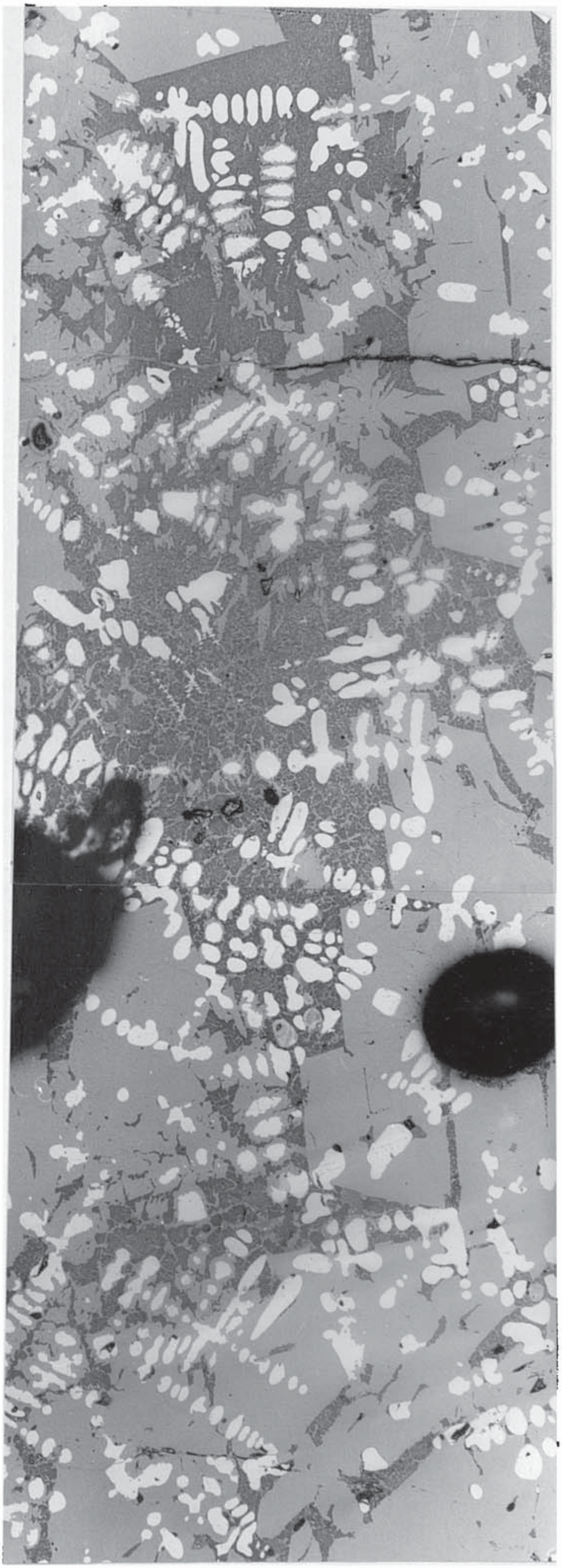

Figure 4.35

(a) Bowl furnace reconstruction slag RR2 in transmitted light showing primary leucite. Plane polarized light. Field of view is 0.57 mm wide.

(b) Leucite in a leucite tephroite from Vesuvius for comparison. Plane polarized light. Field of view is 2.2 mm wide.

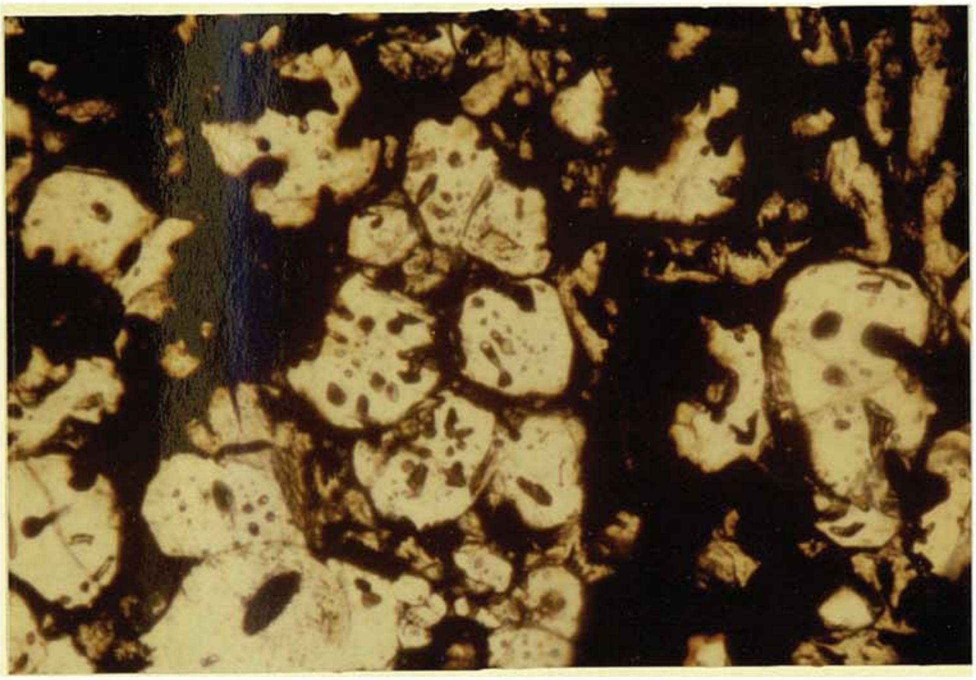

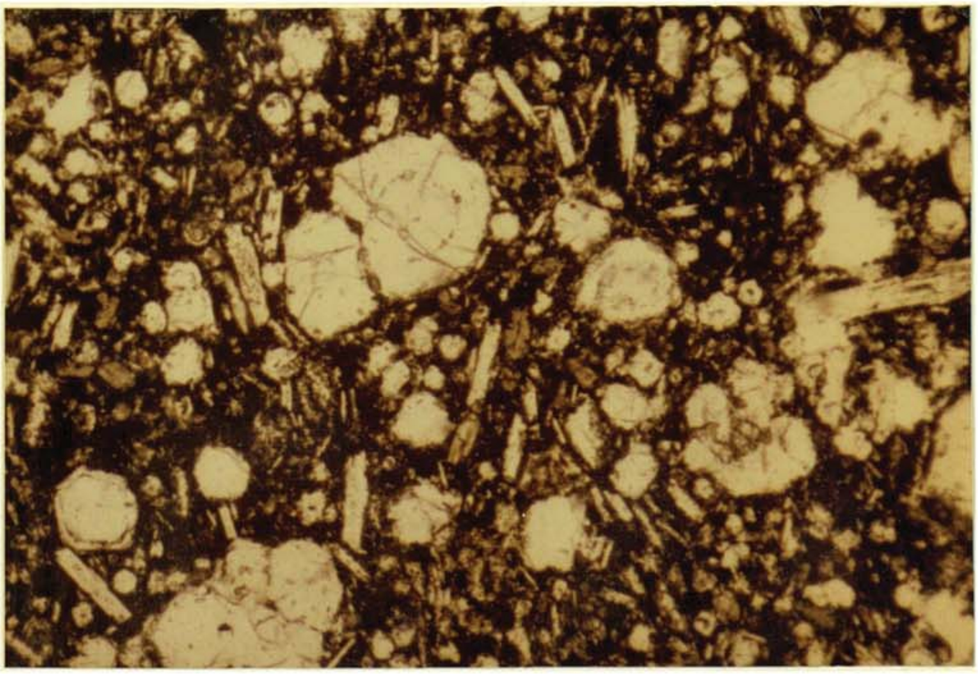

Figure 4.36

(a) Ramsbury slag RAM 5 in reflected light. The pore in the top right hand corner (filled with bake^lite) is rimmed by leucite. Note the absence of wüstite exsolution in the leucite immediately adjacent to the pore, and its abundance in the other patches of leucite. This photograph also illustrates the typical relationships of fayalite, leucite and glass. Field of view is 1.2 mm wide.

(b) Bowl furnace reconstruction slag RR2 in reflected light. Here the leucite is in the form of an arc within slag showing otherwise 'normal' texture. Note also the euhedral crystal of leucite in the top left, with a zone of ?glassy inclusions. Fayalite laths (pale grey) are set in glass containing some crystallites of a phase rich in calcium (slightly darker than fayalite) and a few grains of skeletal magnetite are also visible in the bottom right. Field of view is 0.60 mm wide.

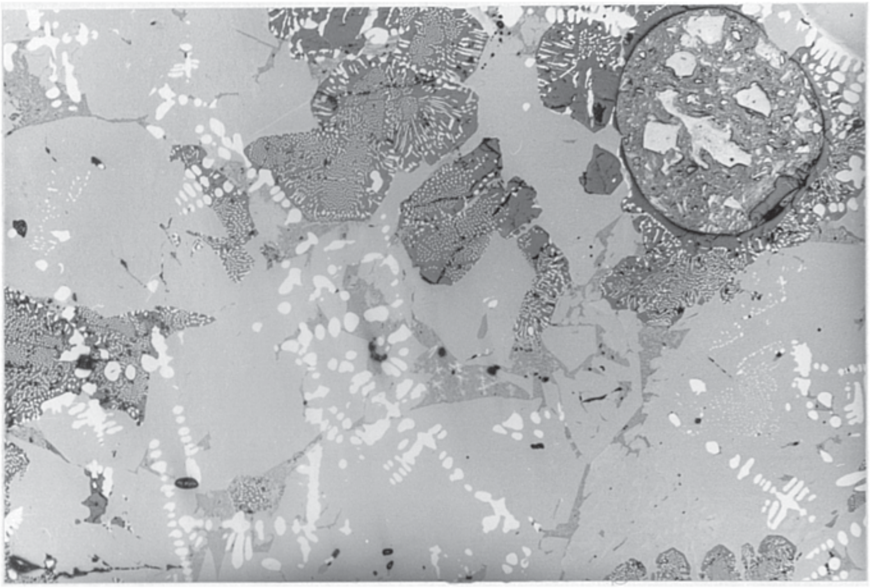

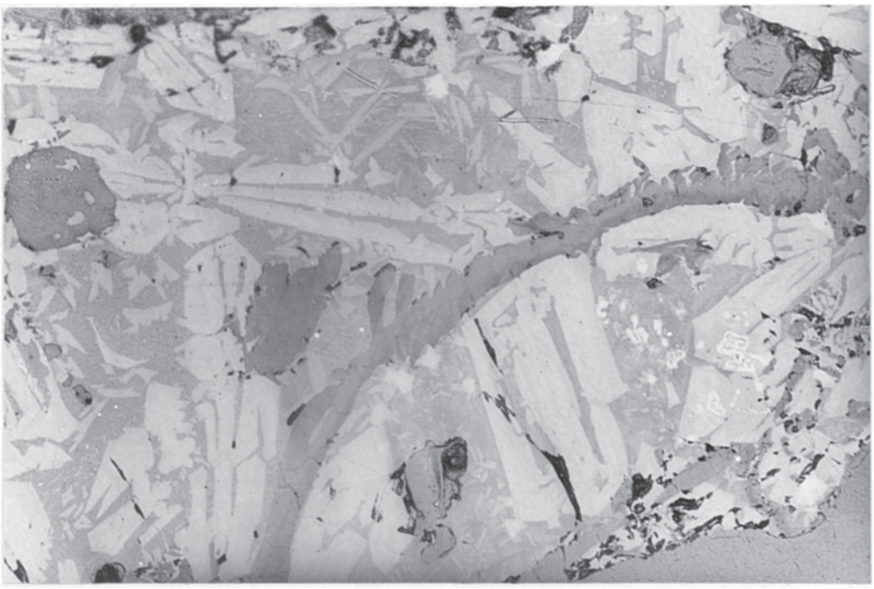

Figure 4.37

Stamford slag 700130 in transmitted light showing bundles of long fayalite laths radiating down from a chilled surface, with short laths (in the next 'flow') radiating upwards from it. Crossed polars; the section is rather thin and the interference colours are therefore of a lower order than they should be. Field of view is 3.4 mm wide.

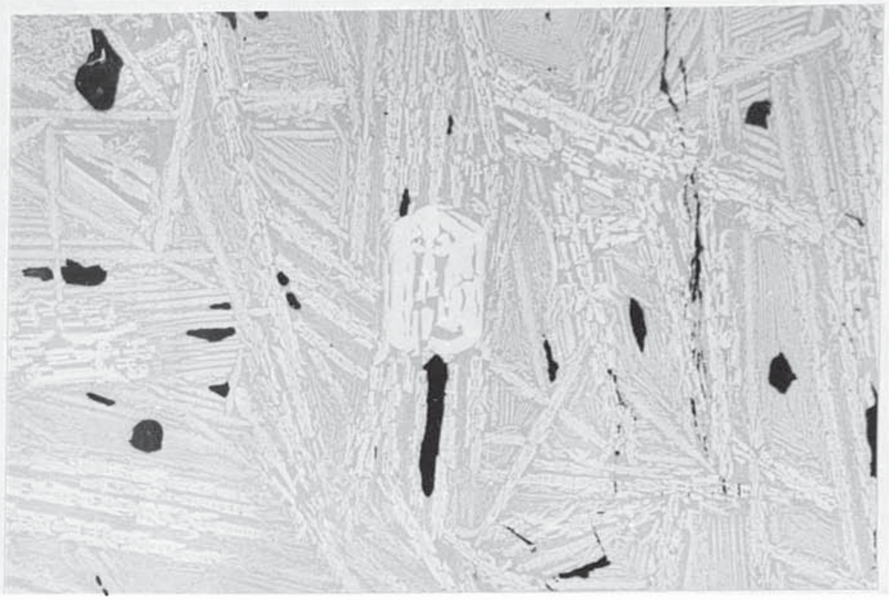

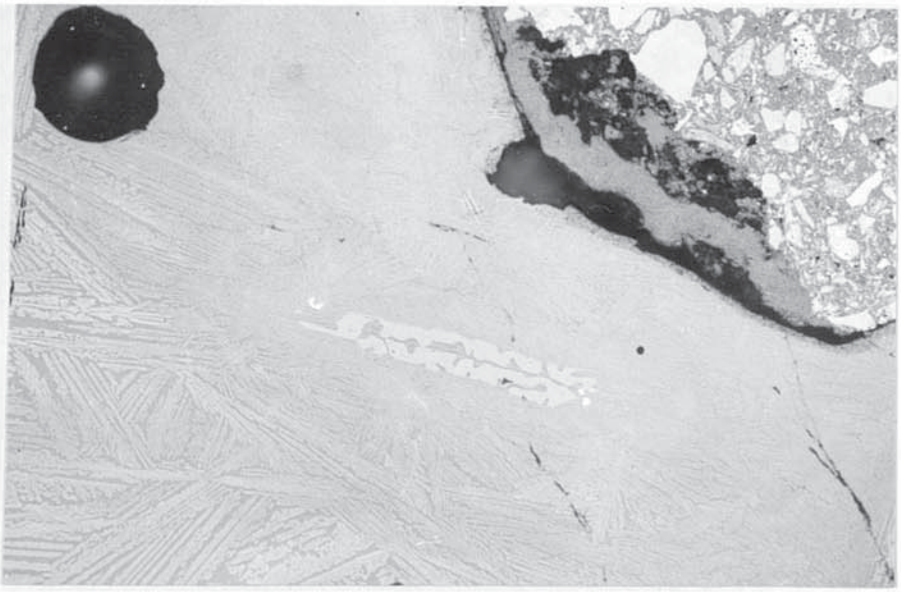

Figure 4.39(a) and (b)

Great Oakley slag GO3 showing euhedral fayalite crystal with concentric zones of hercynite inclusions. In the outer part of the crystal a little wüstite accompanies the hercynite. Contrast this with the fayalite/hercynite intergrowth at the bottom left. (a) Transmitted light, crossed polars. (b) Reflected light. Crystal is 0. mm long.

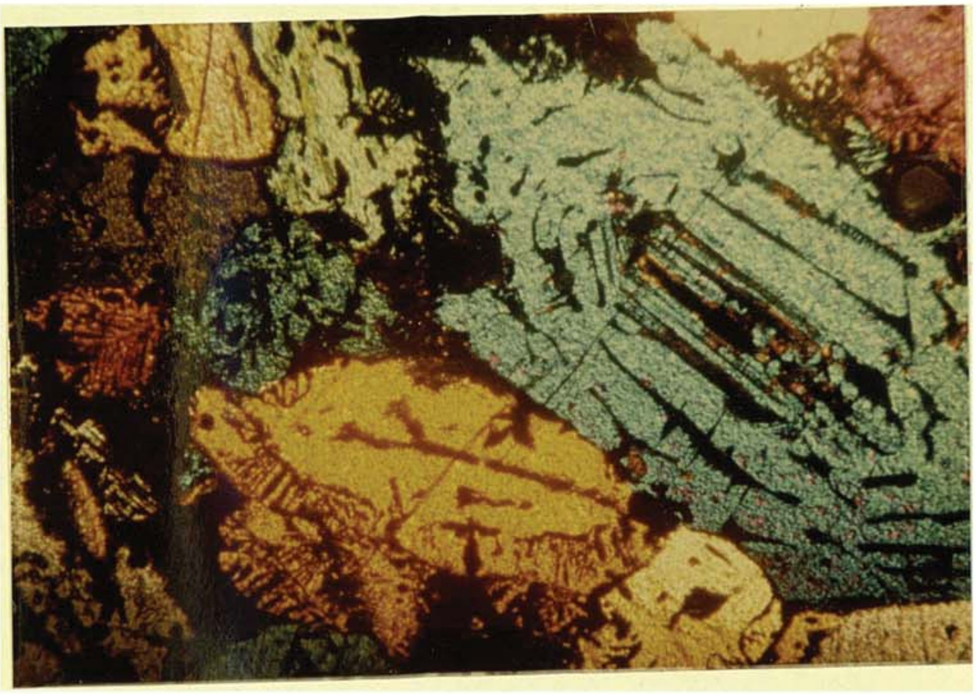

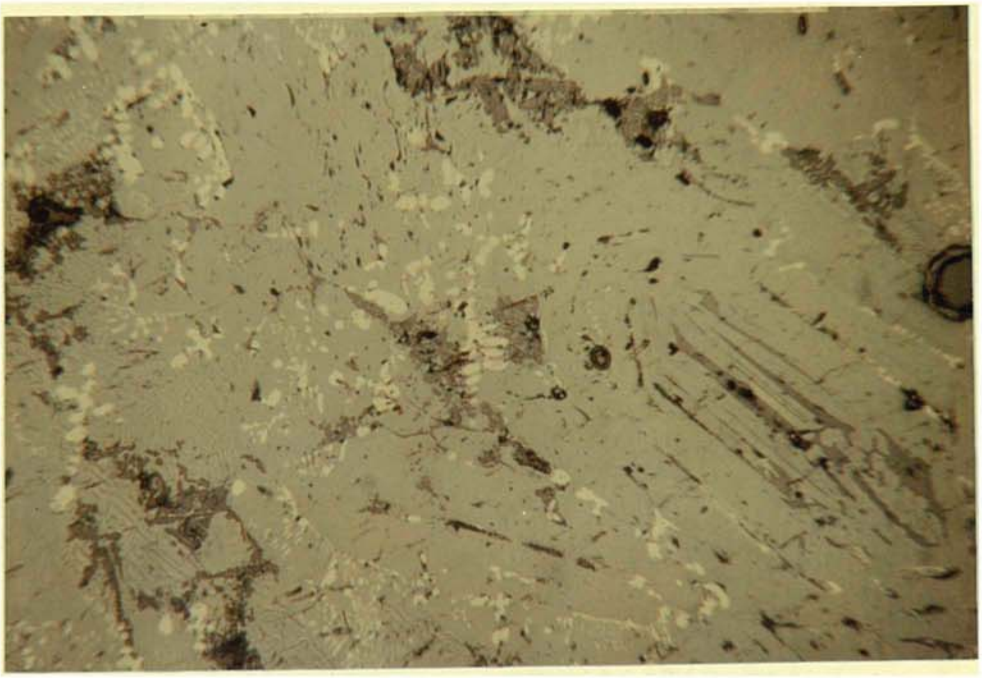

Table 5.1

Mean ($\bar{x}$), standard deviation ( ), and coefficient of variation (c.v.)* of oxide ratios for the three main ironstones investigated

Ratio		Ironstone Junction-Band	Northampton Sand Ironstone		Wadhurst Clay Ironstone	
		(No. of samples = 17)	(No. of samples = 9)	(No. of samples = 15)	(No. of samples = 6)	(No. of samples = 10)
$\frac{Al_2O_3}{MnO}$	$\bar{x}$	24.5	35.7	37.3	1.5	3.1
		60.1	8.3	15.7	0.21	3.6
	c.v.	245%	23%	42%	14%	117%
$\frac{Al_2O_3}{TiO_2}$	$\bar{x}$	13.6	21.5	22.6	9.39	15.1
		7.6	1.4	7.3	0.58	13.0
	c.v.	56%	7%	32%	6%	86%
$\frac{Al_2O_3}{V_2O_5}$	$\bar{x}$	75.1	46.2	59.2	134	
		27.8	2.5	25.5	36.9	No data
	c.v.	73%	5%	43%	28%	
$\frac{MnO}{TiO_2}$	$\bar{x}$	4.1	0.63	0.91	6.4	6.5
		5.0	0.15	0.95	1.04	2.2
	c.v.	122%	24%	104%	16%	34%
$\frac{MnO}{V_2O_5}$	$\bar{x}$	16.9	1.35	2.26	87.9	
		16.4	0.29	2.48	25.4	No data
	c.v.	97%	22%	110%	29%	
$\frac{TiO_2}{V_2O_5}$	$\bar{x}$	6.7	2.2	2.4	14.4	
		4.3	0.20	0.81	4.49	No data
	c.v.	64%	9%	34%	31%	
$\frac{Al_2O_3}{MgO}$	$\bar{x}$	40.7	7.9	6.4	5.89	9.1
		47.0	9.9	7.8	2.94	9.8
	c.v.	116%	125%	122%	50%	108%
$\frac{MnO}{MgO}$	$\bar{x}$	5.0	0.23	0.24	3.32	2.7
		3.2	0.26	0.30	2.25	1.92
	c.v.	64%	113%	125%	68%	70%
$\frac{MgO}{TiO_2}$	$\bar{x}$	0.78	6.2	7.4	3.18	4.0
		0.37	4.1	5.0	3.43	3.8
	c.v.	94%	66%	68%	108%	94%
$\frac{MgO}{V_2O_5}$	$\bar{x}$	3.24	13.8	16.8	37.4	
		2.01	9.7	9.8	23.5	No data
	c.v.	62%	70%	58%	63%	

* coefficient of variation, c.v. = $\frac{\ }{\bar{x}}$ x 100%

Table 5.2

Results of discriminant analysis performed on material from Northamptonshire

The three groups were defined using only those ironstone samples collected at outcrop; supposed ore fragments from archaeological sites were included with the slags as unknowns to be identified

'Unknown'	Probability of belonging to Ironstone Junction-Band Group	Probability of belonging to Northampton Sand Ironstone Group	Probability of belonging to Boulder Clay nodule group
G06: ironstone fragments, Great Oakley	0.893	0.000	0.107
WAK 01: roasted ?ore fragment, Wakerley	1.000	0.000	0.000
WAK: roasted ?ore fragment, Wakerley	1.000	0.000	0.000
STAM roasted: ?ore, Stamford	0.601	0.083	0.316
STAM raw: ?ore, Stamford	0.308	0.535	0.157
WK/AV: furnace slag, Wakerley	0.606	0.001	0.393
WK K(4): furnace slag, Wakerley	0.975	0.000	0.025
WAK 48A: furnace slag, Wakerley	0.734	0.000	0.266
WGW: tap slag, Wakerley Great Wood	0.976	0.000	0.024
G04: furnace slag, Great Oakley	0.553	0.003	0.445
G07: furnace slag (bulk) Great Oakley	0.750	0.001	0.249
BEQ1: tap slag, Blind Eye Quarry	1.000	0.000	0.000
BEQ2: tap slag, Blind Eye Quarry	1.000	0.000	0.000
Brigstock: furnace slag, Brigstock	0.035	0.957	0.009
STAM 700130: tap slag, Stamford	0.098	0.844	0.059
STAM 630532: tap slag, Stamford	0.397	0.086	0.517
Bulwick: tap slag, near Bulwick	0.960	0.000	0.040
S. Witham: tap slag, South Witham	0.005	0.995	0.000

Table 5.3

Application of multiple regression equations to slags from Berkhamsted, Caerwent and Blind Eye Quarry

	Fe_2O_3*	SiO_2	Al_2O_3	MnO	MgO	TiO_2	V_2O_5
Berkhamsted slag (bulk)	74.6	26.4	3.32	1.14	0.25	0.15	0.03
Predicted roasted ore			12.5	1.1	0.0	0.02	0.12
			±0.9	±1.4	±1.1	±0.20	±0.01
Ironstone, L. Greensand nr Leighton Buzzard (after ignition)			1.41	0.11	0.17	0.11	0.06
			1.76	0.18	0.09	0.06	0.06
Marcasite nodules, excavated with slag (after ignition)			0.22	0.01	0.04	0.00	0.02
Caerwent slag	83.9	16.5	2.46	0.15	0.50	0.15	0.02
Predicted roasted ore			-8.1	0.0	0.3	0.02	0.03
			±0.9	±1.4	±1.1	±0.20	±0.01
Forest of Dean			1.64	0.09	3.71	0.06	-
hematite (from Groves)			2.74	0.11	4.00	0.08	-
calculated as roasted			0.95	0.06	0.36	0.06	-
Bristol district hematite			1.84	0.14	0.33	0.00	-
(from Groves)			0.76	0.03	0.24	0.01	-
Blind Eye Quarry slag	75.6	23.5	4.10	0.59	0.19	0.42	0.04
Predicted roasted ore			4.4	0.5	-0.1	0.25	0.07
			±0.9	±1.4	±1.1	±0.20	±0.01
Ironstone Junction-Band, Clipsham (average of rich and poor nodules, all calculated as roasted)			4.79	1.24	0.18	0.36	0.05
Northampton Sand Ironstone, Stamford (average, calculated as roasted)			4.32	0.31	0.18	0.24	0.09

* all iron calculated as Fe_2O_3

Table 5.4

Means and standard deviations of oxides in the Ironstone Junction-Band and Northampton Sand Ironstone

IRONSTONE JUNCTION-BAND		Fe_2O_3	SiO_2	Al_2O_3	CuO	MnO	MgO	TiO_2	V_2O_5	P_2O_5	K_2O
1. Ketton Quarry (4 samples)											
Mean,	$\bar{x}$	74.6	7.5	3.01	2.55	0.38	0.16	0.13	0.05	0.06	0.08
Std dev.,	σ	13.3	8.3	3.13	3.04	0.27	0.03	0.08	0.03	0.03	0.05
2. Wakerley Great Wood (4 samples)											
	$\bar{x}$	69.28	14.0	4.14	0.84	0.29	0.08	0.39	0.07	0.04	0.13
	σ	8.8	11.4	1.80	1.33	0.25	0.03	0.22	0.02	0.02	0.05
3. Average: represents 10 localities (17 samples)											
	$\bar{x}$	71.2	12.5	3.28	1.23	0.55	0.12	0.27	0.04	0.05	0.13
	σ	11.8	11.5	1.95	1.99	0.44	0.06	0.18	0.02	0.02	0.12
NORTHAMPTON SAND IRONSTONE											
1. Brookfield Cottage Pit (8 samples)											
	$\bar{x}$	54.0	9.8	6.38	3.94	0.17	1.87	0.30	0.14	1.41	0.39
	σ	5.6	1.9	1.62	1.85	0.03	1.02	0.06	0.03	0.42	0.07
2. Stanion Lane Pit* (5 samples)											
	$\bar{x}$	51.9	11.9	5.40	7.64	0.22	1.75	0.19	0.09	1.23	0.04[1]
	σ	12.3	5.3	1.59	6.31	0.17	1.24	0.05	0.04	0.56	0.02
3. Average[2]: represents 4 localities (15 samples)											
	$\bar{x}$	53.6	10.3	5.9	5.7	0.19	1.71	0.25	0.11	1.42	0.24
	σ	9.3	3.4	1.5	4.6	0.10	1.05	0.07	0.04	0.45	0.18

* From Riley[11]

1 Includes Na_2O

2 Includes analyses published by Riley[11]

Table 5.5

Weathering effect on Northampton Sand Ironstone and Wadhurst Clay Ironstone

The analyses have been recalculated to eliminate the effect of variable volatiles content, i.e. loss on ignition subtracted and oxides rounded up to 100%

	Fe_2O_3	SiO_2	Al_2O_3	CaO	MnO	MgO	TiO_2	V_2O_5	P_2O_5	K_2O
Raw NSI (boxwall only), Stamford excavation	80.0	11.9	4.14	1.00	0.23	0.17	0.23	0.09	1.76	0.50
Roasted NSI (mainly boxwall, some core), Stamford excavation	73.5	18.6	4.50	0.78	0.38	0.18	0.24	0.08	1.07	0.66
Raw NSI (boxwall, BC8) Brookfield Cottage Pit	69.3	15.2	10.42	0.95	0.23	0.32	0.45	0.23	2.37	0.60
Raw NSI (core, BC8) Brookfield Cottage Pit	66.8	13.2	10.2	3.36	0.28	1.74	0.45	0.20	2.61	0.59
Raw NSI (boxwall, BC6) Brookfield Cottage Pit	75.2	9.1	5.86	6.28	0.18	0.85	0.27	0.13	1.67	0.44
Raw NSI (core, BC6) Brookfield Cottage Pit	72.1	9.5	6.54	6.42	0.21	2.73	0.29	0.14	1.62	0.43
Raw WCI (boxwall, GHR3), W. Hoathly Pit	73.7	18.2	4.45	0.46	2.83	0.38	0.45	0.03	1.02	0.71
Raw WCI (core, GHR3) W. Hoathly Pit	62.2	20.6	5.15	3.71	3.73	1.34	0.59	0.03	0.90	0.83

Table 5.6

Compositions of charcoal and wood ash (wt % oxide)*

	Oak (Q. robur)	Elm (*Ulmus campestris*)		Wild Cherry (*Cerasus avium*)		Beech (*Fagus sylvatica*)	Pine (*Pinus sylvestris*)	Larch (Larix europoea)	Beech[1] (*Fagus sp.*)
	wood	wood	bark	wood	bark	wood	wood	wood)	charcoal
K_2O	8.43	21.92	2.2	25.90	7.94	15.80	2.79	15.24	22.0^2
Na_2O	5.65	13.72	10.09	10.47	15.83	2.87	16.77	7.76	
CaO	75.45	47.80	72.70	35.78	44.67	63.58	31.72	27.05	24.96
MgO	4.49	7.71	3.19	11.47	5.43	11.28	19.76	24.50	7.64
Fe_2O_3	0.57	0.77	0.54	0.07	0.21	0.84	2.70	2.83	tr
Mn_3O_4	-	-	-	-	-	-	18.17	13.51	31.62^3
P_2O_5	3.46	3.59	3.59	9.63	3.47	2.28	2.40	2.82	4.85
SiO_2	0.78	3.07	3.07	2.57	21.28	1.46	3.04	3.60	8.0
SO_3	0.95	1.05	1.05	3.36	0.70	1.35	1.95	1.71	-
Cl_2	0.01	-	-	-	0.20	0.07	0.45	0.28	-
	99.76	99.63	99.78	99.25	99.73	99.53	99.75	99.30	

* All analyses are reported in Percy, except the beech charcoal, which is from Tylecote.

1 Analysis includes Al_2O_3 0.92 wt % and a trace of TiO_2

2 Figure includes CO_2

3 Figure is MnO_2, not Mn_3O_4

It is interesting to note that MnO and dolomite, $(Ca,Mg)CO_3$, were apparently being mined close to where the pine and larch grew

Table 5.7

Contribution of charcoal ash to slag

(a) Contribution of ash from charcoal used in smelting. With the exception of the last column, figures are per kilogram of ore.

	Smelt	Ore Type	Slag Produced (kg)	Amount of charcoal used in smelting (kg)	Weight of ash (assuming charcoal contains 3% ash) (kg)	Ash weight as a percentage of slag weight
1.	Smelt 12*	W. Lothian siderite	0.30	2	0.06	20
2.	Smelt 14*	Northamptonshire Sand Ironstone	0.30	2	0.06	20
3.	Smelt 18	Northamptonshire Sand Ironstone	0.66	0.75	0.02	3
4.	Smelt 17	Northamptonshire Sand Ironstone	0.53	0.75	0.02	3.8
5.	Smelt 19	Northamptonshire Sand Ironstone	0.60	0.50	0.015	2.5
6.	Smelt 20	Northamptonshire Sand Ironstone	0.73	0.25	0.008	1.1
7.	Dimi	Limonite or magnetite	0.6[1]	0.22	0.007	1.2
8.	Chandghur	Unknown	0.6[1]	1.10	0.033	5.5
9.	Tendekura	Unknown	0.6[1]	1.09	0.033	5.5
10.	Catalan process	?Limonite	0.5[2]	1.12	0.034	6.8

(b) Contribution of ash from all charcoal consumed.

	Smelt	Ore Type	Total amount of slag produced (kg)	Total charcoal consumption (kg)	Weight of ash (assuming charcoal contains 3% ash) (kg)	Ash weight as a percentage of slag weight
1.	Smelt 12*	WLS	2.19	80	2.4	-
2.	Smelt 14*	NSI	2.19	92	2.76	-
3.	Smelt 18	NSI	14.98	80	2.4	16.0
4.	Smelt 17	NSI	14.42	74	2.2	15.3
5.	Smelt 19	NSI	16.32	37	1.11	6.8
6.	Smelt 20	NSI	10.59	33	0.99	8.5

Figures are from Tylecote et al. (1-6), Todd (7) and Percy (8-10)

* Cast iron produced

[1] Estimate based on Smelts 17, 19 and 20 of Tylecote et al.

[2] Estimate based on figures obtained by Richard and quoted by Percy

Figure 5.1(a)

Hedges and Salter's[23] graphical representation of their analytical data. The scale is logarithmic and each point represents a single inclusion. Inclusions from the three hoards are grouped in separate columns, in the order Danebury, Gretton, Beckford.

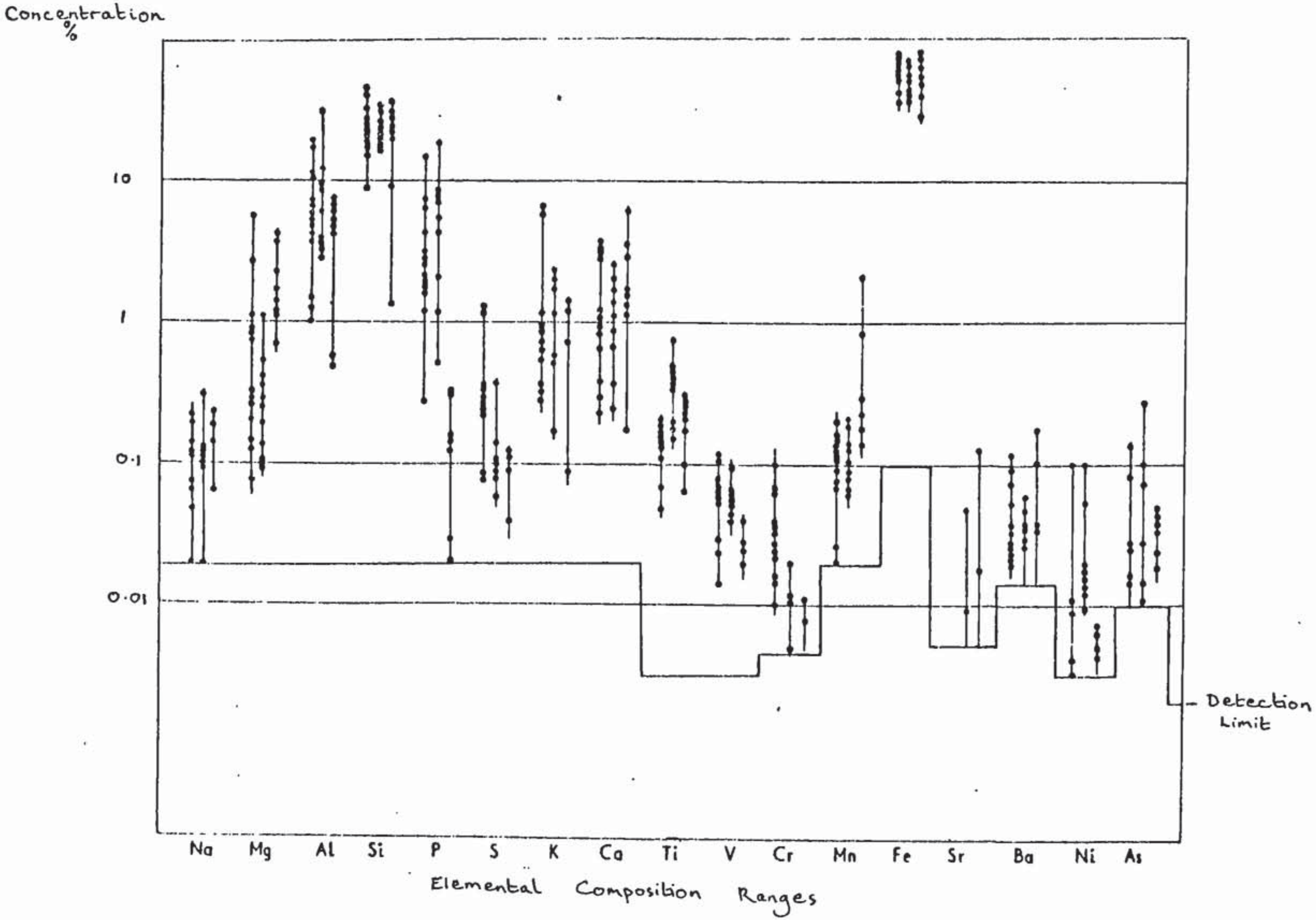
Concentration %
10
1
0·1
0·01
Na
Mg
Al
Si
P
S
K
Ca
Ti
V
Cr
Mn
Fe
Sr
Ba
Ni
As
Elemental Composition Ranges
Detection Limit

Figure 5.1(b)

Hedges and Salter's[23] representation of the results of the linear discriminant analysis performed on their data. The two axes are linear combinations of elemental concentrations selected from the set of 17 such orthogonal axes to display the maximum discrimination.

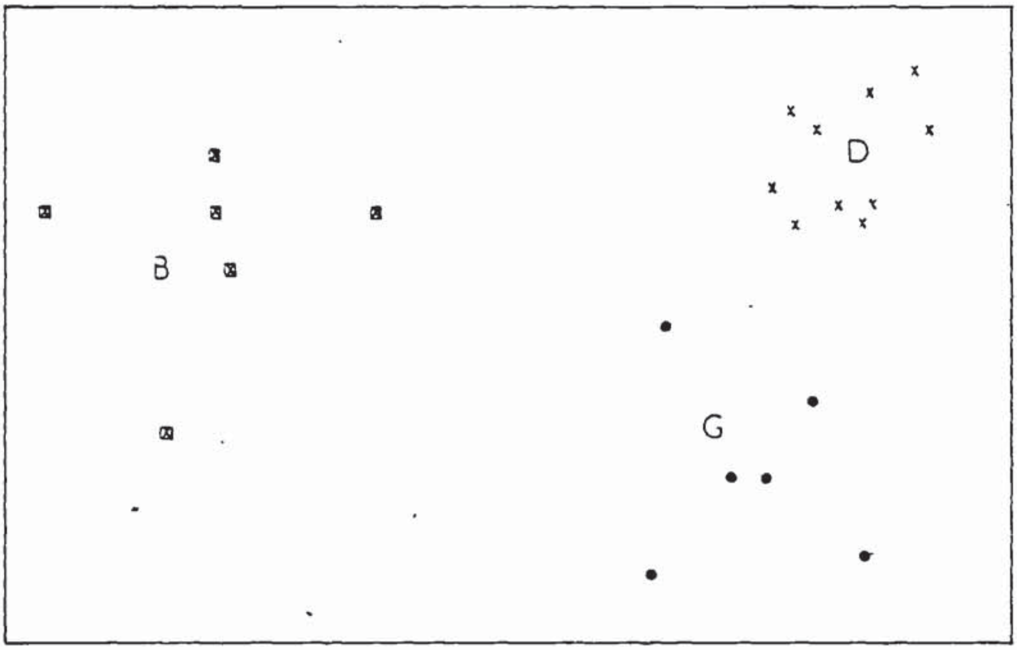
B
D
G

Figure 5.2

Plot of MnO vs Al_2O_3 for the ironstones and slags investigated. Fold-out key is located after Figure 5.12.

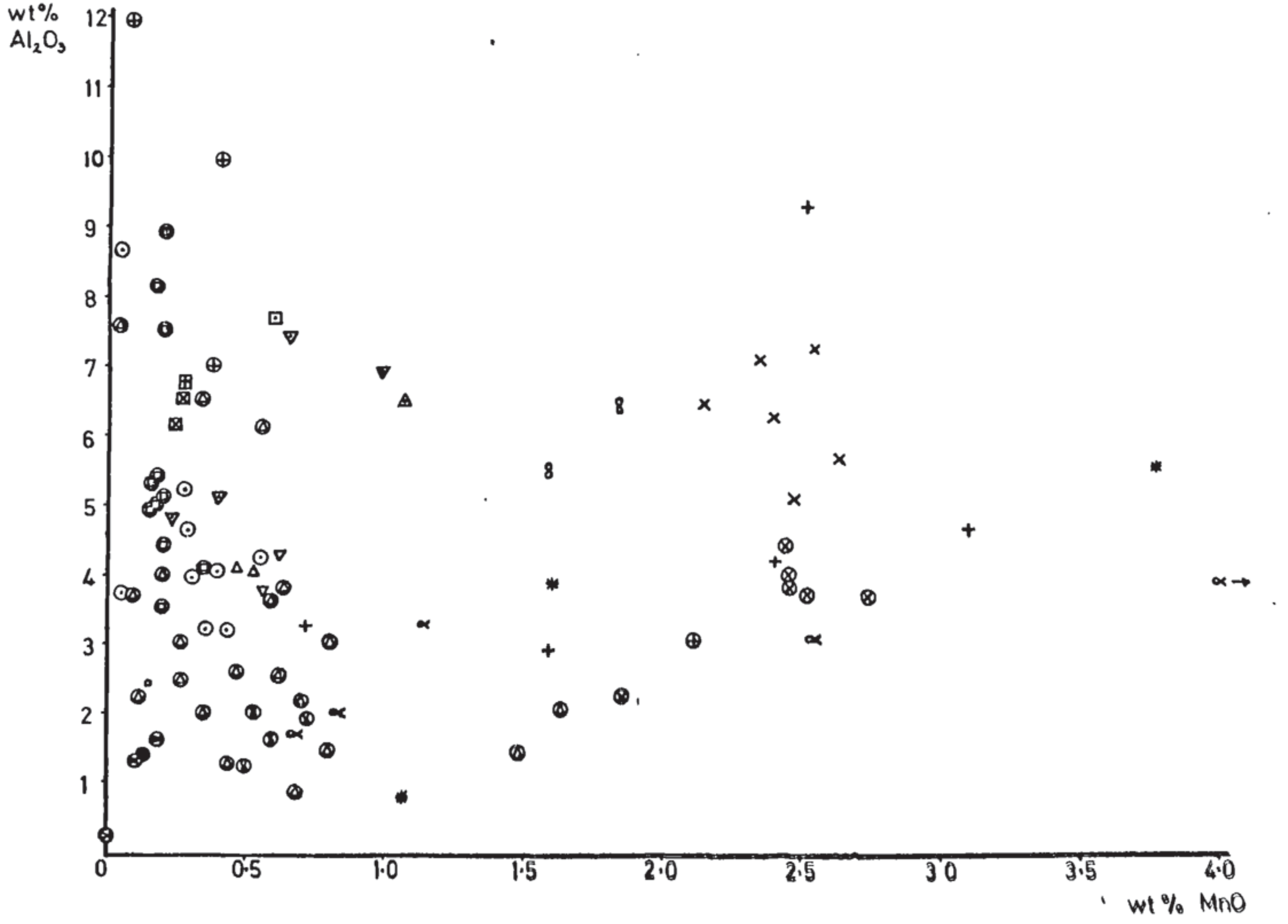
wt%
Al$_2$O$_3$
12
11
10
9
8
7
6
5
4
3
2
1
0
0·5
1·0
1·5
2·0
2·5
3·0
3·5
4·0
wt % MnO

Figure 5.3

Plot of Al_2O_3 vs MgO for the ironstones and slags investigated. Fold-out key is located after Figure 5.12.

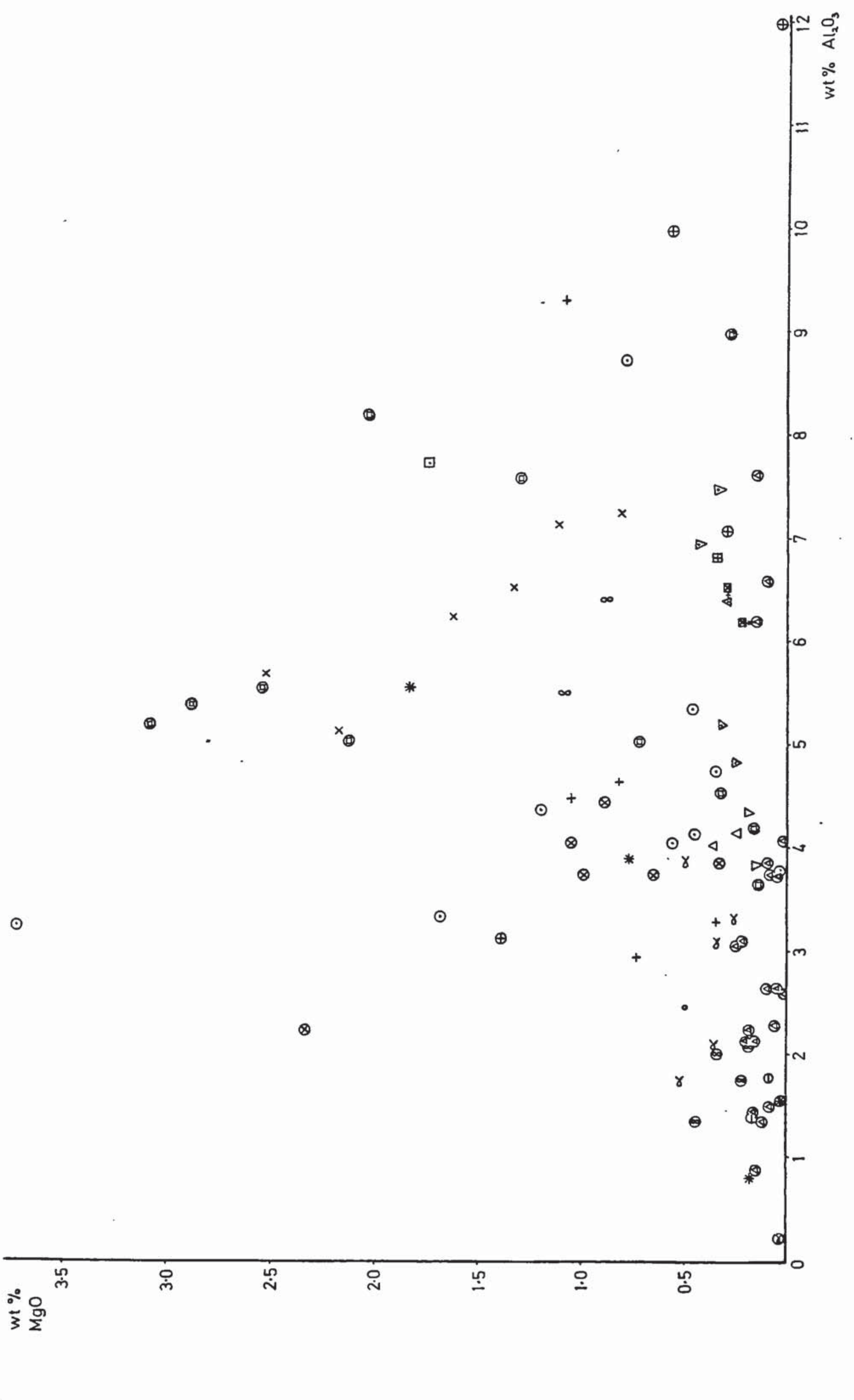
wt %
MgO
3·5
3·0
2·5
2·0
1·5
1·0
0·5
0
1
2
3
4
5
6
7
8
9
10
11
12
wt % Al_2O_3

Figure 5.4

Plot of Al_2O_3 vs TiO_2 for the ironstones and slags investigated. Fold-out key is located after Figure 5.12.

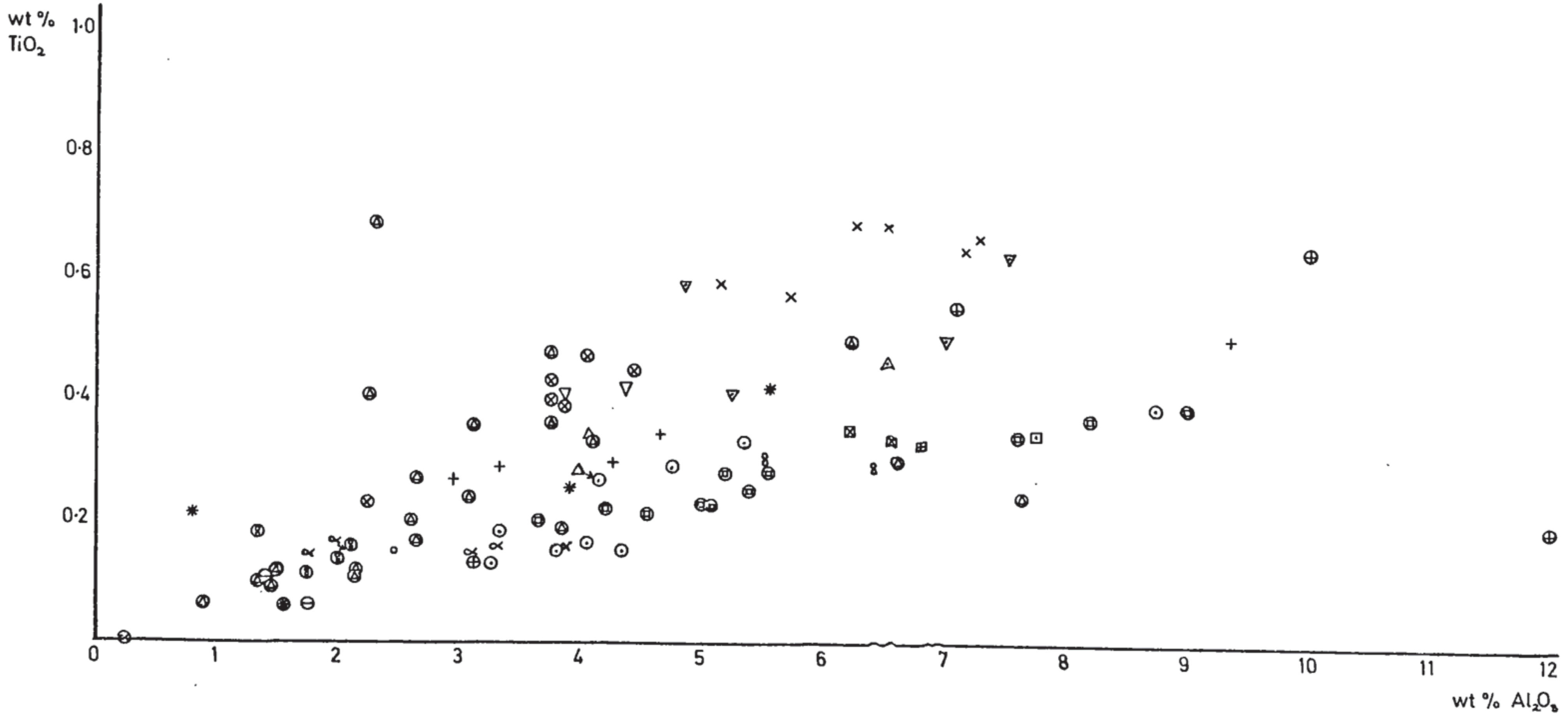
wt %
TiO$_2$
1·0
0·8
0·6
0·4
0·2
0
1
2
3
4
5
6
7
8
9
10
11
12
wt % Al$_2$O$_3$

Figure 5.5

Plot of Al_2O_3 vs V_2O_5 for the ironstones and slags investigated. Fold-out key is located after Figure 5.12.

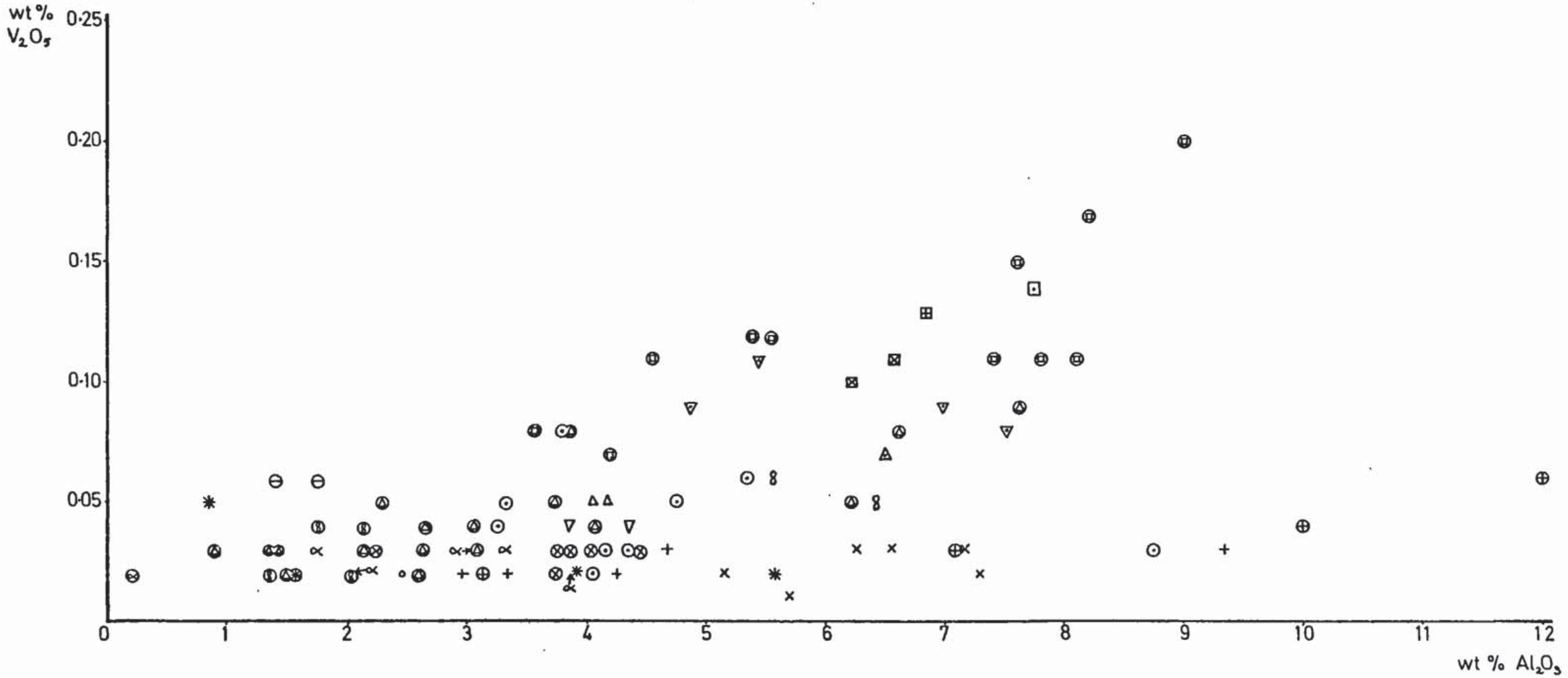
wt %
V₂O₅
0·25
0·20
0·15
0·10
0·05
0
1
2
3
4
5
6
7
8
9
10
11
12
wt % Al₂O₃

Figure 5.6

Plot of MnO vs MgO for the ironstones and slags investigated. Fold-out key is located after Figure 5.12.

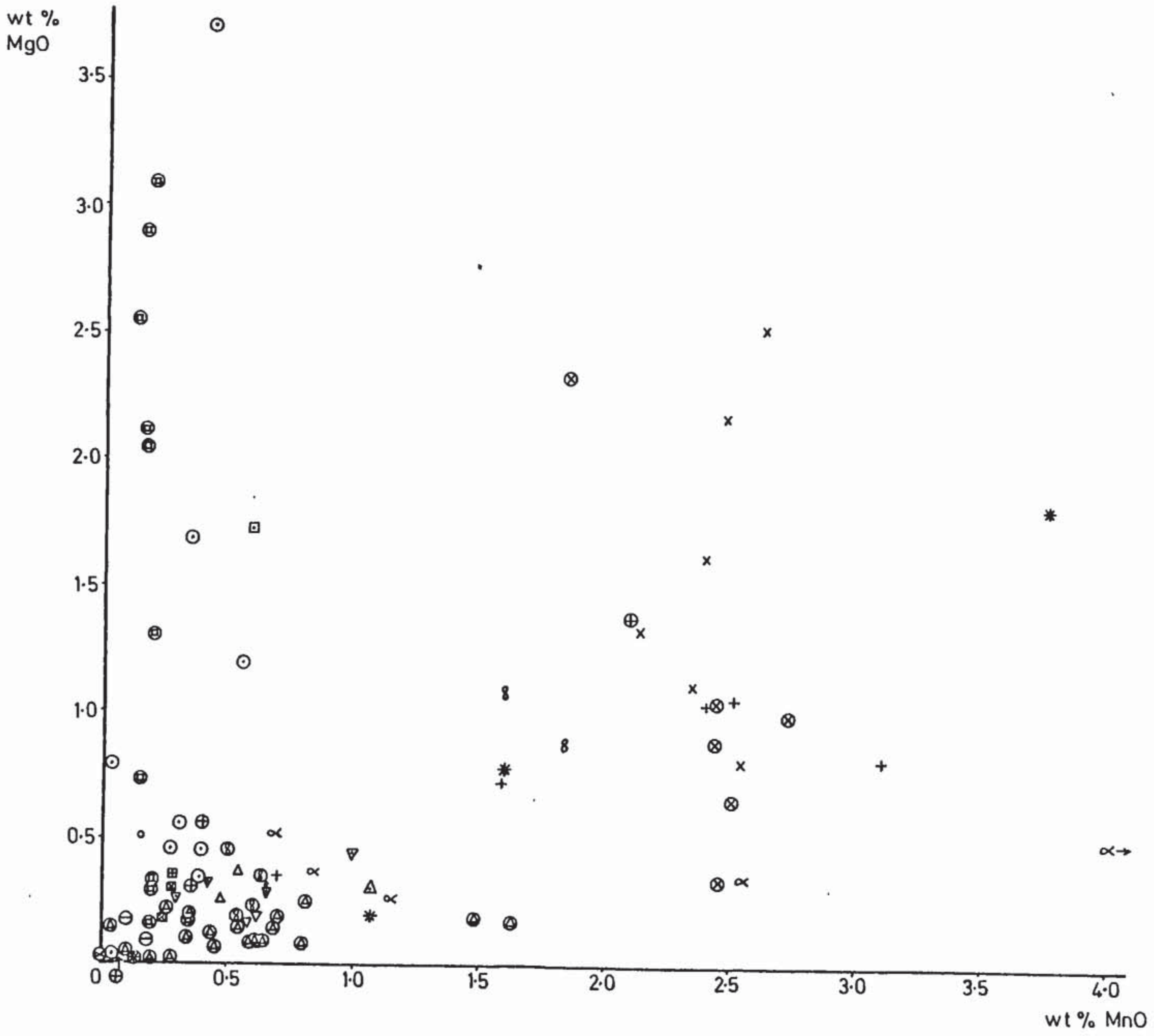
wt %
MgO
3·5
3·0
2·5
2·0
1·5
1·0
0·5
0
0·5
1·0
1·5
2·0
2·5
3·0
3·5
4·0
wt % MnO

Figure 5.7

Plot of MnO vs TiO_2 for the ironstones and slags investigated. Fold-out key is located after Figure 5.12.

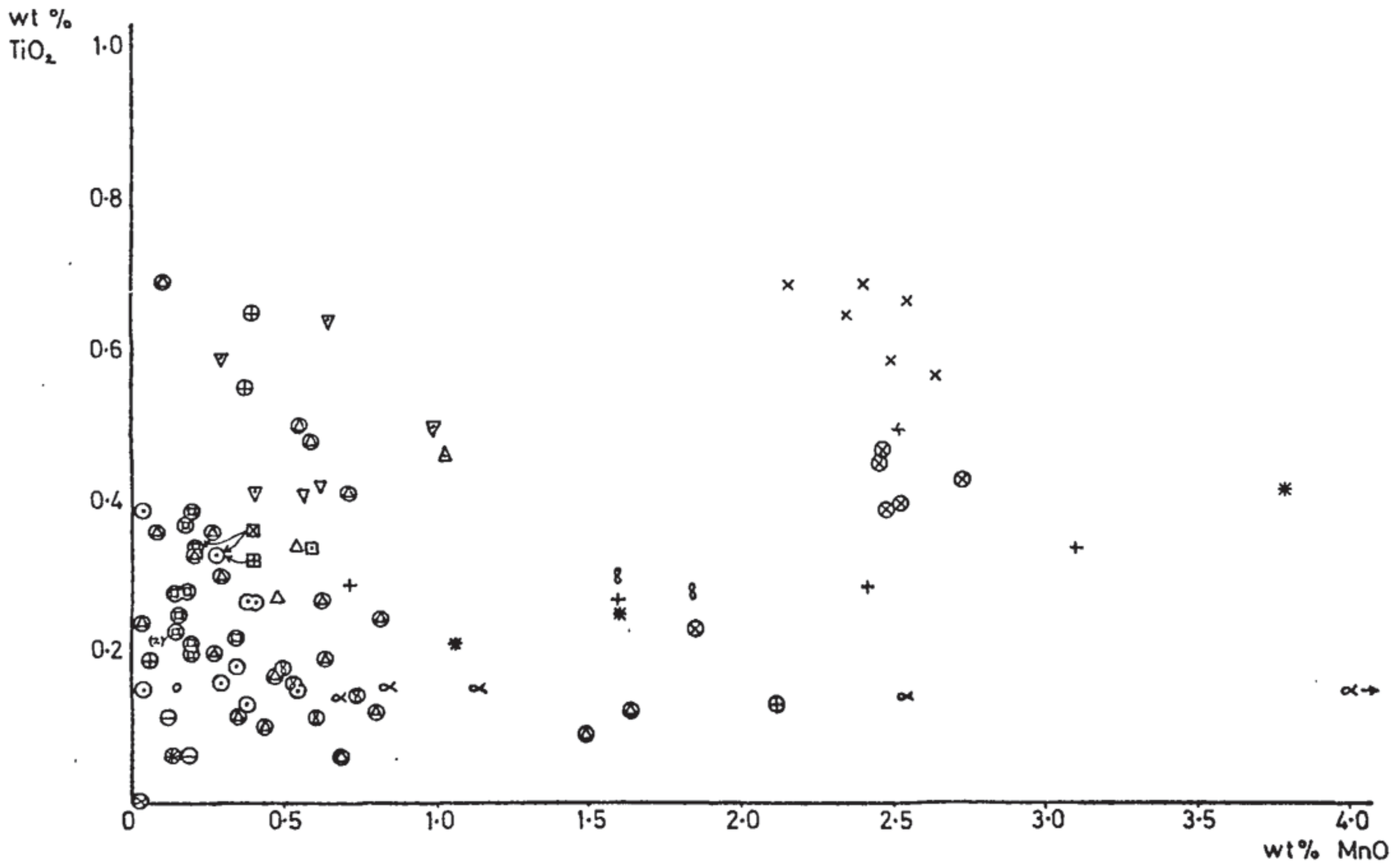
wt %
TiO₂
1·0
0·8
0·6
0·4
0·2
0
0·5
1·0
1·5
2·0
2·5
3·0
3·5
4·0
wt% MnO
(2)

Figure 5.8

Plot of MnO vs V_2O_5 for the ironstones and slags investigated. Fold-out key is located after Figure 5.12.

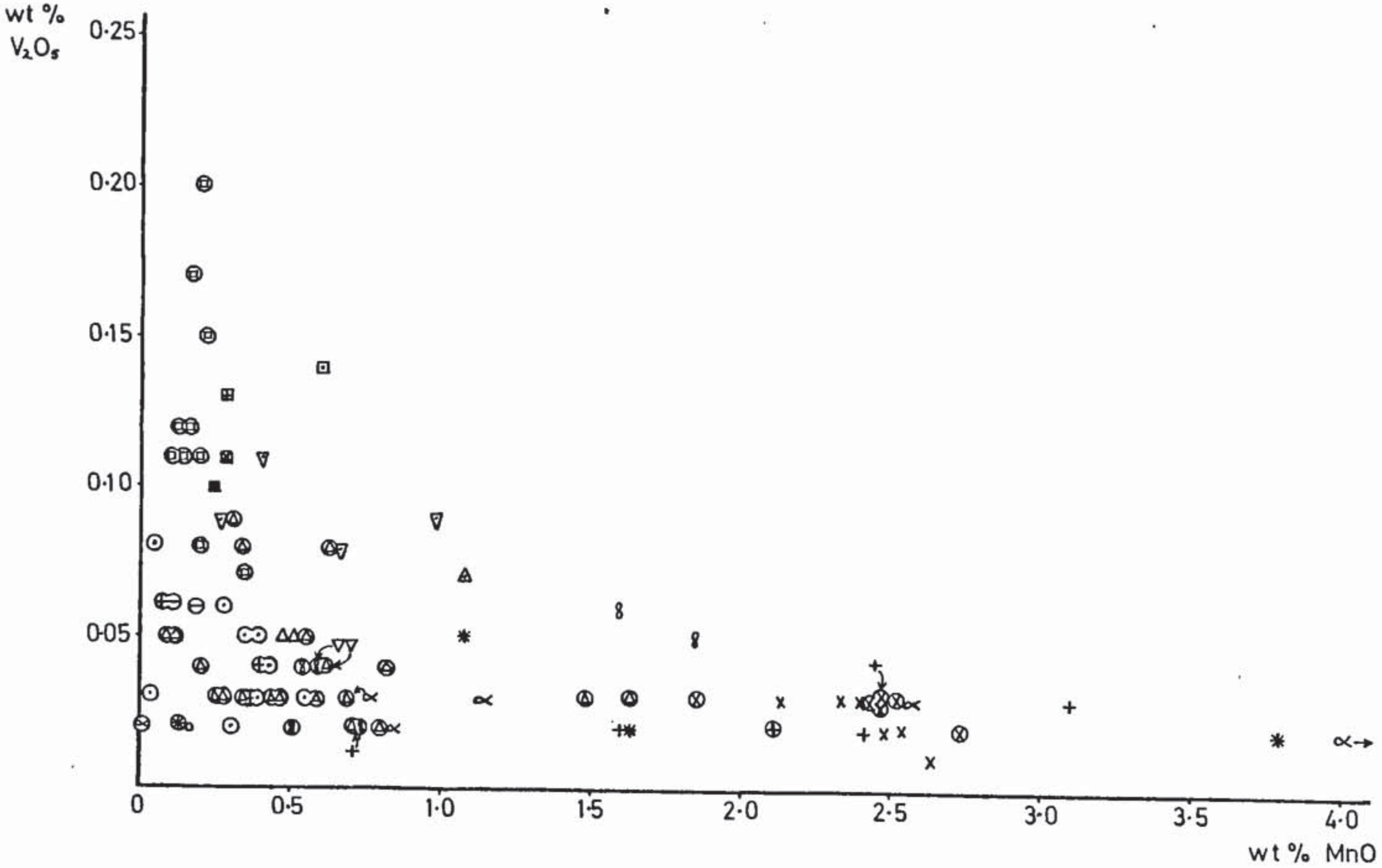
wt %
V_2O_5
0·25
0·20
0·15
0·10
0·05
0
0·5
1·0
1·5
2·0
2·5
3·0
3·5
4·0
wt % MnO

Figure 5.9

Plot of MgO vs TiO_2 for the ironstones and slags investigated. Fold-out key is located after Figure 5.12.

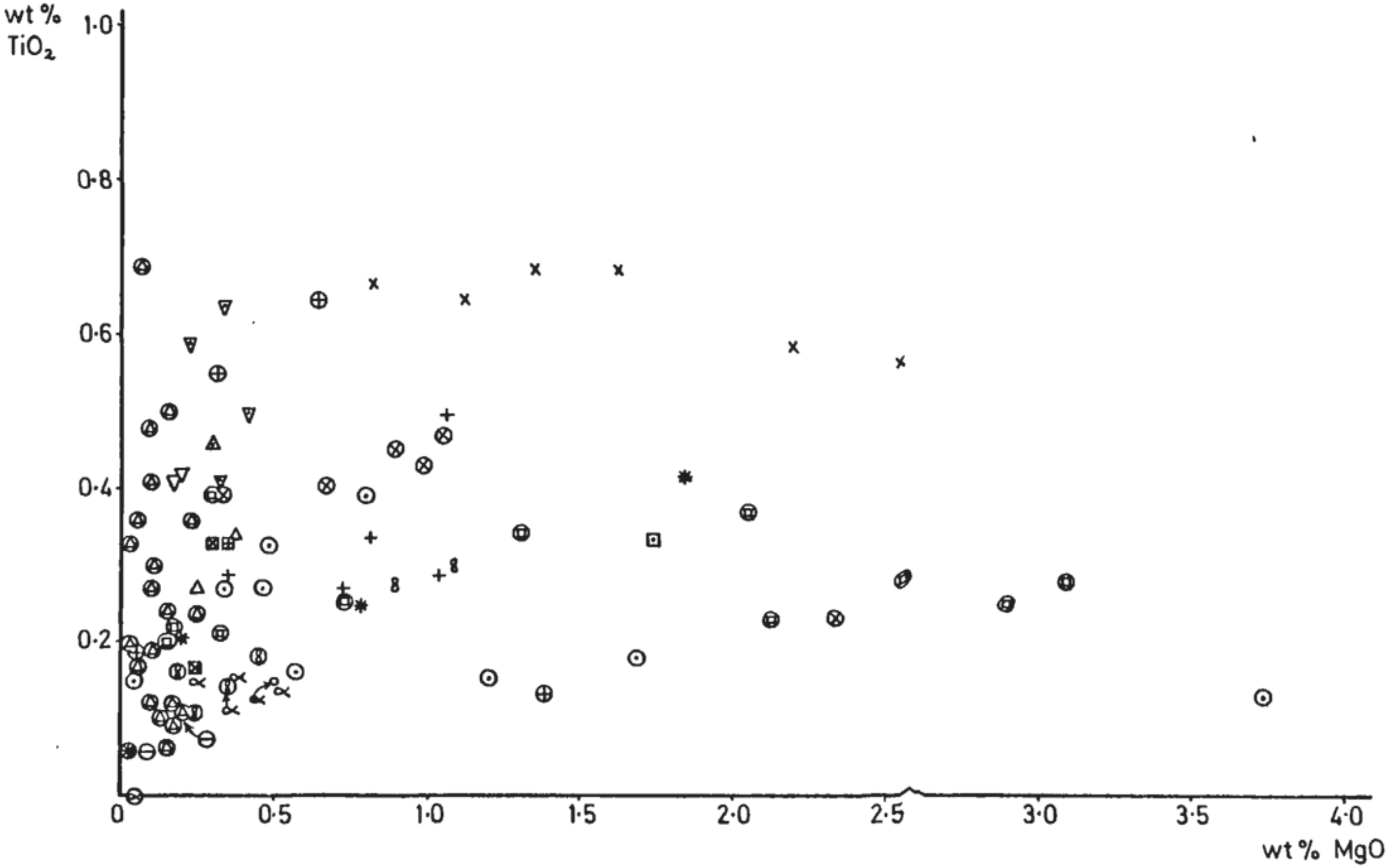
wt % TiO₂
1·0
0·8
0·6
0·4
0·2
0
0·5
1·0
1·5
2·0
2·5
3·0
3·5
4·0
wt % MgO

Figure 5.10

Plot of MgO vs V_2O_5 for the ironstones and slags investigated. Fold-out key is located after Figure 5.12.

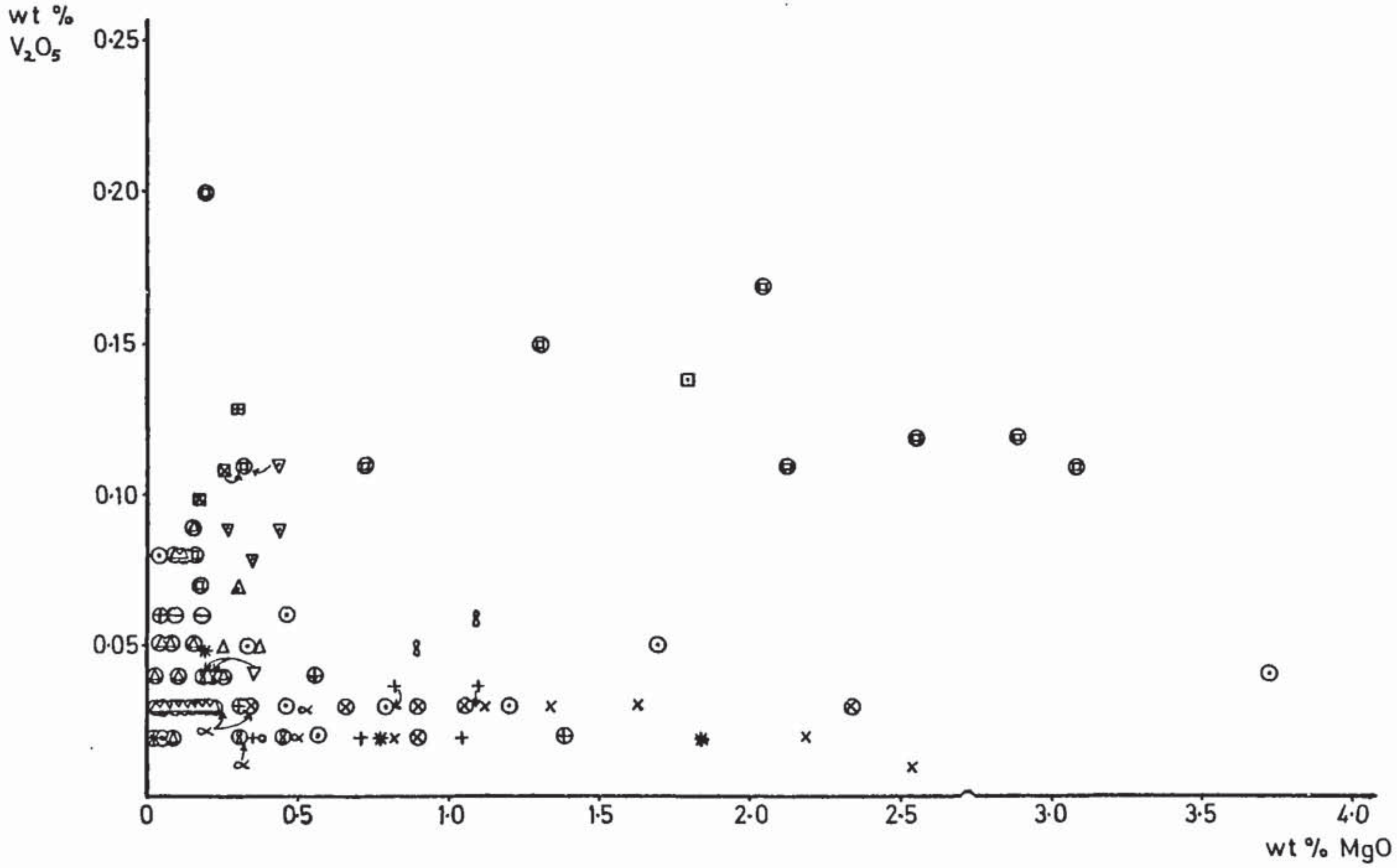
wt %
V$_2$O$_5$
0·25
0·20
0·15
0·10
0·05
0
0·5
1·0
1·5
2·0
2·5
3·0
3·5
4·0
wt % MgO

Figure 5.11

Plot of TiO_2 vs V_2O_5 for the ironstones and slags investigated. Fold-out key is located after Figure 5.12.

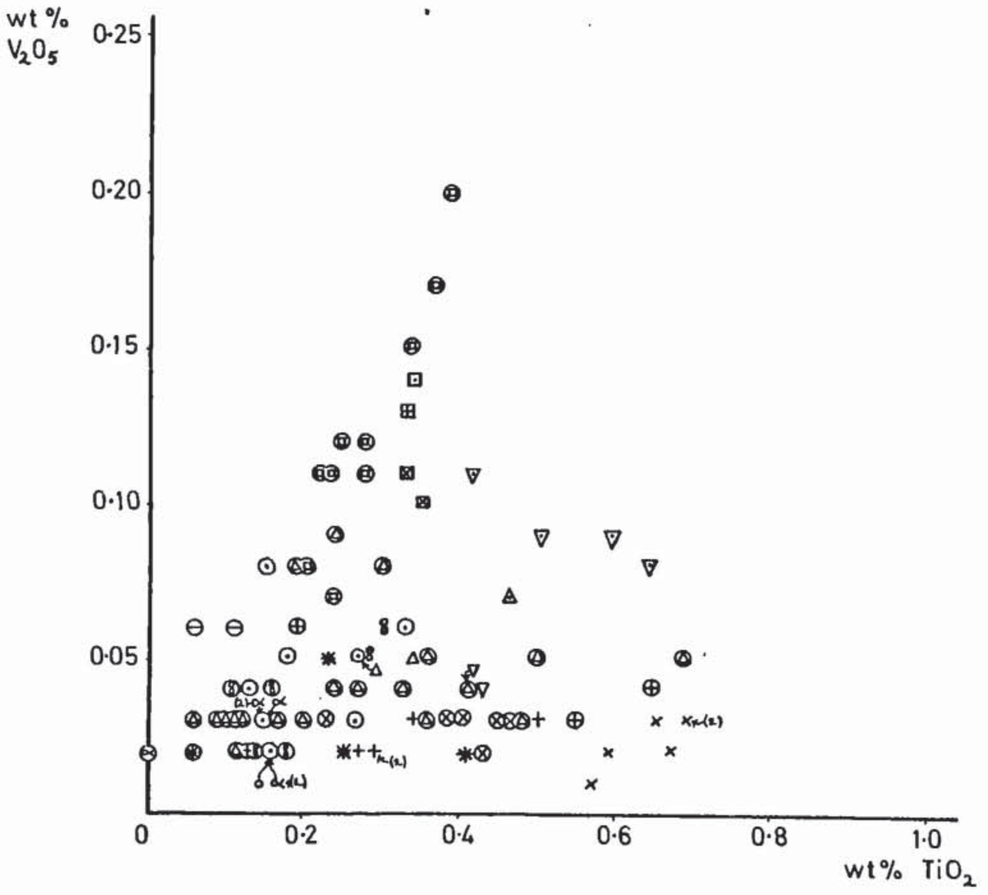
wt %
V$_2$O$_5$
0·25
0·20
0·15
0·10
0·05
0
0·2
0·4
0·6
0·8
1·0
wt% TiO$_2$

Figure 5.12

Plot of MnO vs P_2O_5 for the ironstones and slags investigated. Fold-out key is on following page.

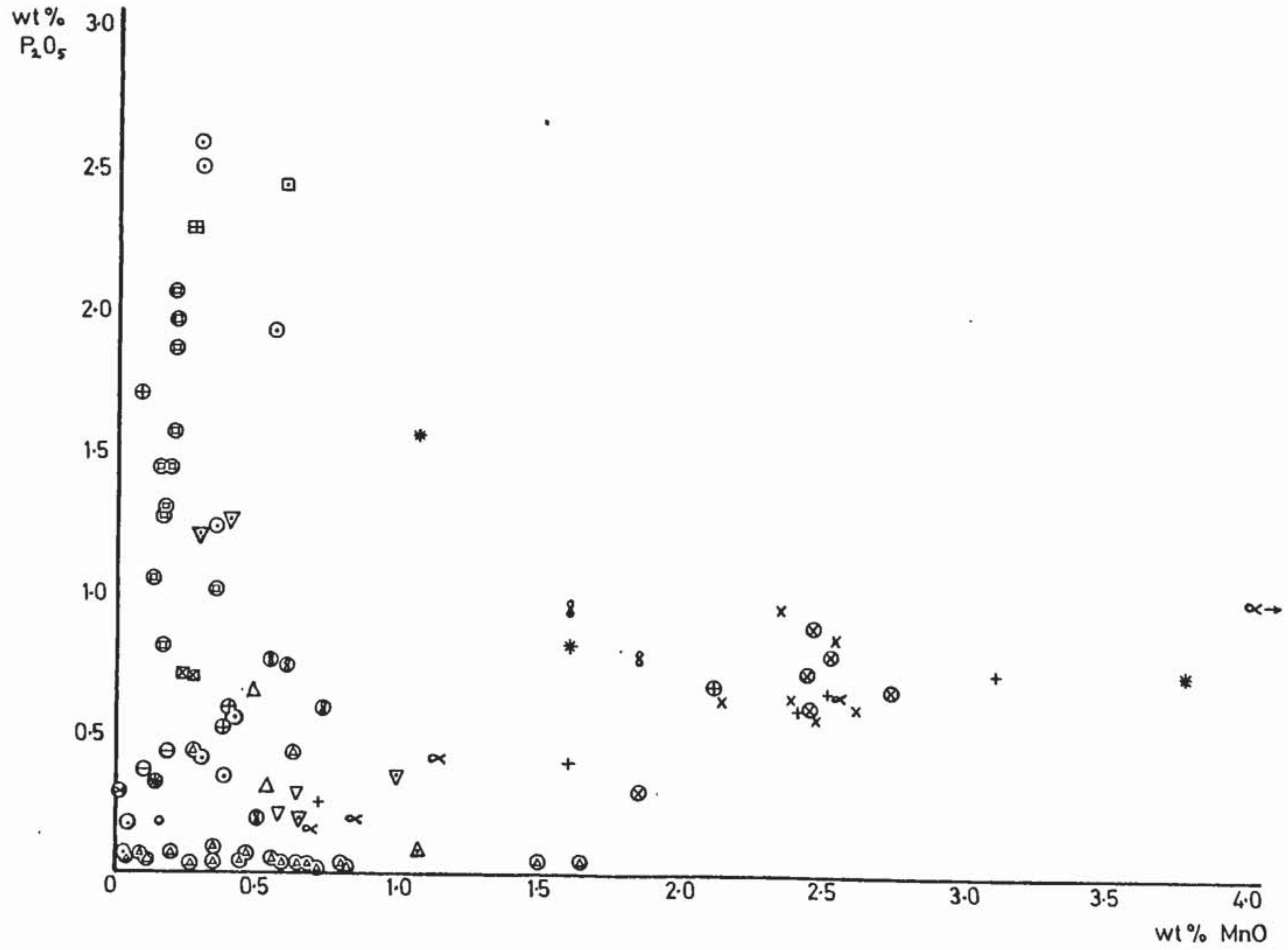
wt % P$_2$O$_5$
3·0
2·5
2·0
1·5
1·0
0·5
0
0·5
1·0
1·5
2·0
2·5
3·0
3·5
4·0
wt % MnO

Key to symbols used on two-component plots (Figures 5.2 to 5.12)

Slags

◬	Wakerley
△	Great Oakley
▽	Blind Eye Quarry
◬	Bulwick
⊞	Brigstock
⊠	Stamford
⊡	South Witham
+	Garden Hill
✱	Millbrook
×	Reconstructions
8	Ramsbury
∝	Bulbourne Valley
∘	Caerwent

Ores

⊚	Ironstone Junction-Band
⦶	Northampton Sand Ironstone
⊙	Boulder Clay Nodules
⊗	Wadhurst Clay Ironstone
⊕	Garden Hill Ores
⊛	Millbrook Limonite
⦻	Ramsbury Ores
⊖	Upper Greensand
⊜	Marcasite

Groups

NSI - Northampton Sand Ironstone
IJB - Ironstone Junction-Band
BC - Boulder Clay

W - Weald
R - Ramsbury
B - Bulbourne Valley

Figure 5.13

Dendrogram showing the results of the application of cluster analysis to the data. Nearest neighbour (single linkage) method.

CLUSTER ANALYSIS USING THE CLUSTAN 1A PROGRAM #CLUS (MARK 2A)
NEAREST NEIGHBOUR

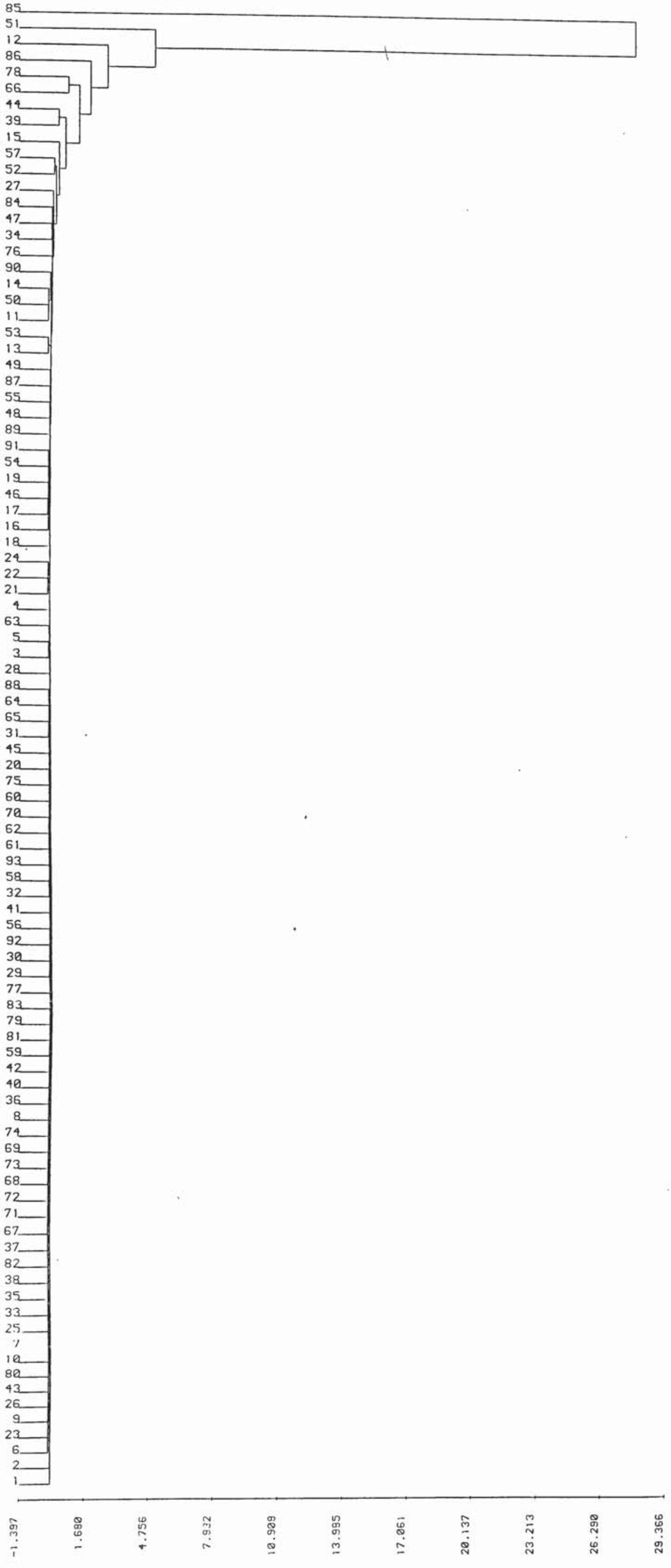

Figure 5.14

Dendrogram showing the results of the application of cluster analysis to the data. Group average (average linkage) method.

CLUSTER ANALYSIS USING THE CLUSTAN 1A PROGRAM #CLUS (MARK 2A)
GROUP AVERAGE

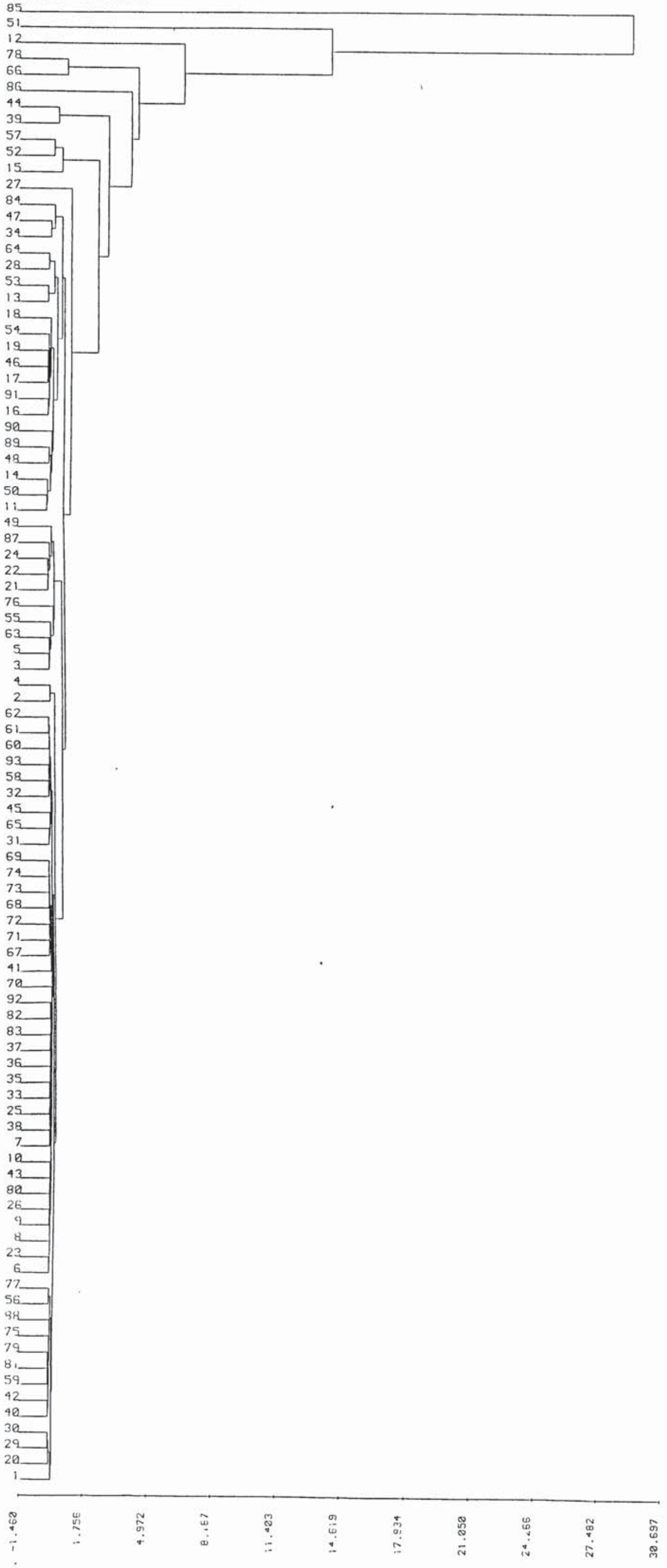

Figure 5.15

Dendrogram showing the results of the application of cluster analysis to the data. Ward's method.

CLUSTER ANALYSIS USING THE CLUSTAN 1A PROGRAM #CLUS (MARK 2A)
WARD'S METHOD

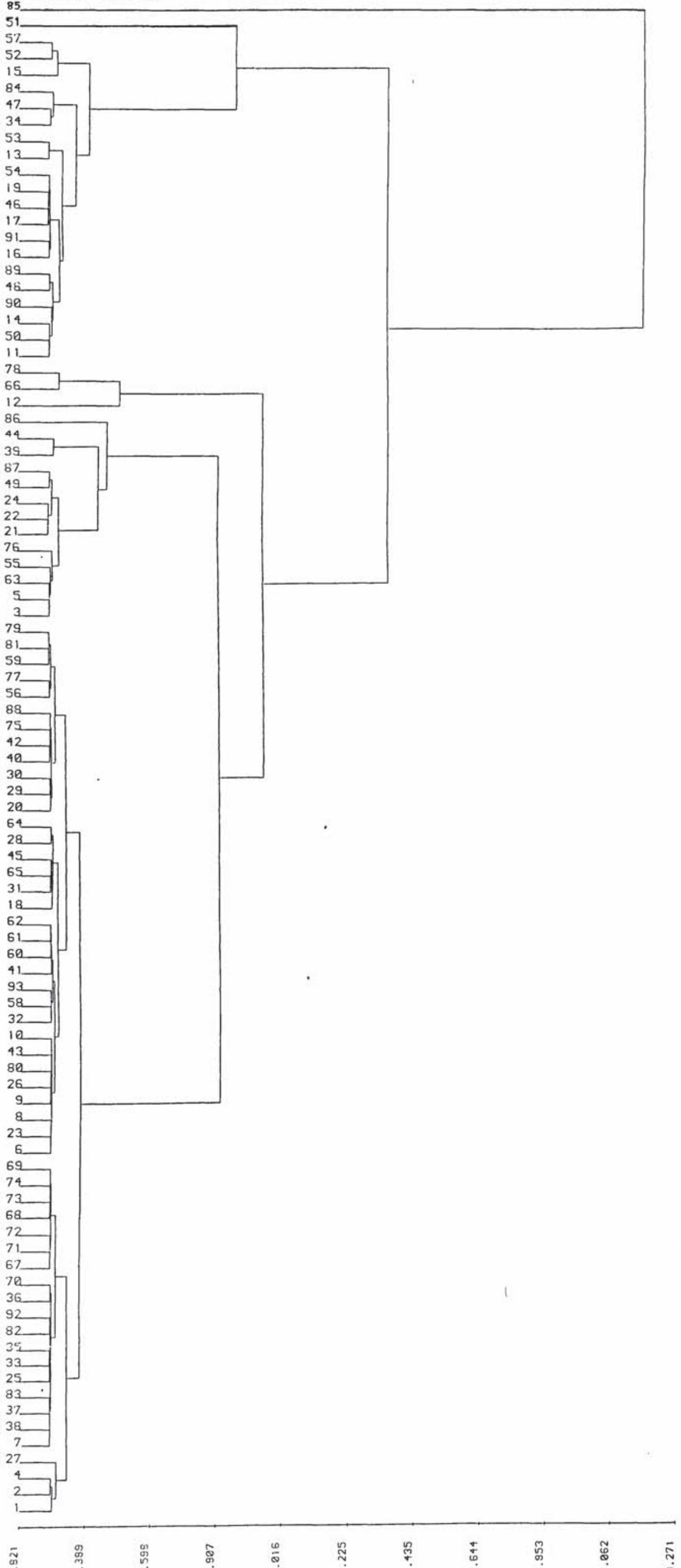

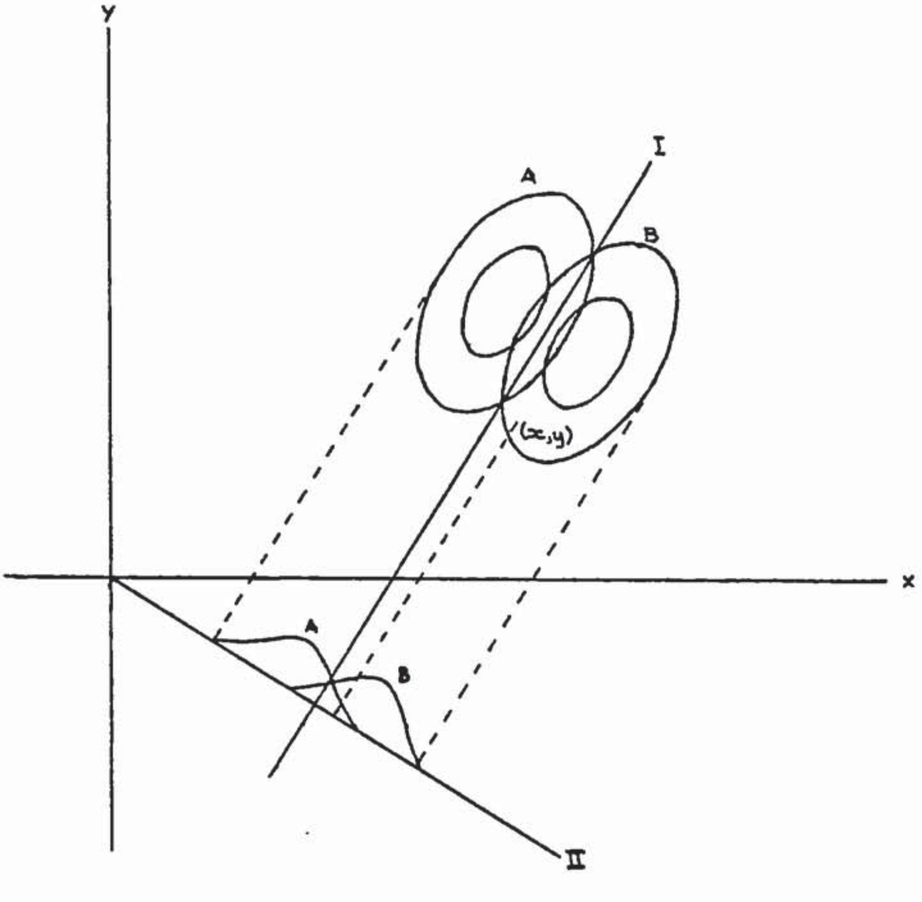
Y
A
I
B
(x,y)
x
A
B
II

Figure 5.16

Diagram illustrating the principle of discriminant analysis. For explanation see text.

Figure 5.17

Results of multiple regression analysis of the data: graph shows the observed Al_2O_3 content of the ores versus the calculated content.

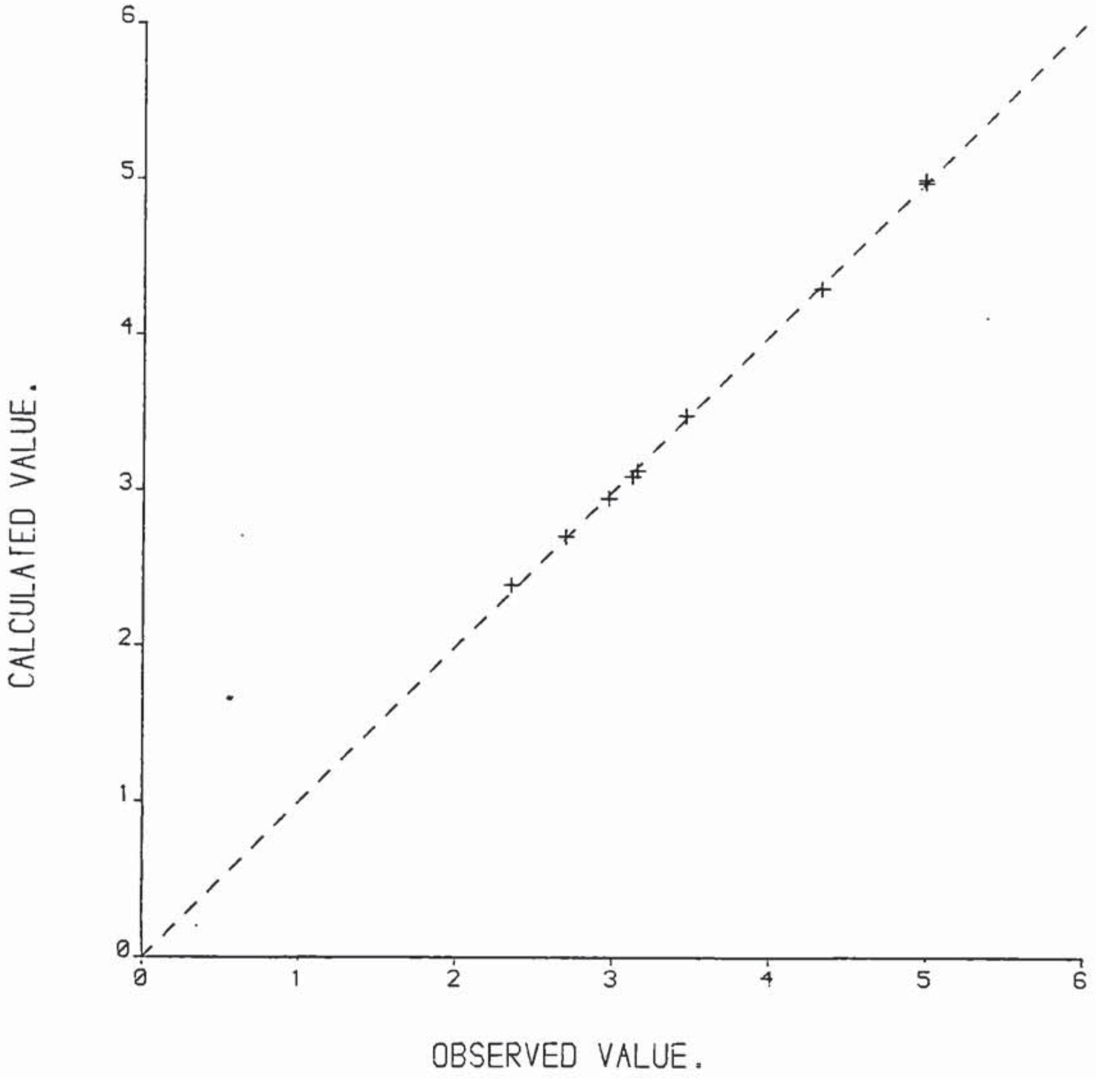

0BSERVED V CALCULATED – Al_2O_3

Figure 5.18

Results of multiple regression analysis of the data: graph shows the observed MnO content of the ores versus the calculated content.

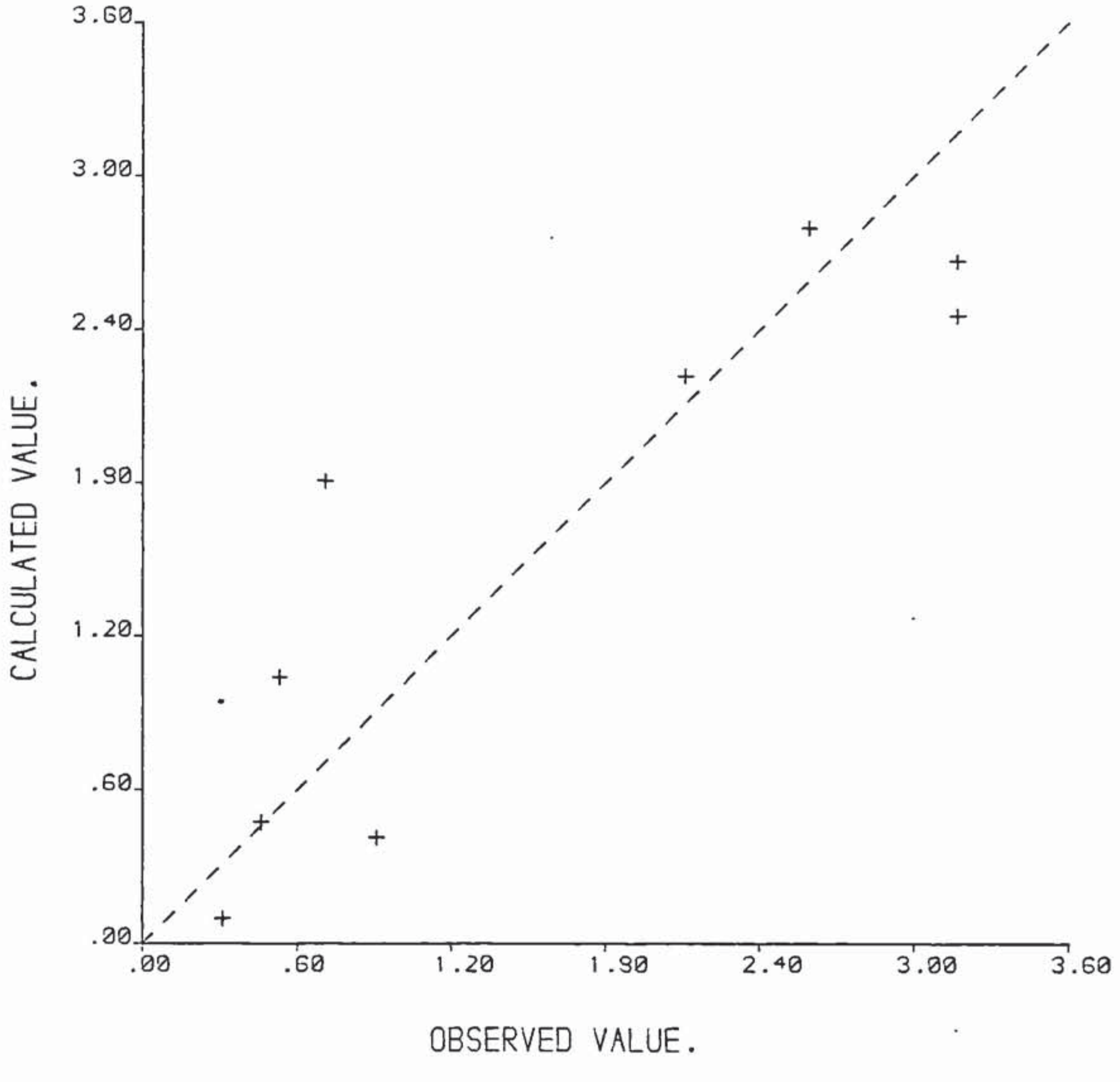

0BSERVED V CALCULATED – MnO

Figure 5.19

Results of multiple regression analysis of the data: graph shows the observed MgO content of the ores versus the calculated content.

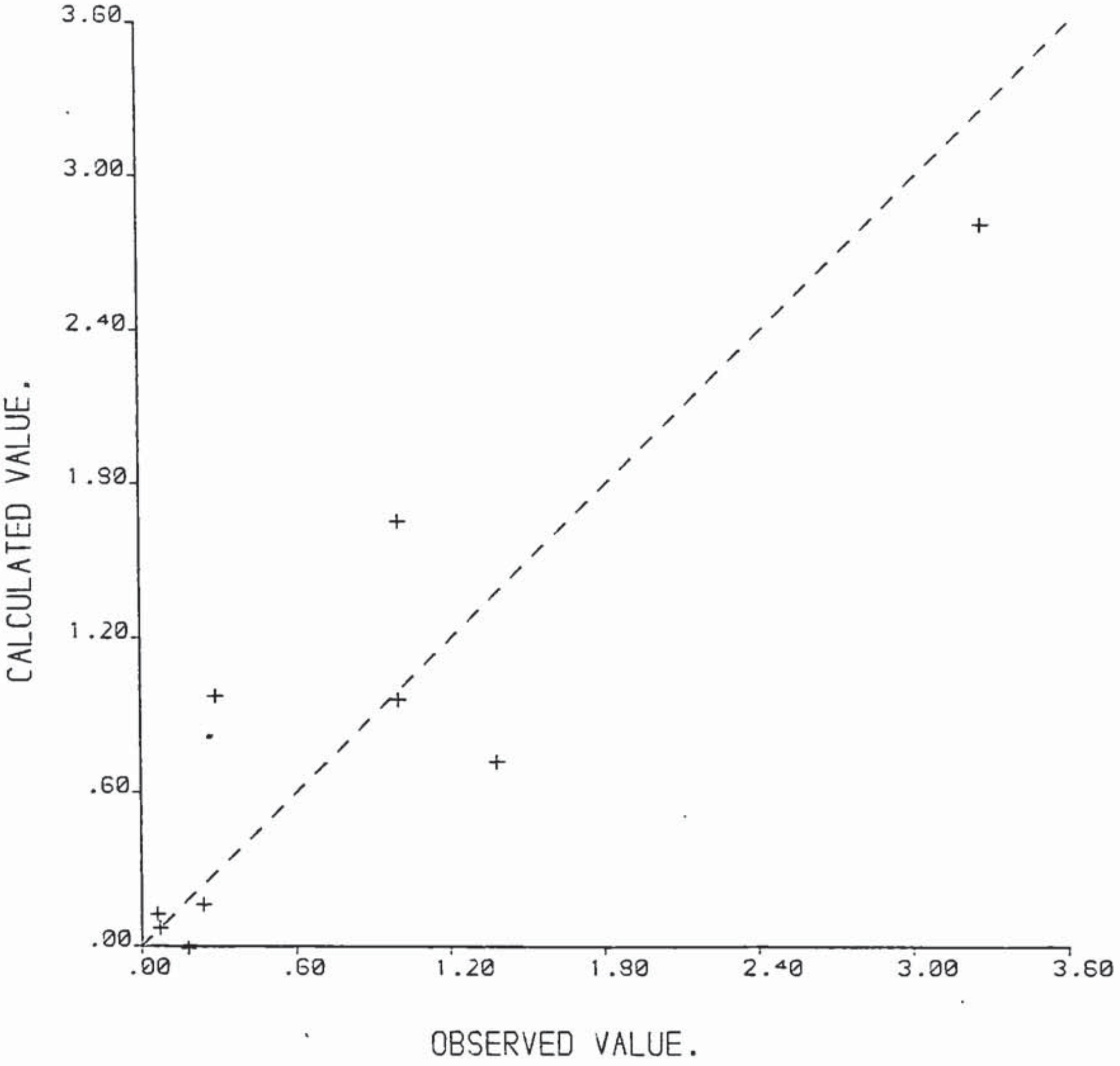

OBSERVED V CALCULATED – MgO

Figure 5.20

Results of multiple regression analysis of the data: graph shows the observed TiO_2 content of the ores versus the calculated content.

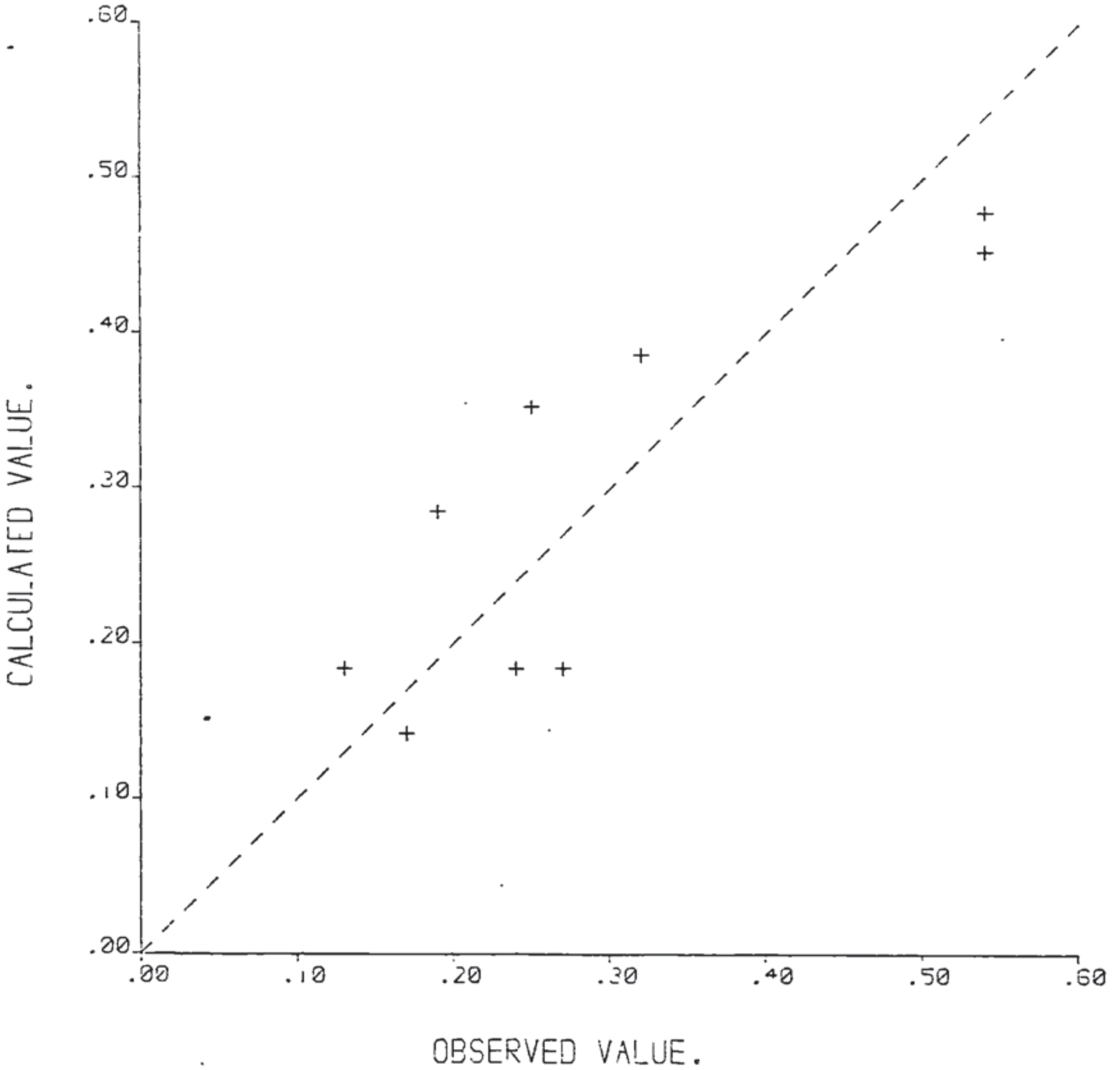

0BSERVED V CALCULATED – TiO_2

Figure 5.21

Results of multiple regression analysis of the data: graph shows the observed V_2O_5 content of the ores versus the calculated content.

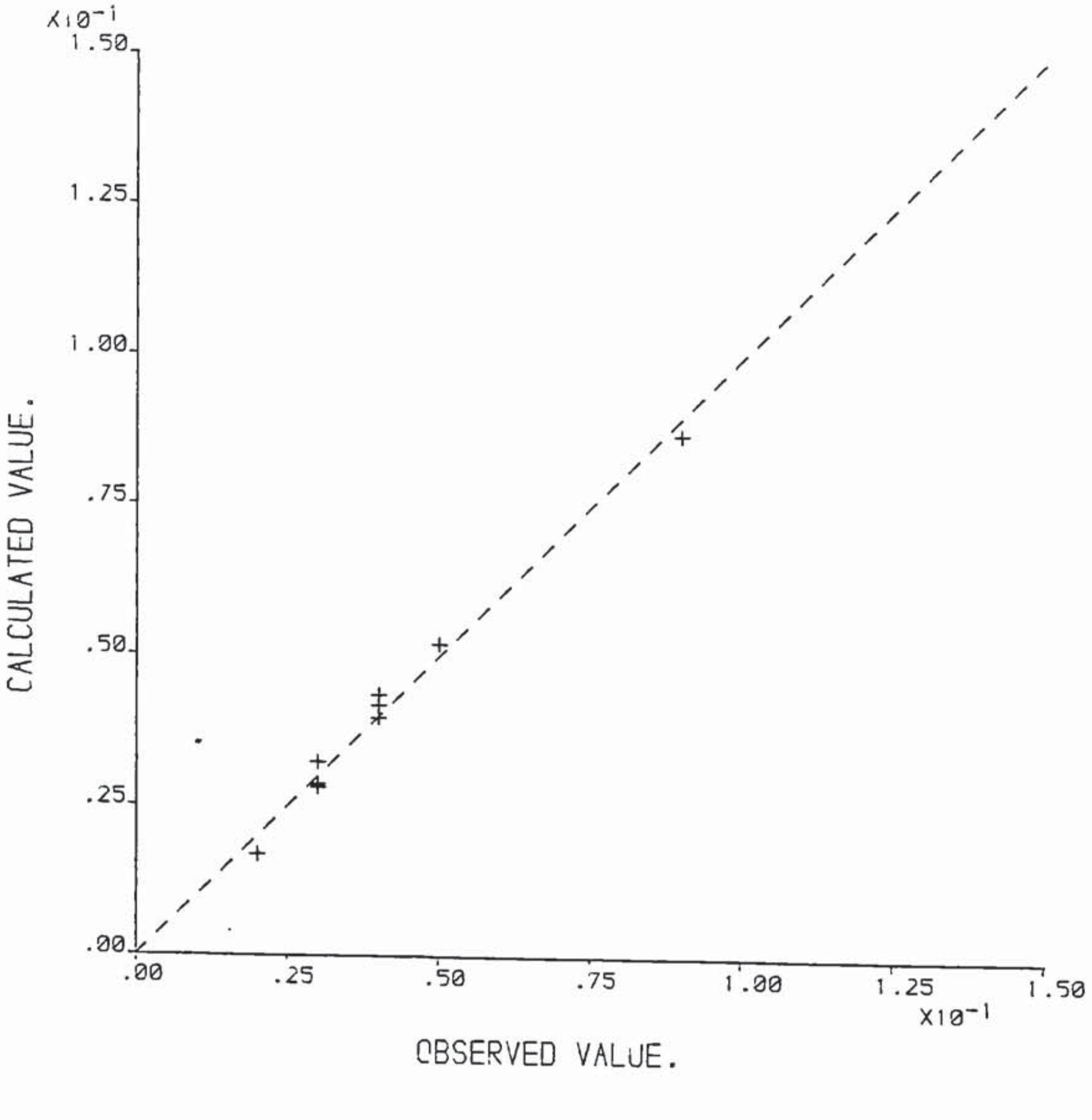

OBSERVED V CALCULATED – V_2O_5

Figure 5.22

Plot of the partially corrected values for Al_2O_3 in the ore against the Fe_2O_3 contents of the slag, all other independent variables being held at their average value.

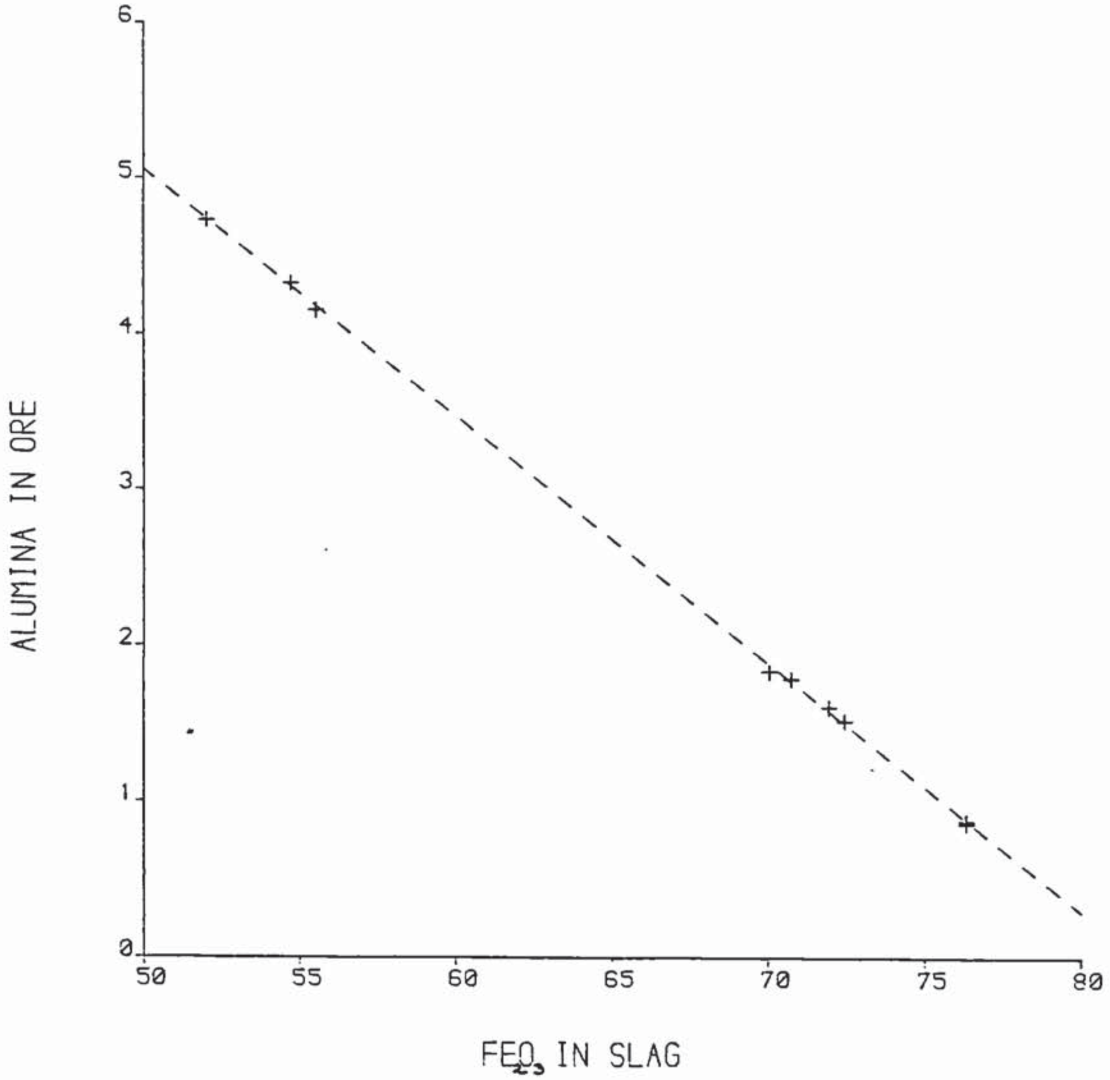

AL_2O_3 IN ORE V FE_2O_3 IN SLAG

Figure 5.23

Plot of the partially corrected values for Al_2O_3 in the ores against the SiO_2 content of the slags, all other independent variables being held at their average value.

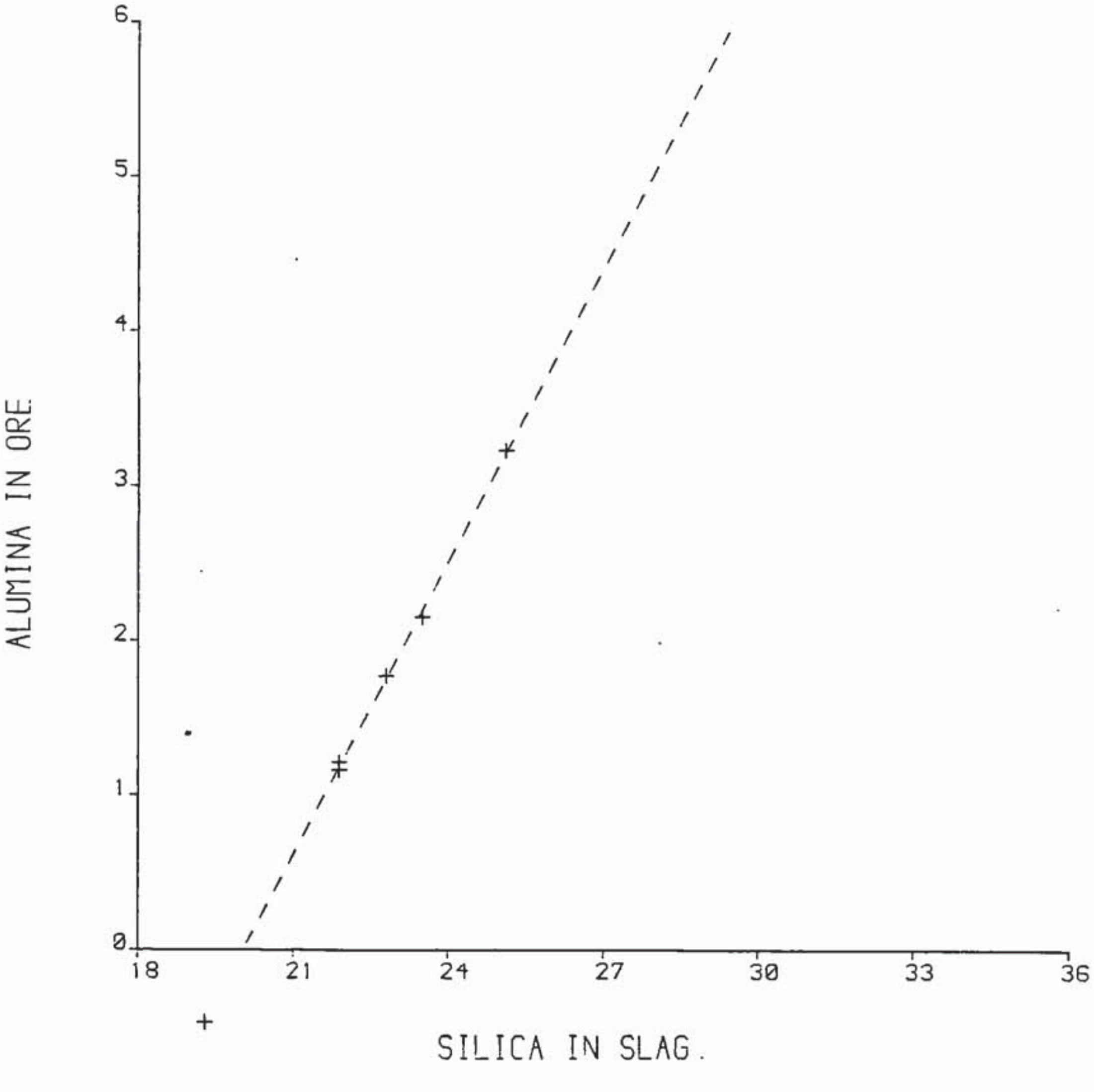

ALUMINA IN ORE V SILICA IN SLAG

Figure 5.24

Plot of the partially corrected values for Al_2O_3 in the ores against the Al_2O_3 content of the slags, all other independent variables being held at their average values.

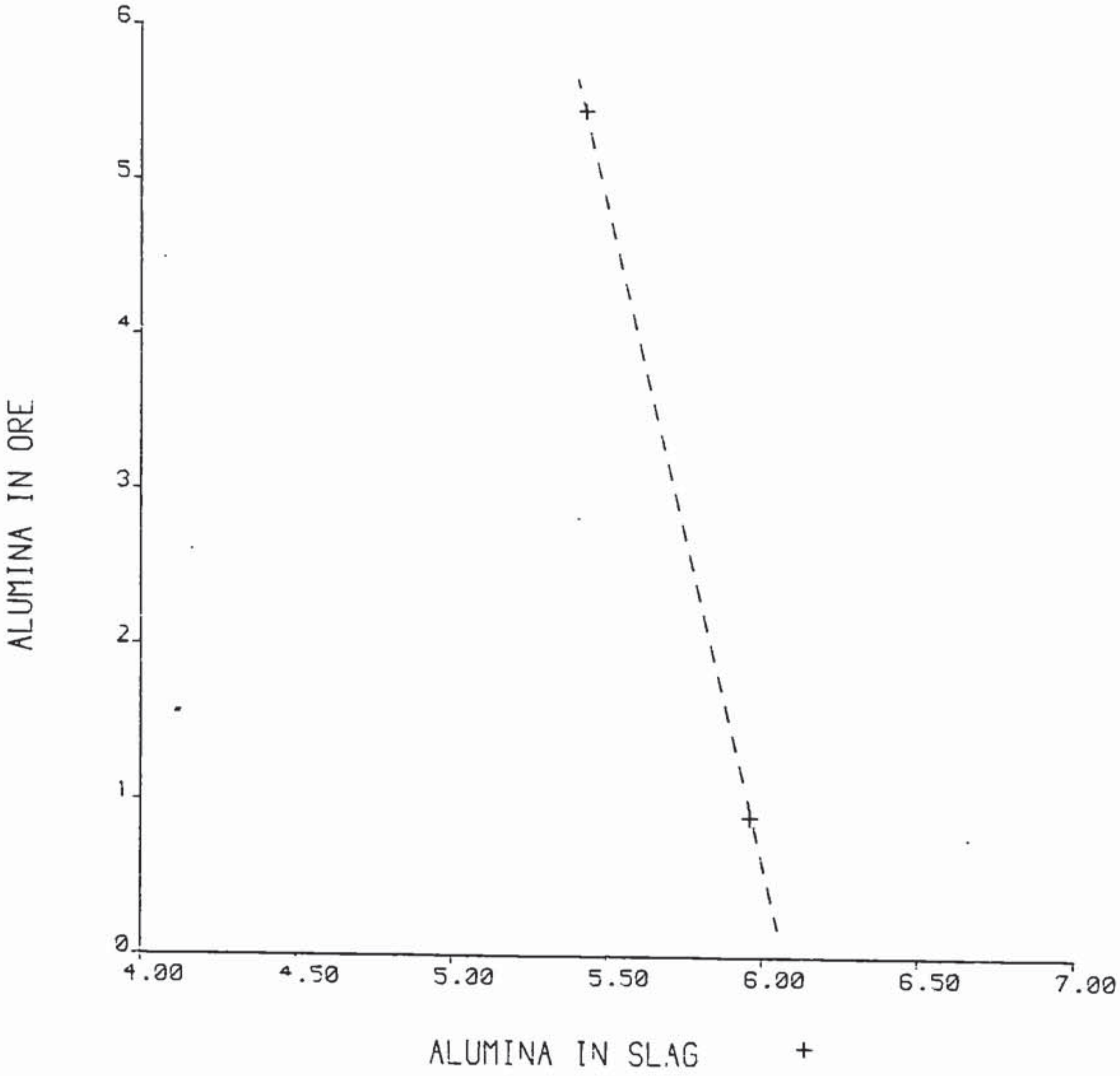

ALUMINA IN ORE V ALUMINA IN SLAG

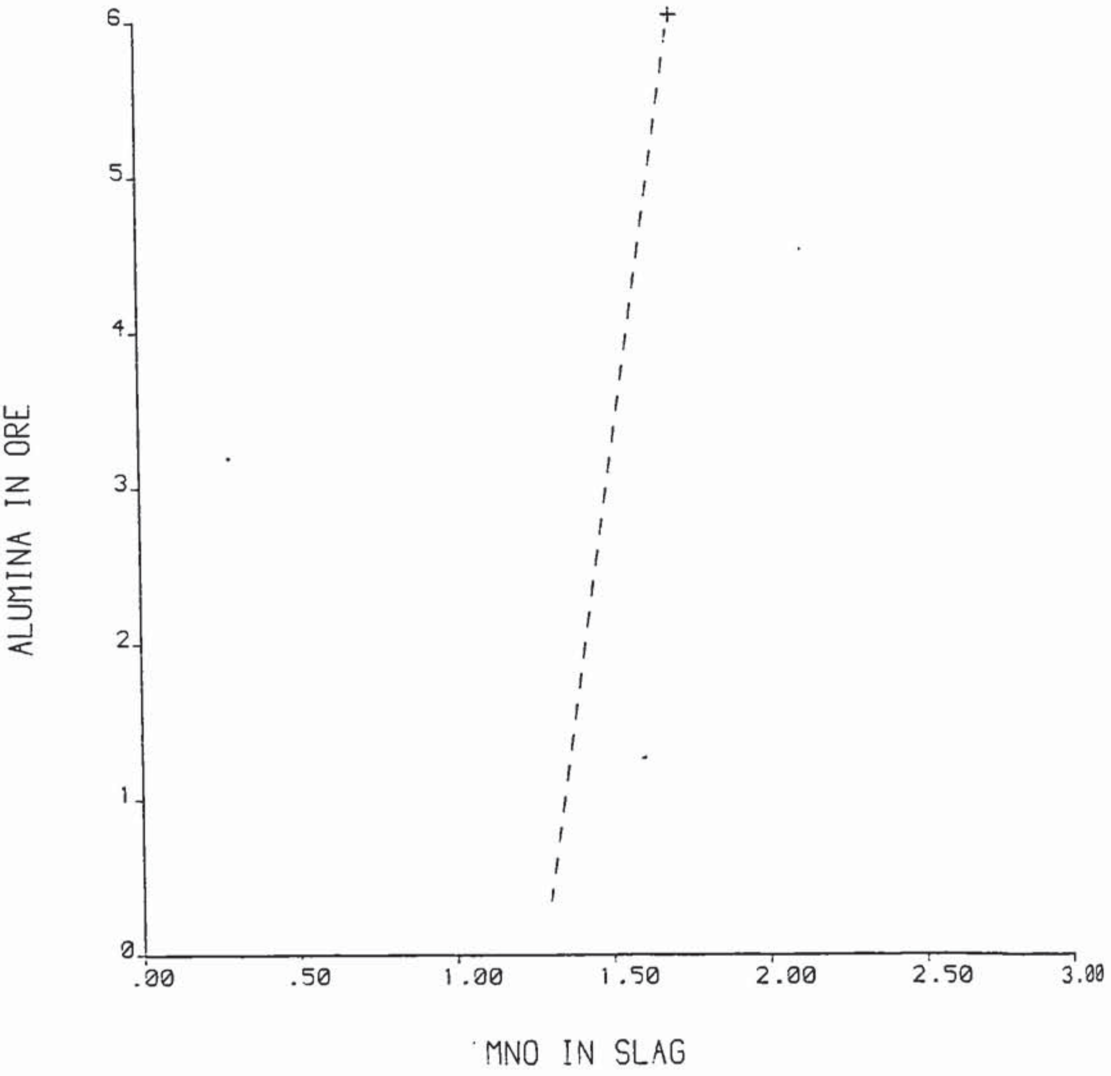

AL_2O_3 IN ORE V MNO IN SLAG

Figure 5.25

Plot of the partially corrected values for Al_2O_3 in the ores against the MnO content of the slags, all other independent variables being held at their average values.

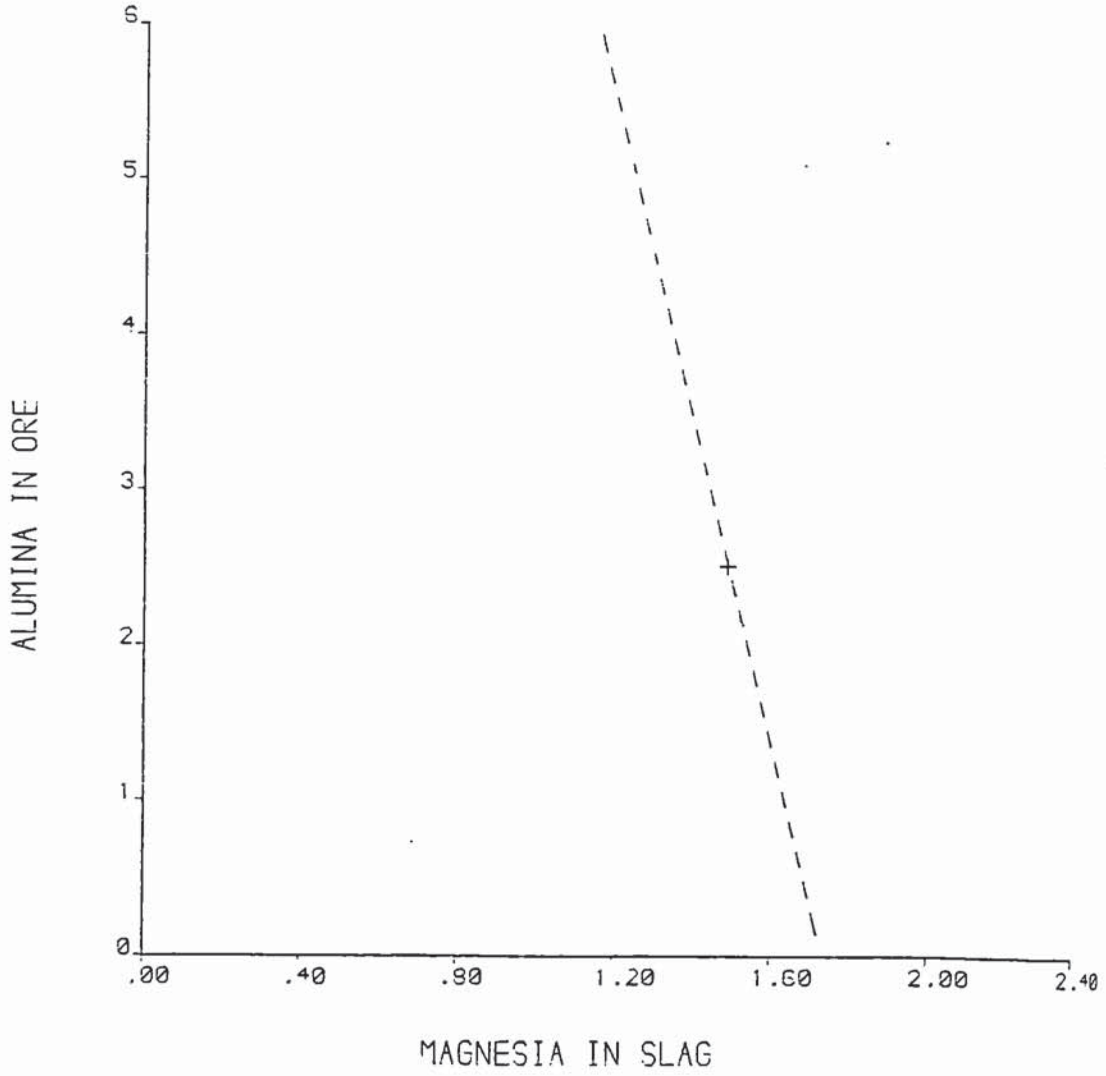

ALUMINA IN ORE V MAGNESIA IN SLAG

Figure 5.26

Plot of the partially corrected values for Al_2O_3 in the ores against the MgO content of the slags, all other independent variables being held at their average values.

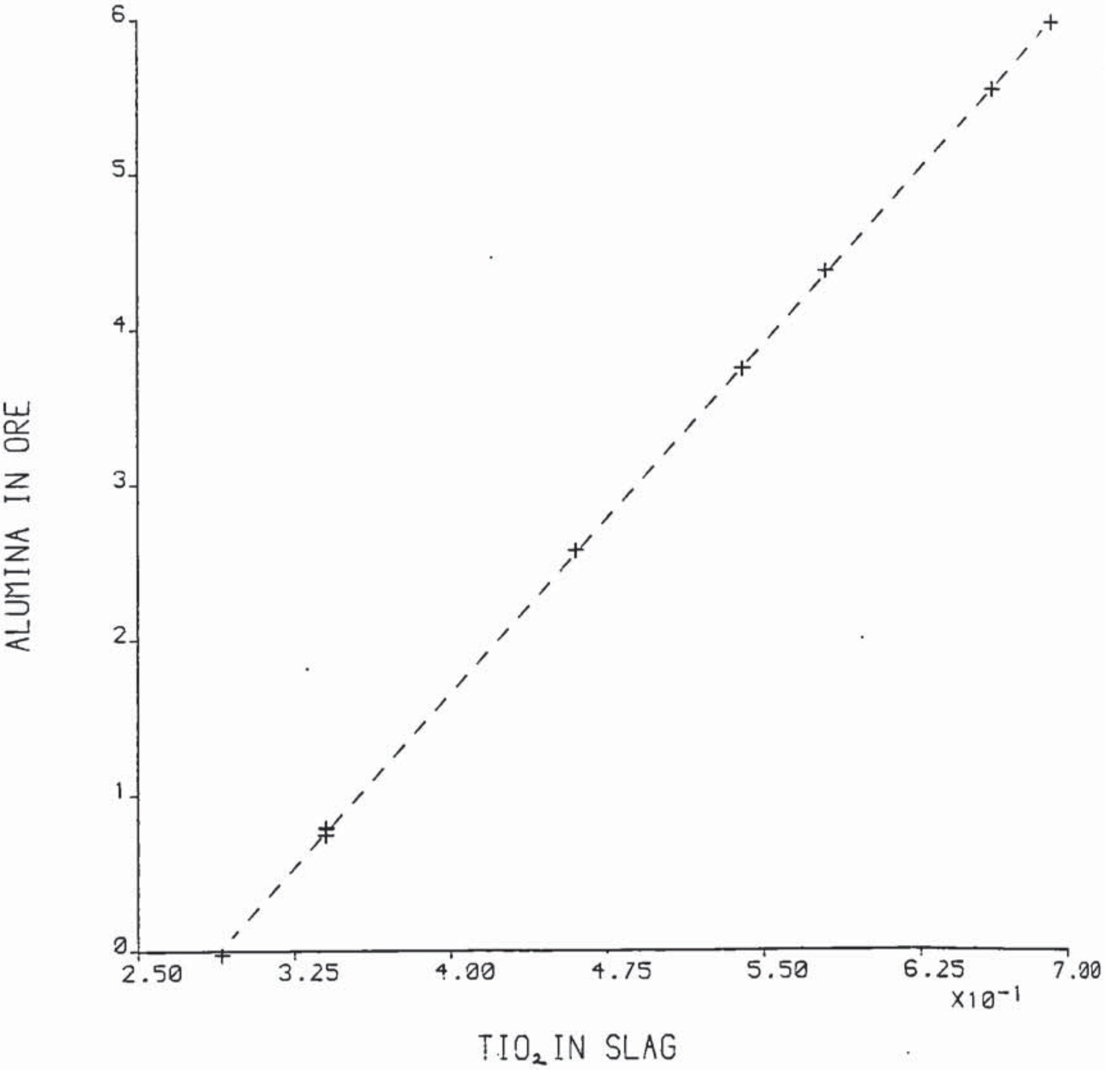

AL_2O_3 IN ORE V TIO_2 IN SLAG

Figure 5.27

Plot of the partially corrected values for Al_2O_3 in the ores against the TiO_2 content of the slags, all other independent variables being held at their average value.

Figure 5.28

Plot of the partially corrected values for Al_2O_3 in the ores against the V_2O_5 content of the slags, all other independent variables being held at their average value.

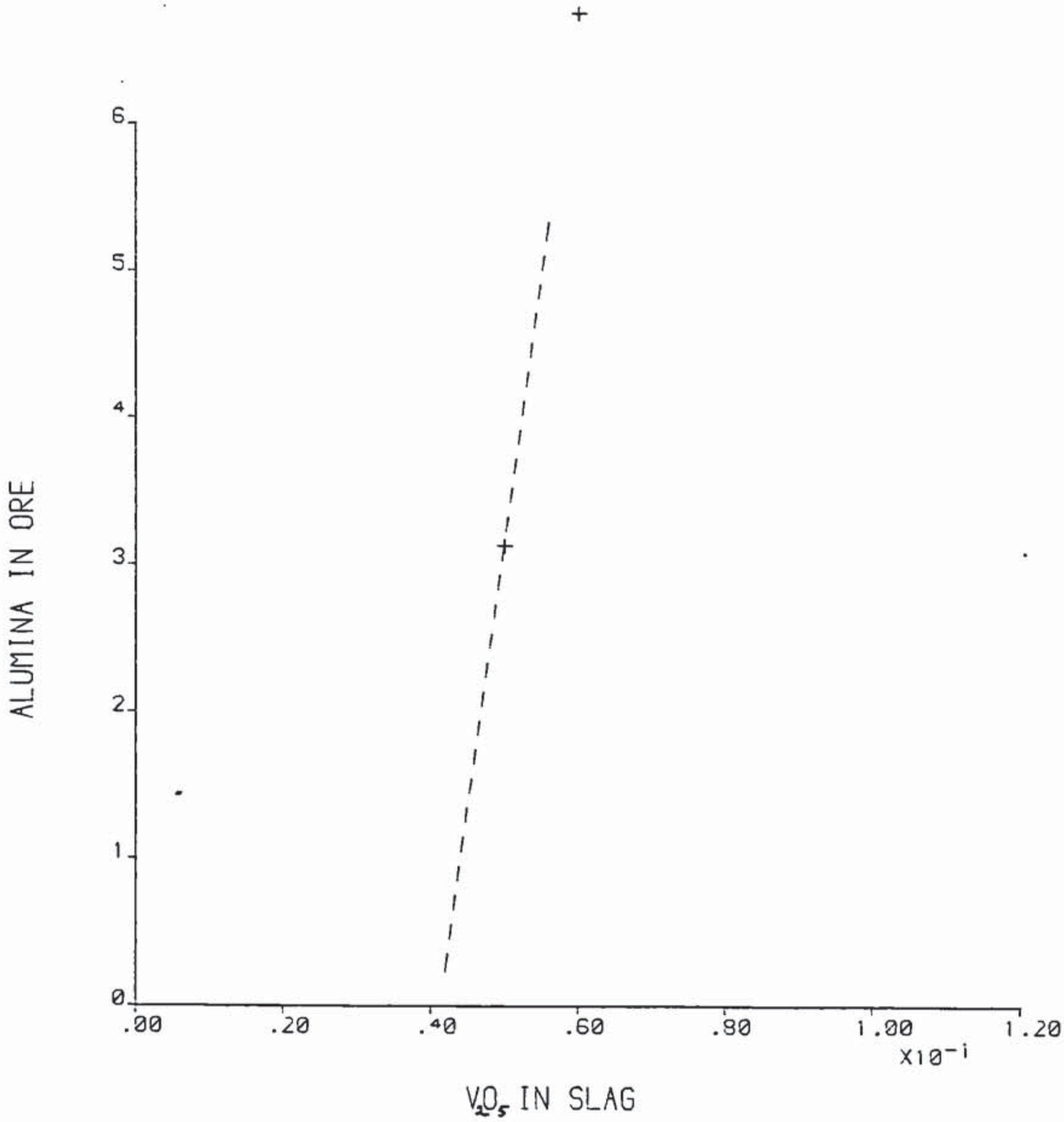

AL_2O_3 IN ORE V V_2O_5 IN SLAG

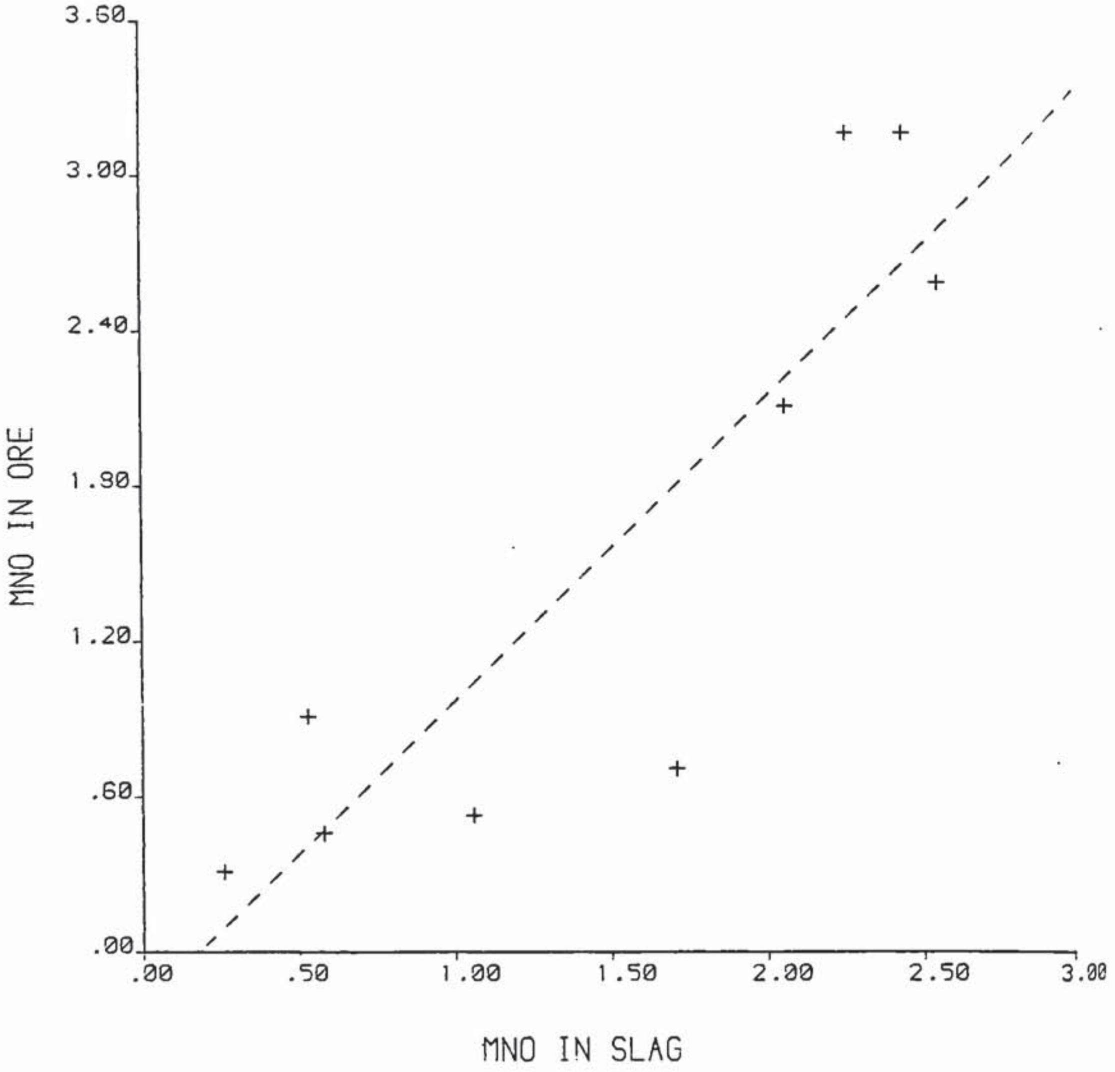

MNO IN ORE V MNO IN SLAG

Figure 5.29

Plot of the calculated values for MnO in the ores against the MnO content of the slags.

Figure 5.30

Plot of the calculated values for MgO in the ores against the MgO content of the slags.

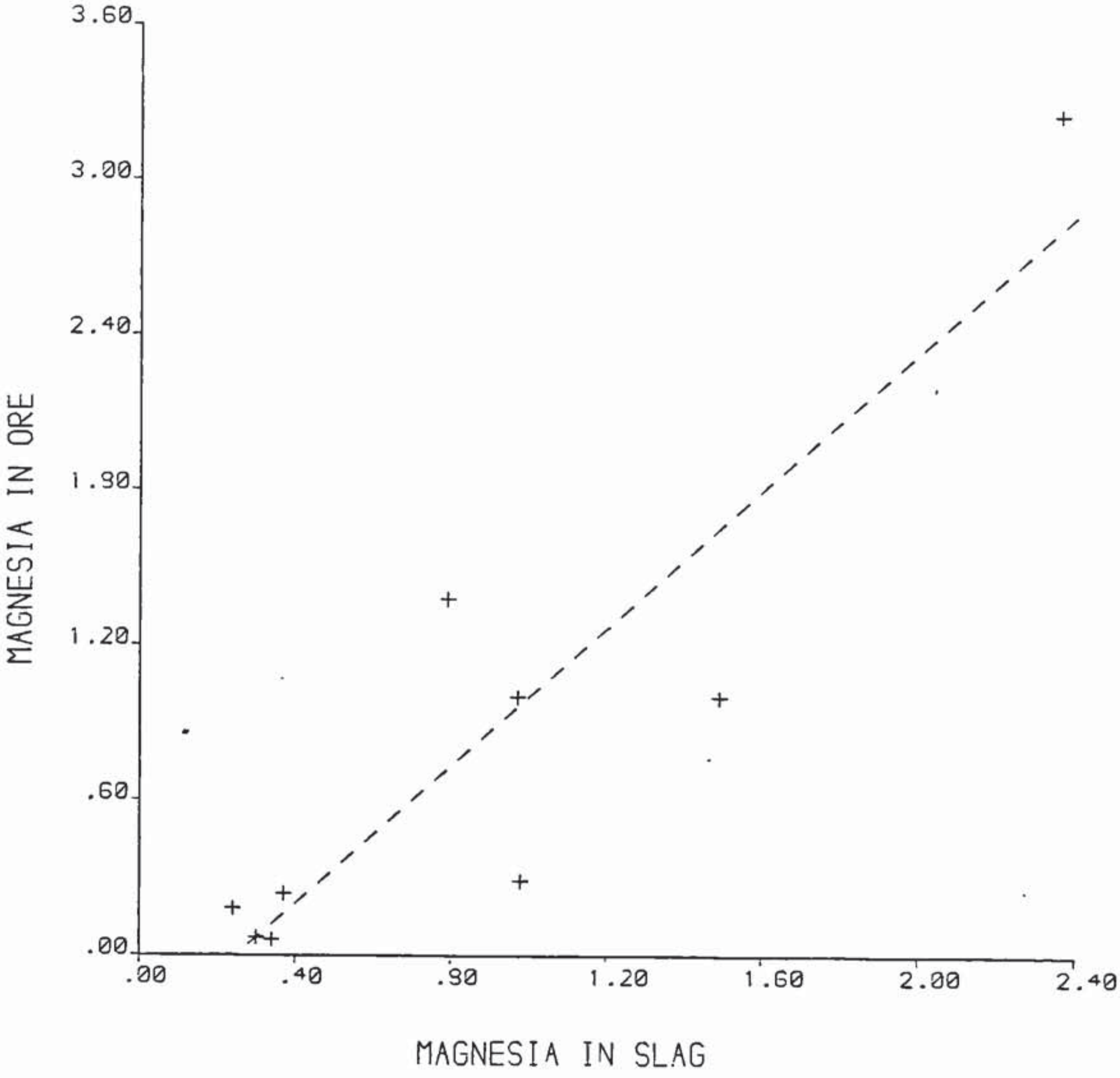

MAGNESIA IN ORE V MAGNESIA IN SLAG

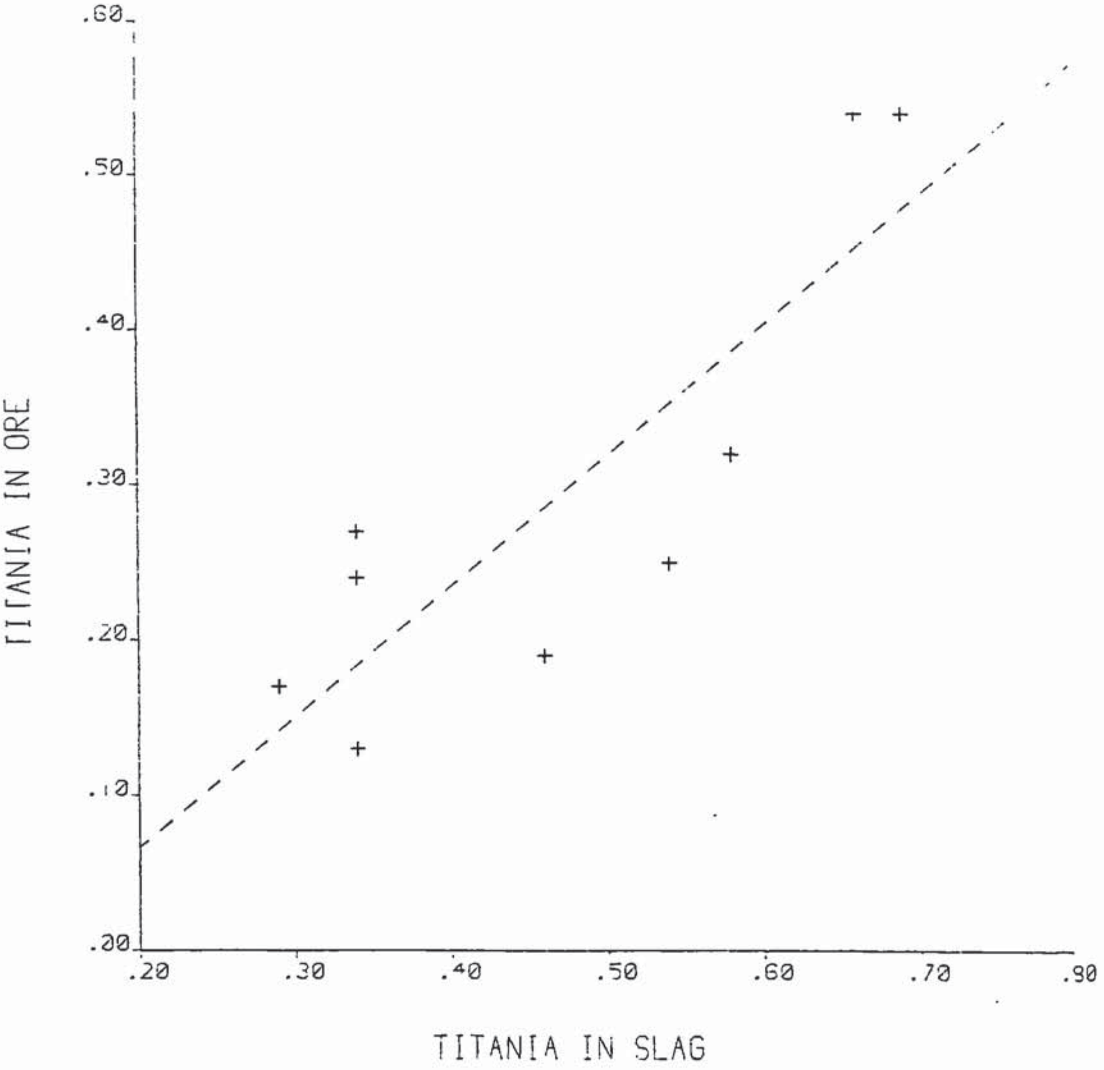

TITANIA IN ORE V TITANIA IN SLAG

Figure 5.31

Plot of the calculated values for TiO_2 in the ores against the TiO_2 content of the slags.

Figure 5.32

Plot of the partially corrected values for V_2O_5 in the ores against the Fe_2O_3 contents of the slags, all other independent variables being held at their average values.

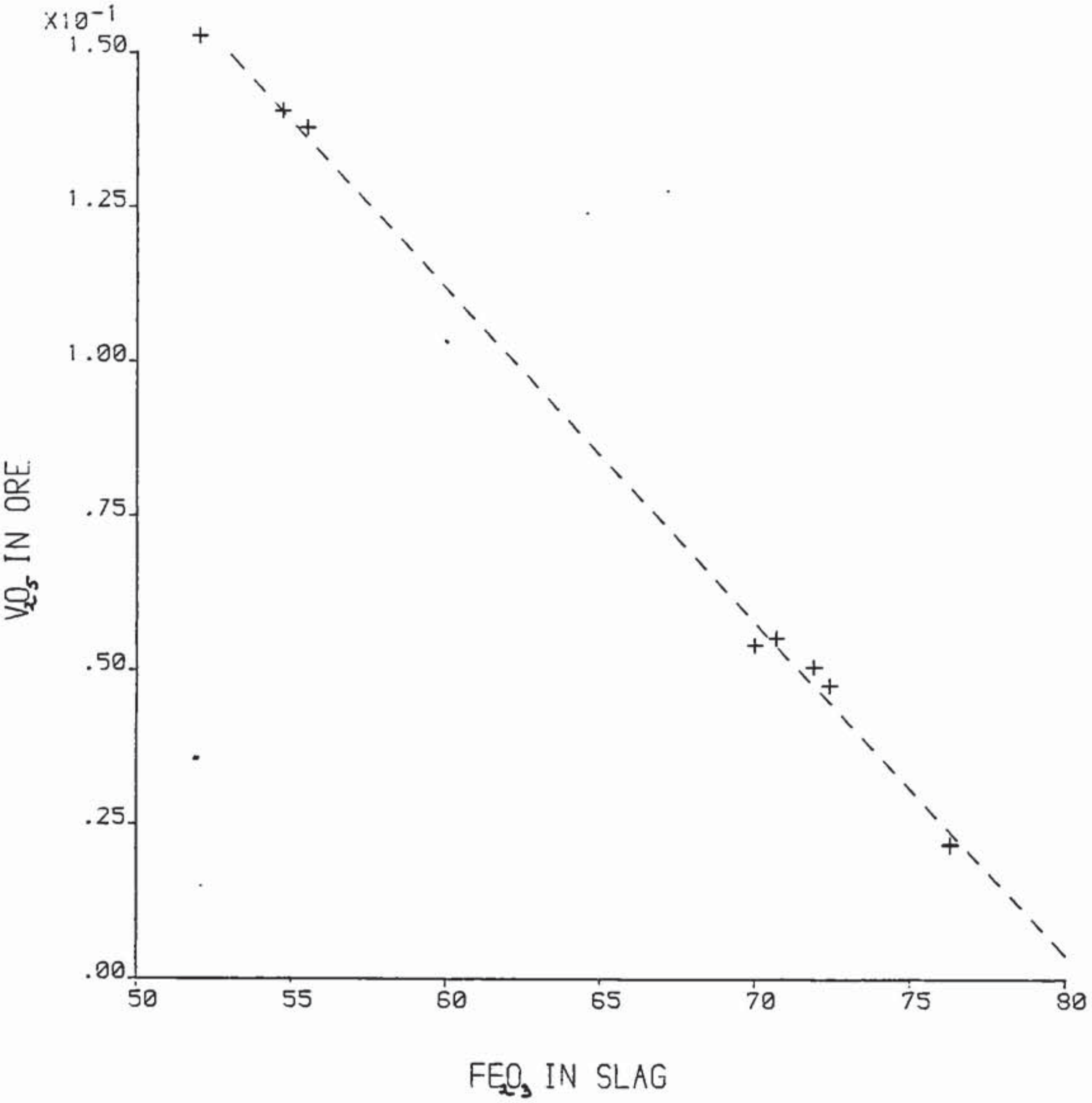

V_2O_5 IN ORE V FE_2O_3 IN SLAG

Figure 5.33

Plot of the partially corrected values for V_2O_5 in the ores against the Al_2O_3 contents of the slags, all other independent variables being held at their average values.

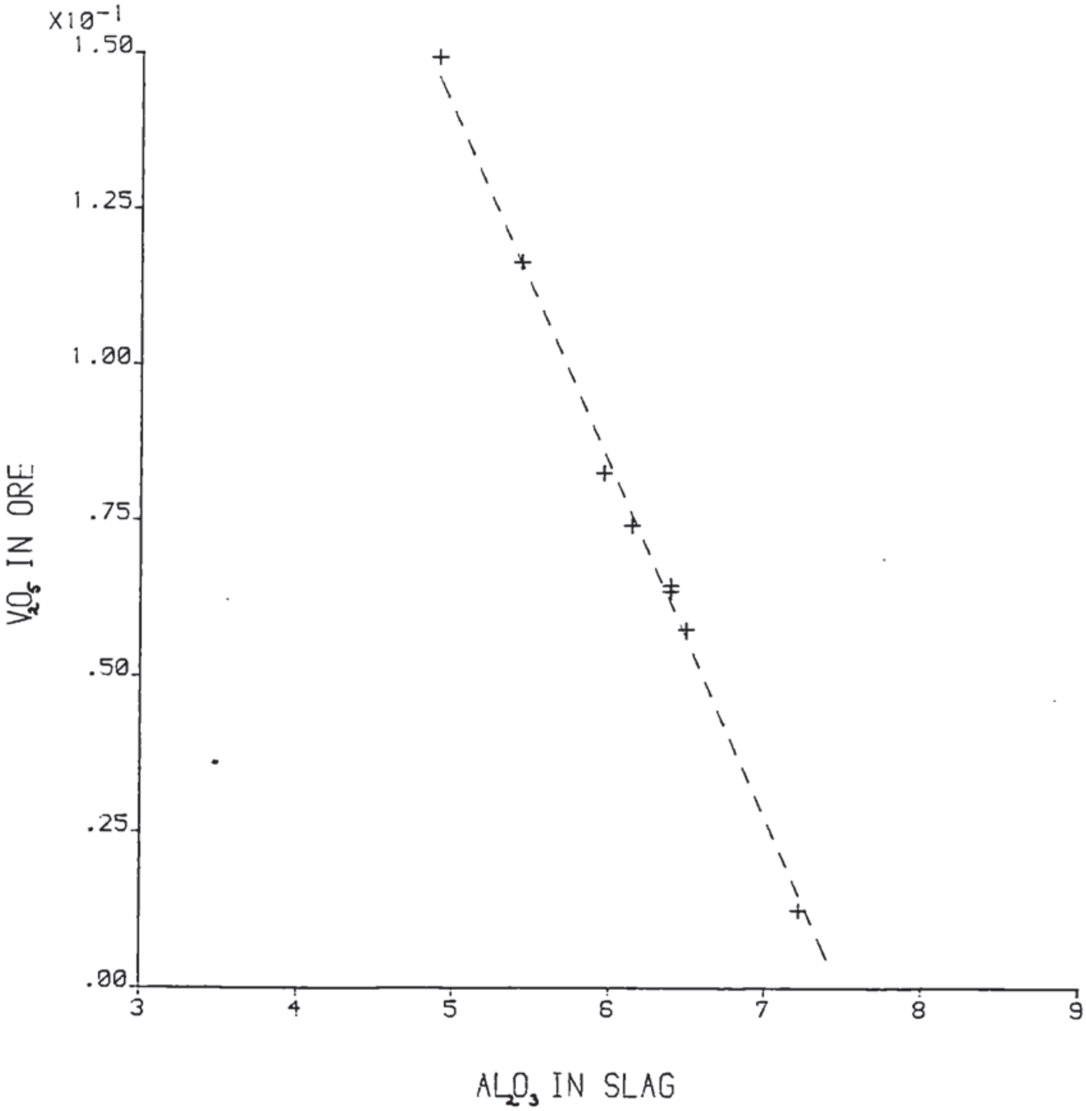

V_2O_5 IN ORE V AL_2O_3 IN SLAG

Figure 5.34

Plot of the partially corrected values for V_2O_5 in the ores against the MnO contents of the slags, all other independent variables being held at their average values.

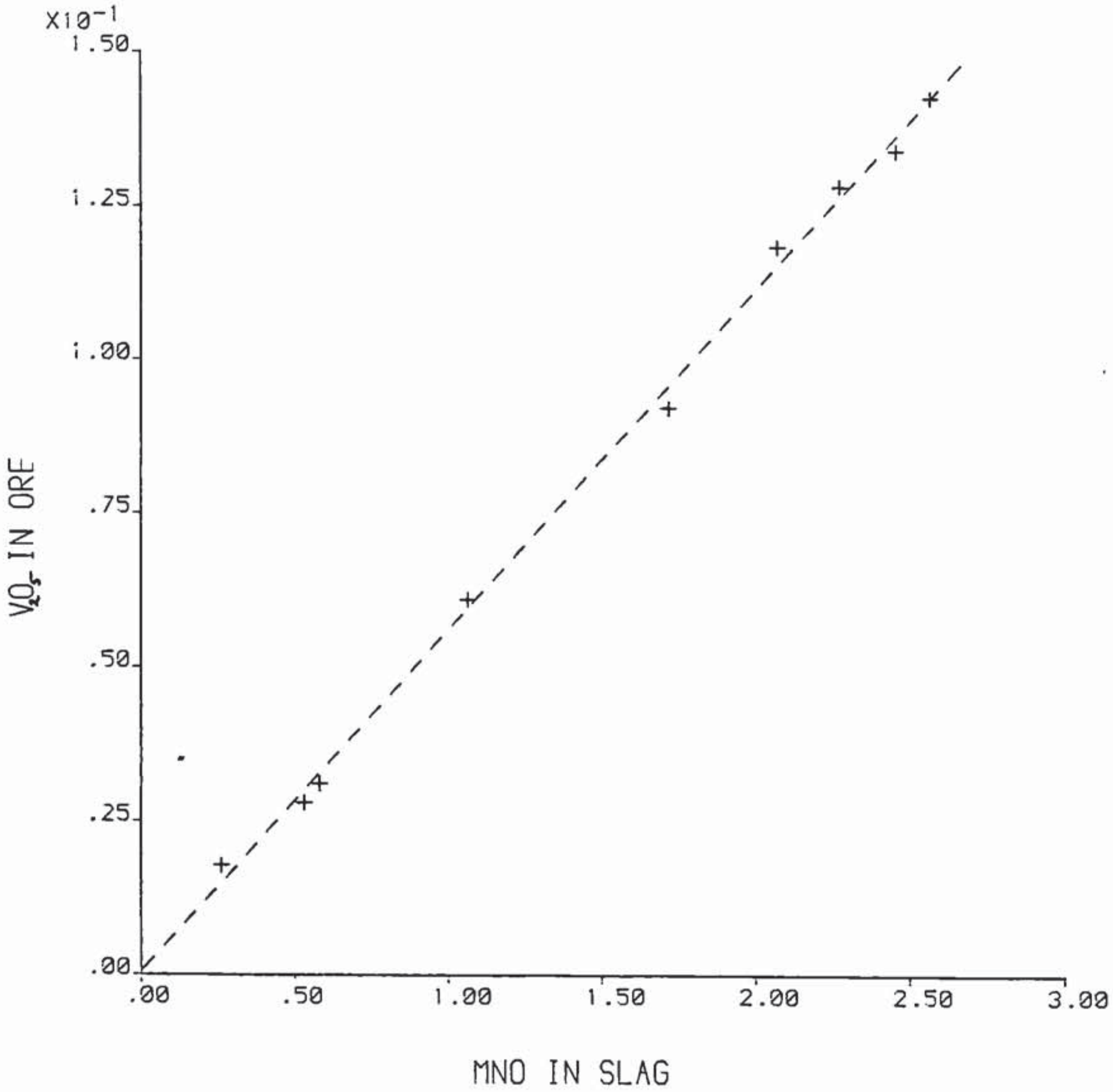

V_2O_5 IN ORE V MNO IN SLAG

Figure 5.35

Plot of the partially corrected values for V_2O_5 in the ores against the MgO contents of the slags, all other independent variables being held at their average values.

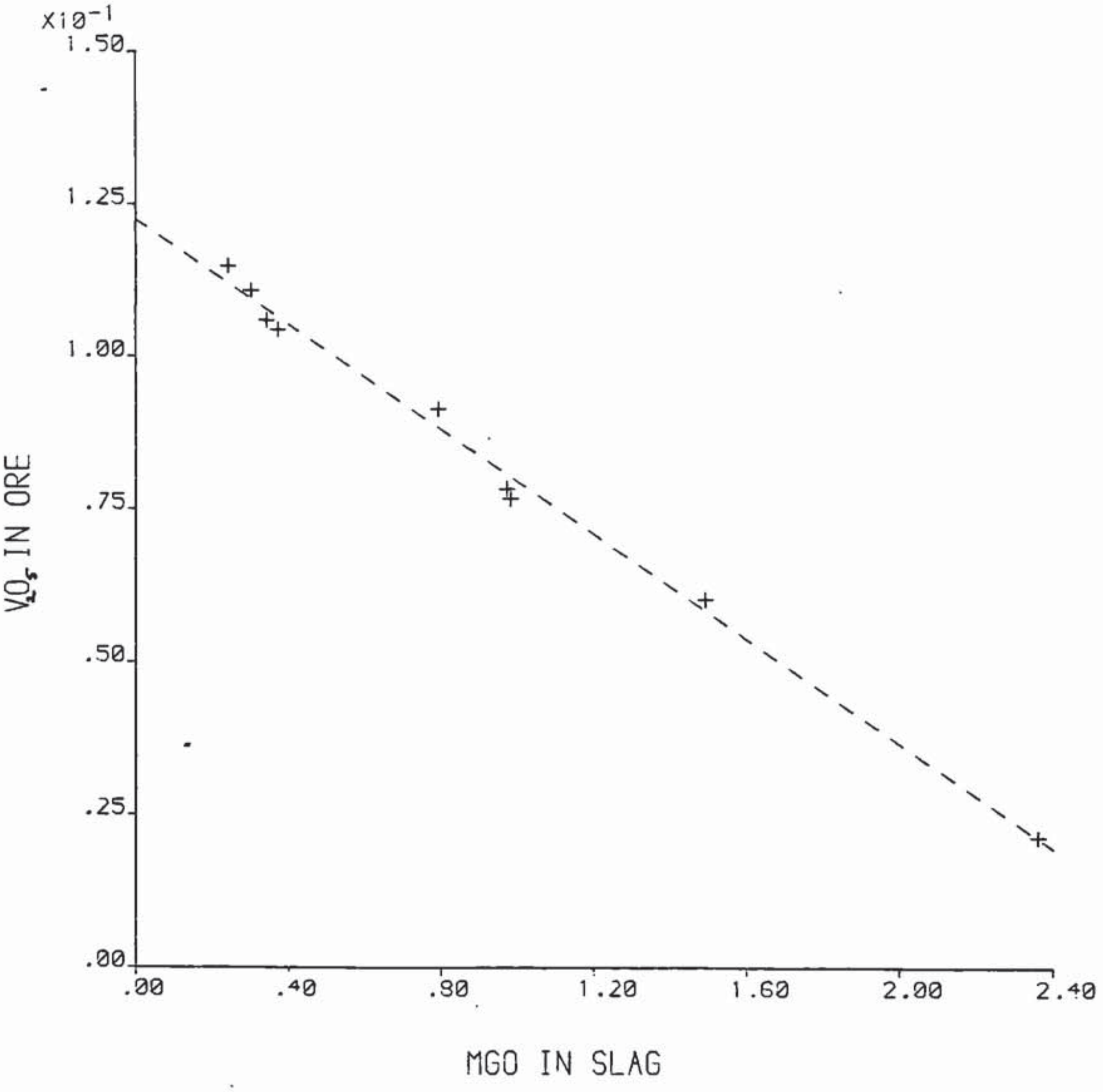

V_2O_5 IN ORE V MGO IN SLAG

Figure 5.36

Plot of the partially corrected values for V_2O_5 in the ores against the V_2O_5 contents of the slags, all other independent variables being held at their average values.

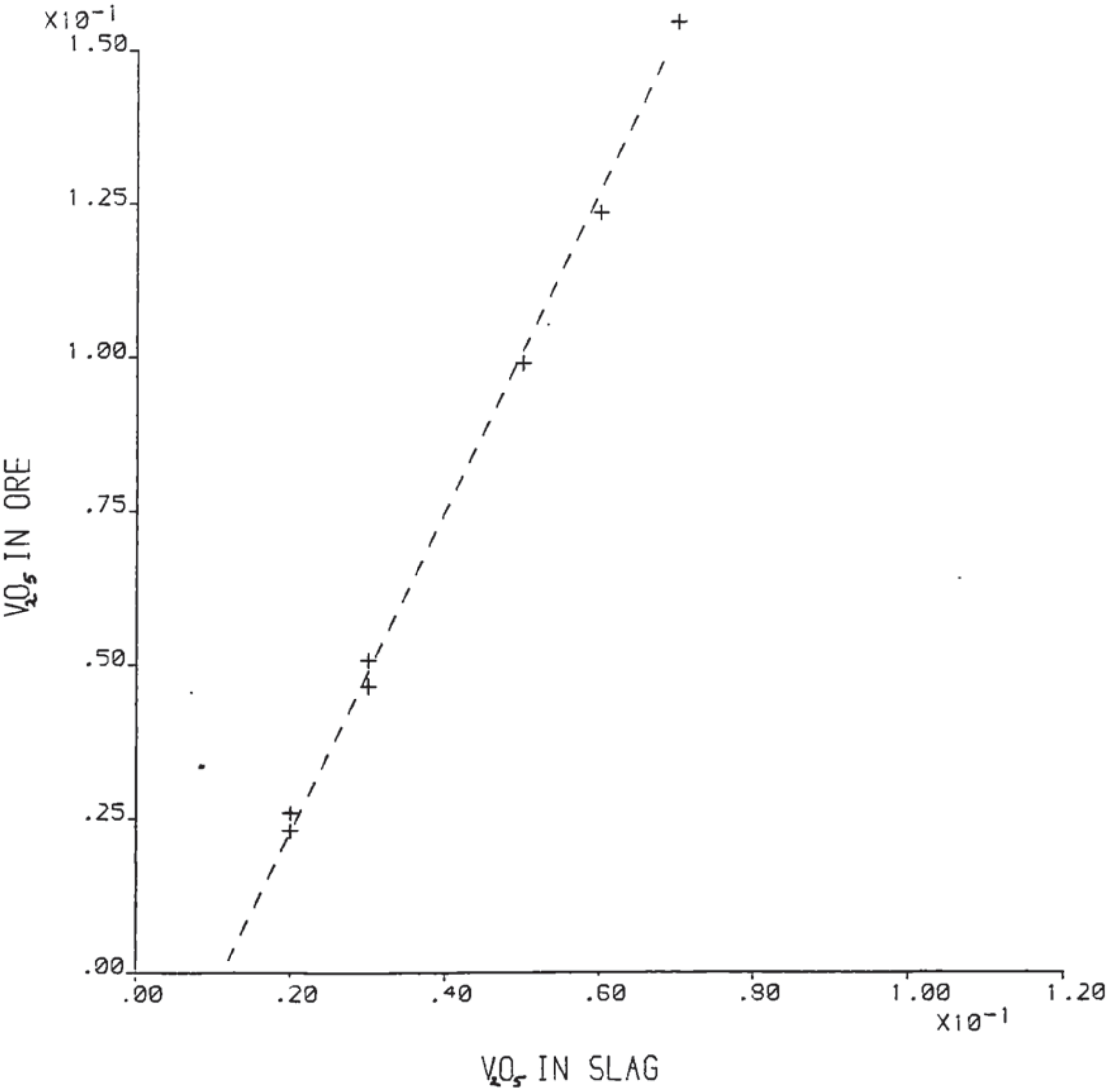

V_2O_5 IN ORE V V_2O_5 IN SLAG

APPENDIX A

List of localities from which samples were obtained, with code numbers used for individual samples.

LOCALITY AND DATE	SAMPLE	FURNACE TYPE	A.M. LAB NUMBER	EXCAVATOR'S NUMBER	NO USED IN THIS THESIS	
GREAT OAKLEY 800 BC						
	Slag	?	–	–	GO3	
	Slag	?	–	–	GO4	26
	Slag	?	–	–	GO7	43
Stream Course	Slag	?	GO 792017	–	GO 792017	–
Feature 1	Slag	?	–	from F1	from F1	–
Pit F22	Slag	?	–	from F22	from F22	–
	ore	–	–	–	GO6	42
WAKERLEY 1st BC to 3rd AD						
Ditch C	Slag	?	–	Tr. 1 (9)	WAK	–
Ditch B	Slag	?		Tr. B VII (1)	WAK 48A	9
Furnace 4, Site 4	Slag	bowl/ domed	7312610	WK/BK K4	WK K 4	8
Furnace 2, Site 4	Slag	sunken shaft	7312607	WK/AV	WK AV	7
Ditch B	ore	–	–	Tr. BVII (1)	WAK 01	5
?	ore	–	–	–	WAK 02	–
Ditch B	ore	–	–	Tr. Bx(1)		39
Field brash	Slag	Tapping	–	–	WGW	10
BLIND EYE QUARRY 2nd AD						
	Slag	Shaft Tapping	610135	–	BEQ1	29
	Slag	Shaft Tapping	610134	–	BEQ2	30
BRIGSTOCK PRE 2nd/3rd AD						
	Slag			BK 479		33
BULWICK ROMANO-BRITISH						
	Slag	Shaft Tapping	–	–	BUL.	40
BULBORNE VALLEY I.A. and R.B.						
Northchurch	Slag	Tapping	740451	T8 (26)(58)	NOR	32
	Slag	Tapping	740451	T5 (68)(215)	NOR 2	62
Bridgewater School	Slag	shaft tapping	–	–	BBS1	87
Cow Roast Marina Site	Slag	tapping	–	–	BCR 1	86
Cow Roast Orchard Site	Slag	tapping	–	–	BCR2	–
Cow Roast Esso Site	Slag	tapping	–	–	BCR3	–
(Bulk)	Slag	tapping	–	–	Bulk slag	88
Cow Roast + School	? ore	–	–	–	Bulk ore	85

LOCALITY AND DATE	SAMPLE	FURNACE TYPE	A.M. LAB NUMBER	EXCAVATOR'S NUMBER	NO USED IN THIS THESIS	REF NO
GARDEN HILL c50 BC-c35D AD						
Furnace 1, base	slag	shaft tapping	-	SL346(F433)	GH1	18
Furnace 1, pit	slag	shaft tapping	-	SL361(F431)	GH2	19
Furnace 2, base	slag	shaft tapping	-	SL357(F067)	GH3	-
Furnace on J4/5	slag	? domed	-	SL671(F773)	GH671	91
Furnace on J4/5	slag	?domed	-	SL666(F773)	FH666	-
Rampart Quarry	slag	?	-		GH631	90
Rampart Quarry	slag	?	-		GH653	89
On L10/11	? ore	-	-	GE130	GH4	-
Dump on L10	? ore	-	-	GE132	GH5	13
Under Rampart	? ore	-	-	GE126(L3,56)	GH6	53
Quarry on Site	? ore	-	-	GE127	GH7	12
	ore	-	-	SL673(I2(3))	GH673	84
PIPPINGFORD 1st AD	slag		-	-	GHE1	-
CAERWENT 1st to 4th AD						
	slag	tapping	697282	-	697282	-
	slag	tapping	697096	-	CAER	31
RAMSBURY c800 AD						
	slag	non-tapping	-	-	RAM	-
	slag	non-tapping	-	-	RAM5	61
	slag	tapping	-	RA74/15	RAM6	93
(bulk roasted)	ore	-	-	-	RAM1	58
(bulk raw)	ore	-	-	-	RAM2	59
(boxwall, raw)	ore	-	-	-	RAM3	81
(box core, raw)	ore	-	-	-	RAM4	60
MILLBROOK 9th AD						
	Slag	non-tapping	-	-	bulk	54
	Slag	non-tapping	-	-	Millbrook C	-
	slag	non-tapping	-	-	Millbrook D	57
	slag	non-tapping	-	-	Millbrook E_1	56
	slag	non-tapping	-	-	Millbrook E_2	
	slag	non-tapping	-	-	Millbrook F	-
	ore	-	-	-	limonite	55

LOCALITY AND DATE	SAMPLE	FURNACE TYPE	A.M. LAB NUMBER	EXCAVATOR'S NUMBER	NO USED IN THIS THESIS	REF NO
STAMFORD CO-OP c.1000-1050						
	slag	tapping	700128	-	700128	-
	slag	tapping	700130	-	700130	35
	slag	tapping	630532	-	630532	36
	ore	-	700075	-	700075	-
(bulk, raw)	ore	-	-	-	STAM RAW	38
(bulk, roasted)	ore	-	-	-	STAM ROASTED	37
SOUTH WITHAM c.1170-1225						
	slag	tapping	753058	s.w. 1335	South Witham	92
	ore	-	753058	s.w. 1361		
FURNACE RECONSTRUCTIONS						
Tapped	slag	shaft, tapping	-	-	GHR1	11
Furnace	slag	shaft, tapping	-	-	GHR4	50
(roasted)	ore	-	-	-	GHR2	17
(bulk raw)	ore	-	-	-	GHR3	16
(boxwall, raw)	ore	-	-	-	GHR3 box	49
(core, raw)	ore	-	-	-	GHR3 core	48
(core, raw)	ore	-	-	-	WH3	46
(bulk, raw)	ore	-	-	-	Hustmonceux	47
	slag	small shaft	-	-	GHR10	51
	slag	non-tapping	-	-	GHR11	52
	slag	bowl	-	-	RR1	14
	slag	bowl	-	-	RR2	15

ORE TYPE	LOCALITY	SAMPLE NUMBER	NO. OF XEF ANALYSIS
Ironstone Junction Band	Creeton railway cutting	Creeton	44
	Cipsham New Quarry	Clipsham, rich	21
		Clipsham, poor	20
	Ketton Portland Cement Quarry	K1	77
		K2	78
		K3	79
		K4	80
	Field brash, w. of Wakerley Great Wood	WAK 03	1
		WAK 04	2
		WAK 05	3
		WAK 06	4
	Adamix Refractories Quarry, Kings Cliffe	Adamix	24
	Woodside Quarry Wansford	Y 1 + 2	75
	Pipe trench, Castor	CAS 3	45
	Redland Aggregates Quarry, Southorpe	S 1 + 2	76
	Brookfield Cottage Pit	BC 1 + 2	63
	Cowthick Pit	Cowthick	22
Northampton Sand Ironstone	Wakerley Pit	WAK NS1	25
	Brookfield Cottage Pit	B.C.6 box	67
		B.C.6 core	68
		B.C.7	69
		B.C.8 box	70
		B.C.8 core	71
		B.C.9	72
		B.C.10	73
		B.C.11	74

ORE TYPE	LOCALITY	SAMPLE NUMBER	NO. OF XEF ANALYSIS
Boulder Clay Nodules	Wakerley Pit	WAK 010	6
		WAK B.C.	23
	Brookfield Cottage Pit	B.C. 3 + 4	64
		B.C. 4 (2)	65
		B.C. 5	66
	Great Oakley Pit	G01 (goeth)	27
		G02 (carb)	28
		G05 (bulk)	41
	Beeby's Sand Pit, Brigstock	Beeby's	34
Upper Green-Sand	Silica Sand Quarry Leighton Buzzard	LBA	82
	Arnold's Quarry Health and Reach	LBB	83

APPENDIX B

Electron probe micro-analyses of individual phases within slags. Some raster analyses of ore samples are also included.

Standards used:

Apatite	37.45%	Ca
	18.11%	P
	55.56%	0
Alkali Feldspar	13.25%	K
	9.79%	Al
	30.39%	Si
	0.40%	Na
	46.17%	0
Wollastonite	34.32%	Ca
	24.00%	Si
	0.30%	Fe
	0.12%	Mn
	41.26%	0
$Al_2 0_3$	52.91%	Al
	47.09%	0
$V_2 0_5$	56.00%	V
	44.00%	0
Mg0	60.32%	Mg
	39.68%	0
PbS	86.62%	Pb
	13.38%	S
Metallic	Fe, Ti & Mn	

- not detected
n.d. not determined

* Potassium loss under the probe beam has led to anomalously low values for this element in many of the leucite analyses. The SiO_2 and Al_2O_3 values are also correspondingly high, the normal values for these oxides being of the order of 55 wt % and 22 wt % respectively, while K_2O should be around 20 wt %. Some loss of potassium from the glass phase probably also occurred.

GREAT OAKLEY SLAG GO4

	Fayalite Area A	Fayalite Area B	Fayalite Area C	Wüstite Area A	Wüstite Area B	Wüstite Area C	Glass Area D
FeO	65.96	68.03	69.11	95.93	98.66	96.96	36.09
SiO_2	22.99	27.38	26.84	0.34	0.25	0.39	41.41
CaO	0.89	2.60	0.44	0.15	0.07	0.05	0.91
Al_2O_3	8.23	-	0.38	0.48	0.54	0.59	3.60
MnO	0.62	0.73	0.98	0.17	0.24	0.28	0.12
MgO	0.10	0.20	0.56	-	0.04	0.04	0.21
K_2O	-	0.02	0.01	0.05	0.02	0.06	0.47
P_2O_5	0.09	0.14	0.11	-	-	-	1.26
TiO_2	0.36	0.08	0.06	1.48	1.12	1.16	0.10
V_2O_5	0.08	0.02	-	0.30	0.24	0.28	0.02
	99.32	99.20	98.49	98.90	101.18	99.81	84.19

	Hercynite Area A	Hercynite Area B	Hercynite Area C	Leucite Area A *	Leucite Area B *	Leucite Area C *	Glass Area D
FeO	51.51	51.23	51.59	1.65	8.43	2.77	34.98
SiO_2	0.43	0.35	0.43	48.88	47.42	52.14	46.21
CaO	0.03	0.07	0.03	0.17	0.48	0.12	1.05
Al_2O_3	42.74	45.87	42.23	21.63	18.12	23.13	4.13
MnO	0.23	0.38	0.26	0.05	0.08	-	0.18
MgO	0.04	-	0.02	-	0.06	-	0.13
K_2O	0.01	-	-	11.09	4.51	18.10	0.60
P_2O_5	-	0.02	-	0.09	0.32	0.04	1.24
TiO_2	1.70	0.94	1.60	0.22	0.18	-	0.06
V_2O_5	0.44	0.40	0.44	0.06	0.08	0.02	-
	97.13	99.26	96.60	83.84	79.68	96.32	88.58

WAKERLEY SLAG WAK 48A

	Fayalite Area 1	Fayalite Area 2	Fayalite Area 3	Wüstite Area 1	Wüstite Area 2	Wüstite Area 3	Leucite Area 1*
FeO	64.67	63.72	69.26	95.48	95.38	98.89	1.47
SiO_2	28.09	27.43	27.21	0.32	0.64	0.39	60.77
CaO	0.66	1.75	1.15	0.04	0.15	0.10	0.01
Al_2O_3	0.15	0.21	0.11	0.63	0.93	0.43	25.76
MnO	2.30	2.13	2.17	0.81	0.60	0.65	0.03
MgO	1.53	0.30	0.42	0.10	0.02	0.06	-
K_2O	-	0.01	-	-	0.03	0.01	11.05
P_2O_5	0.05	0.09	0.02	0.02	0.02	0.02	0.02
TiO_2	0.08	0.12	0.10	1.38	2.25	0.98	0.04
V_2O_5	-	0.04	0.04	0.26	0.38	0.18	0.02
	97.53	95.80	100.48	99.04	100.40	101.71	99.17

	Leucite Area 3		Iron Grain	Iron Grain	Iron Grain	Iron Grain	Iron Grain
FeO	1.54	Fe	99.56	99.49	100.00	100.29	99.39
SiO_2	61.83	Si	-	0.09	0.03	0.02	0.03
CaO	0.04	Ca	0.03	0.09	0.03	0.02	0.03
Al_2O_3	25.98	Al	-	-	-	0.02	-
MnO	0.10	Mn	0.09	-	-	-	0.06
MgO	0.02	Mg	-	-	-	-	-
K_2O	11.49 *	K	n.d	n.d	n.d	n.d	n.d
P_2O_5	0.70	P	-	-	-	-	-
TiO_2	0.04	T	0.05	0.08	0.06	0.08	0.04
V_2O_5	-	V	0.02	0.02	0.01	0.03	-
		S	0.03	-	-	-	-
	101.74		99.78	99.74	100.11	100.47	99.54

WAKERLEY SLAG WAK 48A

	Hercynite Area 1	Hercynite Area 1	Hercynite Area 2	Hercynite Area 3	Glass Area 1	Glass Area 2	Glass Area 3
FeO	47.07	48.80	48.80	49.52	22.28	25.61	14.99
SiO_2	0.30	0.61	0.43	0.30	32.80	31.86	30.92
CaO	0.01	0.05	0.03	0.04	12.48	12.22	15.87
Al_2O_3	44.66	44.40	44.33	45.48	14.04	15.91	14.83
MnO	0.71	0.75	0.72	0.78	0.30	0.42	0.19
MgO	0.61	0.70	0.68	0.74	0.59	-	0.02
K_2O	-	-	-	0.01	5.35	3.03	5.60
P_2O_5	-	0.02	-	-	0.16	1.81	3.58
TiO_2	0.92	0.80	0.80	0.74	0.84	0.08	0.36
V_2O_5	0.57	0.46	0.57	0.53	0.04	-	-
	94.85	96.59	96.36	98.14	88.88	90.94	86.36

	Fayalite Area A	Fayalite Area A	Fayalite Area B	Glass Area A	Glass Area B	Glass nr iron	nr iron
FeO	35.20	67.52	74.76	40.85	39.86	36.03	27.62
SiO_2	34.20	24.02	20.18	21.01	28.32	26.66	24.40
CaO	0.40	0.35	0.65	10.39	7.48	9.13	15.26
Al_2O_3	23.07	3.70	1.02	8.11	9.61	12.53	12.42
MnO	0.49	0.76	0.65	0.33	0.43	0.18	0.12
MgO	0.21	0.54	0.12	0.08	-	-	0.02
K_2O	0.01	-	0.01	0.93	2.59	3.29	3.17
P_2O_5	0.64	0.64	0.57	9.17	5.04	7.47	12.33
TiO_2	0.94	0.30	0.42	0.32	0.24	0.26	0.28
V_2O_5	0.12	0.06	0.08	-	-	0.02	-
	95.08	97.89	98.46	91.19	93.57	95.57	95.62

WAKERLEY SLAG WK-AV

	Fayalite	Wüstite Area A	Wüstite Area B		Metal Area B	Iron Grain	Iron Grain
FeO	66.86	91.51	97.27	Fe	99.73	98.81	99.35
SiO_2	25.95	6.23	0.64	Si	0.02	0.05	0.03
CaO	0.96	0.14	0.05	Ca	0.07	0.08	0.04
Al_2O_3	1.10	0.37	0.65	Al	0.06	-	-
MnO	0.70	0.46	0.40	Mn	0.14	0.08	-
MgO	0.52	0.21	0.08	Mg	0.01	-	-
K_2O	0.11	-	-	K	-	0.05	0.03
P_2O_5	1.33	0.30	0.02	P	-	0.01	0.01
TiO_2	0.18	0.80	0.94	Ti	0.06	0.06	0.04
V_2O_5	0.04	0.30	0.34	V	0.02	-	0.02
S	n.d.	n.d.	n.d.	S	n.d.	0.02	0.01
	97.75	100.32	100.37		100.11	99.16	99.53

	Iron Grain	Iron Grain	Iron Grain	Iron Grain	Iron Grain	Iron Grain	Iron Grain
Fe	99.16	98.96	99.10	98.37	100.00	98.49	98.87
Si	0.13	0.04	0.02	0.04	-	0.06	0.09
Ca	0.03	0.03	0.03	0.04	0.03	0.04	0.08
Al	-	-	-	-	-	0.03	0.03
Mn	-	-	-	-	-	-	-
Mg	-	0.01	-	-	-	-	0.01
K	0.01	0.01	0.01	0.01	0.01	0.05	0.02
P	0.01	0.01	0.01	0.01	0.01	0.01	-
Ti	0.05	0.02	0.01	0.02	0.07	0.05	0.16
V	0.01	0.02	-	-	0.01	-	0.02
	99.40	99.10	99.18	98.59	100.13	98.73	

WAKERLEY SLAG WK K4

	Fayalite Area A	Fayalite Area A	Fayalite Area B	Fayalite Area C	Fayalite Area D	Wüstite Area A	Wüstite Area B
FeO	68.13	64.35	70.45	69.92	67.41	94.78	91.21
SiO_2	25.93	27.81	25.92	26.27	28.00	0.25	0.45
CaO	0.71	0.35	0.41	0.38	0.42	0.20	0.10
Al_2O_3	0.32	0.48	0.36	0.42	0.46	0.35	0.33
MnO	0.64	0.85	0.64	0.70	0.56	0.32	0.25
MgO	0.38	0.50	0.58	0.42	0.42	0.04	0.04
K_2O	0.16	0.01	-	-	0.01	0.07	0.04
P_2O_5	0.32	0.57	0.50	0.41	0.41	0.05	0.02
TiO_2	n.d.	n.d.	0.08	0.18	0.12	n.d.	0.80
V_2O_5	0.02	0.02	0.04	0.06	-	0.30	0.26
	96.61	94.97	98.98	98.76	97.81	96.37	93.50

	Wüstite Area C	Hercynite Area B	Hercynite Area D	Hercynite	Hercynite	Ca-P Phase
FeO	90.16	51.95	50.43	55.07	53.07	8.34
SiO_2	0.79	0.45	0.43	0.53	0.40	0.68
CaO	0.01	0.01	0.03	0.01	-	41.90
Al_2O_3	0.65	40.33	43.49	41.24	41.52	0.11
MnO	0.25	0.32	0.18	0.06	0.06	0.17
MgO	0.02	0.10	0.10	0.08	0.08	0.08
K_2O	0.23	-	0.01	0.01	0.38	0.55
P_2O_5	0.02	-	0.02	0.02	-	39.80
TiO_2	1.42	2.99	3.40	3.16	2.71	0.04
V_2O_5	0.42	0.79	0.61	0.95	0.04	-
	93.97	96.94	98.70	101.13	98.26	91.67

WAKERLEY SLAG WK K4

	Leucite Area C *	Leucite *	Leucite *	Leucite *	Leucite * (raster)	Leucite *	Glass Area D Oxide
FeO	4.31	2.29	1.07	1.58	1.76	1.52	12.82
SiO_2	53.45	55.11	54.02	57.39	50.81	59.56	46.61
CaO	0.25	0.04	0.01	0.01	0.03	-	10.95
Al_2O_3	23.69	22.82	19.71	23.13	23.22	26.01	13.42
MnO	0.14	-	0.03	0.03	0.05	-	0.06
MgO	0.02	0.02	-	-	-	-	0.06
K_2O	5.45	19.37	18.74	19.20	19.04	7.84	1.99
P_2O_5	0.34	0.11	0.50	0.25	0.11	0.12	6.97
TiO_2	0.08	0.08	0.06	0.06	0.08	0.06	0.12
V_2O_5	0.04	-	0.04	0.02	-	-	-
	89.77	99.84	94.23	101.67	95.1	95.51	93.05

	Glass Area B	Glass	Glass		Iron Grain	Iron Grain	Iron Grain
FeO	8.43	4.43	30.10	Fe	95.05	98.28	99.07
SiO_2	41.50	39.50	25.80	Si	-	-	0.04
CaO	9.03	1.63	7.51	Ca	-	0.03	-
Al_2O_3	19.40	17.55	3.71	Al	-	-	-
MnO	0.11	-	0.05	Mn	-	0.04	-
MgO	0.02	-	0.02	Mg	0.03	-	-
K_2O	7.57	12.83	8.69	K	0.02	-	-
P_2O_5	9.42	8.25	6.03	P	0.01	-	0.05
TiO_2	0.10	0.32	0.72	Ti	n.d.	0.06	
V_2O_5	-	0.09	0.15	V	0.02	-	-
	95.58	84.6	82.78		95.14	98.41	99.16

WAKERLEY ORES

	WAK 02 (from site)			WAK 03 (field brash)		
	Area A	Area B	Area C	Area A	Area B	Area C
Fe_2O_3	76.57	81.51	80.19	67.96	52.34	63.80
SiO_2	2.88	2.33	2.15	12.36	19.43	16.48
CaO	0.36	0.34	0.31	0.07	0.12	0.05
Al_2O_3	1.02	0.59	0.78	0.94	2.85	1.21
MnO	0.51	0.35	0.29	0.16	0.14	0.05
MgO	0.05	0.06	0.04	0.08	0.06	-
K_2O	0.20	0.11	0.13	0.08	0.22	0.08
P_2O_5	0.05	0.02	0.05	-	0.05	0.02
TiO_2	0.04	0.06	0.04	0.28	0.10	0.14
V_2O_5	0.02	-	0.04	0.04	0.04	0.02
	81.70	85.36	84.02	81.97	75.35	81.85

WEST HOATHLY ORE (roasted: A, B & C core, D, E, F, boxwall)

	Area A	Area B	Area C	Area D	Area E	Area F
Fe_2O_3	57.00	58.25	55.84	49.46	42.52	52.34
SiO_2	14.13	23.64	19.16	22.88	27.69	18.33
CaO	1.92	3.18	3.24	2.30	2.02	2.50
Al_2O_3	4.33	5.35	5.78	6.53	7.66	7.05
MnO	1.27	2.21	2.27	1.83	1.75	1.91
MgO	1.51	1.68	1.57	1.74	1.80	1.97
K_2O	0.50	0.77	0.97	0.99	1.07	0.01
P_2O_5	0.46	0.69	0.62	0.37	0.37	0.50
TiO_2	0.28	0.44	0.74	1.06	0.60	0.96
V_2O_5	0.06	0.08	0.08	0.12	0.12	0.10
	81.46	96.29	90.27	87.28	85.60	85.67

GARDEN HILL ORES

	GH5 (unroasted boxstone)			GH6 (roasted boxstone)		
	Area A	Area B	Area C	Area A	Area B	Area C
Fe_2O_3	57.14	60.91	57.97	44.85	55.67	44.04
SiO_2	28.20	23.54	22.42	27.19	18.16	25.03
CaO	0.08	0.07	0.11	0.20	0.25	0.25
Al_2O_3	6.27	4.62	4.52	10.01	8.96	8.84
MnO	0.36	0.34	0.36	0.31	0.21	0.18
MgO	0.10	0.10	0.12	0.51	0.50	0.35
K_2O	0.87	0.72	0.80	1.76	1.31	1.02
P_2O_5	0.66	0.64	0.64	0.55	0.71	0.50
TiO_2	0.54	0.56	0.30	1.14	0.50	0.40
V_2O_5	0.10	0.10	0.06	0.18	0.10	0.10
	94.32	91.65	87.30	86.69	86.37	80.71

GH4 (Boxstone from sandstone)

	Area A	Area B	Area C
Fe_2O_3	16.56	10.42	17.70
SiO_2	79.53	89.00	79.36
CaO	0.07	0.03	0.08
Al_2O_3	2.63	2.58	1.08
MnO	0.03	-	0.08
MgO	0.11	-	0.04
K_2O	0.13	0.08	0.08
P_2O_5	0.02	0.02	0.07
TiO_2	0.14	0.08	0.14
V_2O_5	0.06	-	0.02
	99.28	102.21	98.65

GARDEN HILL SLAG GH1

	Fayalite Area 1	Fayalite Area 2	Fayalite Area 3	Wüstite Area 1	Wüstite Area 2	Wüstite Area 3
FeO	67.99	68.25	67.52	97.72	97.13	98.88
SiO_2	27.40	27.25	27.20	0.34	0.48	0.48
CaO	1.04	1.22	3.00	0.09	0.10	0.26
Al_2O_3	0.21	0.25	0.17	0.52	0.33	0.48
MnO	1.11	1.21	0.86	0.43	0.40	0.24
MgO	0.62	0.52	0.28	0.06	0.08	0.02
K_2O	-	0.01	0.01	0.02	0.01	0.07
P_2O_5	0.12	0.18	0.12	0.02	-	0.02
TiO_2	0.08	0.08	0.10	0.68	0.66	0.98
V_2O_5	0.04	0.04	0.04	0.10	0.12	0.18
	98.61	97.55	99.30	99.98	99.31	101.61

	Glass Area 1	Glass Area 2	Glass Area 3	Glass nr clay	Glass nr clay
FeO	27.67	26.53	31.28	25.02	29.82
SiO_2	33.15	35.02	34.26	42.56	40.93
CaO	12.71	13.31	14.44	7.37	4.77
Al_2O_3	18.23	17.33	12.30	14.55	12.98
KnO	0.34	0.43	0.26	0.28	0.26
MgO	0.04	0.06	0.04	0.08	0.11
K_2O	2.87	3.00	4.55	1.98	2.73
P_2O_5	1.35	1.28	1.60	0.76	0.62
TiO_2	0.22	0.18	0.42	1.10	1.10
V_2O_5	0.04	0.02	0.08	0.16	0.66
	95.62	97.16	99.23	93.86	93.98

GARDEN HILL SLAG GH2

	Fayalite Area 1	Fayalite Area 2	Fayalite Area 3	Wüstite Area 1	Wüstite Area 2	Wüstite Area 4
FeO	61.30	61.89	62.13	91.07	93.03	93.83
SiO_2	26.31	27.19	27.73	0.59	0.47	0.41
CaO	2.46	2.23	3.14	0.07	0.41	0.12
Al_2O_2	0.11	0.06	0.13	0.69	0.48	0.93
MnO	2.71	2.47	1.97	0.80	0.59	0.64
MgO	2.21	1.67	2.18	0.08	-	0.06
K_2O	-	0.03	1.04	-	0.05	-
P_2O_5	0.09	0.12	0.12	-	0.02	0.02
TiO_2	0.06	0.08	0.04	0.74	0.90	0.78
V_2O_5	0.02	0.02	-	0.16	0.16	0.16
	95.27	95.76	98.48	94.20	96.11	96.95

	Glass Area 1	Glass Area 2	Glass Area 3
FeO	26.14	27.57	41.28
SiO_2	31.62	32.53	30.59
CaO	14.81	15.09	3.58
Al_2O_3	15.42	12.16	10.30
MnO	0.71	0.77	0.90
MgO	0.04	0.02	0.08
K_2O	2.94	3.11	0.59
P_2O_2	1.56	1.17	1.28
TiO_2	0.34	0.38	0.10
V_2O_5	0.08	0.04	-
	93.66	92.84	88.70

GARDEN HILL SLAG GH631

	Fayalite Area 1	Fayalite Area 2	Fayalite Area 3	Wüstite Area 2	Wüstite Area 3	Hercynite Area 1	Hercynite Area 2
FeO	65.25	61.73	67.19	95.26	98.12	43.76	46.93
SiO_2	26.87	26.64	25.86	0.25	0.41	0.18	0.28
CaO	0.36	1.99	0.62	0.06	0.17	0.03	0.01
Al_2O_3	0.19	0.84	0.23	0.09	0.35	48.69	44.99
MnO	2.60	2.46	2.57	0.56	0.67	1.08	0.91
MgO	0.84	1.47	0.82	0.02	-	1.67	1.30
K_2O	-	0.02	-	0.04	0.03	-	-
P_2O_5	0.21	0.16	0.34	-	-	-	0.02
TiO_2	0.08	0.10	0.06	0.48	0.34	0.24	0.50
V_2O_5	0.02	-	-	0.12	0.10	0.18	0.16
	96.42	95.41	97.69	96.88	100.19	96.03	95.10

	Hercynite Area 3	Leucite Area 1 *	Leucite Area 3 *	Leucite Area 4 *	Glass Area 1	Glass Area 2	Glass Area 4
FeO	51.68	6.33	9.22	1.68	21.75	38.56	19.76
SiO_2	0.18	52.20	45.89	60.11	30.65	32.53	37.90
CaO	0.04	0.06	0.87	0.01	10.79	3.83	11.25
Al_2O_2	41.99	22.68	20.19	25.31	13.85	14.80	16.75
MnO	0.79	0.03	0.13	0.05	0.89	0.32	0.59
MgO	0.15	-	0.02	-	0.02	0.02	-
K_2O	-	15.48	16.11	18.58	1.16	7.40	3.36
P_2O_5	0.02	0.14	1.63	0.09	1.13	0.21	3.35
TiO_2	0.74	0.06	0.08	0.06	3.52	0.54	0.86
V_2O_5	0.22	0.04	0.04	0.02	0.85	0.16	0.20
	95.81	97.02	94.18	105.91	84.81	98.37	94.20

GARDEN HILL SLAG GH671

	Fayalite Area A	Fayalite Area B	Wüstite Area A	Wüstite Area B	Hercynite Area A	Hercynite Area B
FeO	63.28	61.55	95.78	89.23	51.90	50.12
SiO_2	25.64	26.94	1.04	3.05	5.58	2.27
CaO	0.45	0.35	0.07	0.09	0.29	0.13
Al_2O_3	0.27	0.51	0.20	1.23	35.04	40.03
MnO	2.76	2.98	0.88	1.13	1.27	1.08
MgO	0.28	0.62	0.02	0.04	0.10	0.15
K_2O	0.01	0.02	0.08	0.04	0.01	0.01
P_2O_5	0.23	0.39	0.02	0.16	0.07	0.05
TiO_2	0.16	0.18	0.58	4.87	2.00	1.62
V_2O_5	-	0.04	0.07	0.74	0.35	0.31
	93.08	93.91	98.74	100.61	96.61	95.87

	Leucite Area A*	Leucite Area B*	Ca-P Phase A	Ca-P Phase B
FeO	3.50	2.83	35.46	12.71
SiO_2	57.10	56.26	18.74	5.13
CaO	-	-	14.22	32.21
Al_2O_3	24.28	24.31	2.41	0.26
MnO	0.05	0.05	1.46	0.50
MgO	-	-	0.16	0.10
K_2O	16.85	17.55	0.33	0.42
P_2O_5	0.12	0.07	20.83	28.82
TiO_2	0.02	-	0.06	0.06
V_2O_5	0.02	0.02	-	0.02
	101.94	101.09	93.67	80.23

GARDEN HILL SLAG GH653a

	Fayalite Area A	Fayalite Area B	Fayalite Area C	Wüstite Area A	Wüstite Area B	Wüstite Area C
FeO	59.51	60.57	60.30	97.94	96.90	95.08
SiO_2	28.41	28.71	27.85	0.30	0.43	0.32
CaO	5.65	4.80	4.34	0.16	0.20	0.17
Al_2O_3	0.27	0.06	0.06	0.46	0.54	0.61
MnO	2.83	2.90	2.83	0.89	0.72	0.82
MgO	1.35	1.47	1.29	0.04	0.06	0.10
K_2O	0.23	0.01	0.02	0.01	0.03	0.07
P_2O_5	0.09	0.09	0.09	-	-	-
TiO_2	0.04	0.06	0.06	0.70	0.72	0.66
V_2O_5	-	-	-	0.10	0.10	0.10
	98.38	98.67	96.84	100.60	99.70	97.93

	Glass Area A	Glass Area B	Glass Area C		Iron Area B
FeO	18.51	24.25	21.69	Fe	101.46
SiO_2	39.11	38.66	37.04	Si	0.03
CaO	9.82	10.45	9.81	Ca	0.11
Al_2O_3	19.22	15.76	17.71	Al	-
MnO	0.53	0.71	0.73	Mn	0.03
MgO	0.08	0.23	0.11	Mg	-
K_2O	5.55	7.95	7.04	K	0.03
P_2O_5	1.90	1.56	2.09	P	-
TiO_2	0.14	0.12	0.16	Ti	0.02
V_2O_5	-	0.04	-	V	0.01
	94.86	99.73	96.38		101.69

GARDEN HILL SLAG GH666

	Fayalite Area A	Fayalite Area B	Fayalite Area C	Wüstite Area A	Wüstite Area B	Wüstite Area C
FeO	68.06	68.94	68.97	90.57	95.17	95.79
SiO_2	26.69	26.49	26.36	4.89	1.34	1.56
CaO	0.41	0.74	0.44	0.25	0.23	0.09
Al_2O_3	0.25	0.23	0.25	0.67	0.63	0.61
MnO	3.12	2.88	3.16	1.13	0.82	1.09
MgO	1.83	1.12	1.43	0.39	0.04	0.06
K_2O	0.01	-	0.01	0.01	0.01	0.26
P_2O_5	0.11	0.21	0.21	0.07	0.16	-
TiO_2	0.08	0.10	0.10	1.62	1.02	0.72
V_2O_5	0.02	0.04	-	0.24	0.16	0.14
	100.58	100.75	100.93	99.84	99.58	100.32

	Hercynite Area A	Hercynite Area B	Hercynite Area C	Leucite Area A*	Glass Area B	Glass Area C
FeO	51.66	48.94	51.76	5.56	33.54	45.02
SiO_2	0.55	0.18	0.72	52.27	39.75	25.76
CaO	0.01	0.04	0.04	-	0.30	2.65
Al_2O_3	40.95	42.14	38.47	24.71	15.51	9.98
MnO	1.12	1.08	1.15	0.18	0.05	1.94
MgO	1.28	1.25	0.56	0.01	0.02	0.94
K_2O	-	0.01	-	14.29	9.48	3.77
P_2O_5	-	-	0.02	0.21	0.07	1.19
TiO_2	1.50	0.90	1.54	0.26	0.52	0.56
V_2O_5	0.49	0.46	0.30	-	0.12	0.08
	97.56	95.00	94.56	97.49	96.01	91.84

PIPPINGFORD BLOOMERY SLAG GHE1

	Fayalite Area A	Fayalite Area B	Fayalite Area C	Fayalite Area D	Hercynite Area C	Hercynite Area C
FeO	66.49	61.62	65.92	62.23	48.21	47.50
SiO_2	27.01	27.29	26.83	27.86	0.43	0.40
CaO	0.26	0.12	0.26	0.12	0.03	0.03
Al_2O_3	0.17	0.13	0.17	0.11	42.52	44.51
MnO	2.41	3.73	2.54	3.68	-	1.01
MgO	0.32	1.18	0.52	1.78	0.44	0.21
K_2O	0.02	0.02	-	0.03	-	-
P_2O_5	0.25	0.21	0.14	0.12	0.02	0.02
TiO_2	0.14	0.12	0.18	0.14	1.95	1.89
V_2O_5	0.08	0.06	-	0.02	0.34	0.28
	97.15	95.11	96.56	96.04	93.94	95.85

	Leucite Area A *	Glass Area A	Glass Area B	Glass Area D
FeO	2.06	54.60	12.31	12.68
SiO_2	58.54	8.40	57.48	52.39
CaO	0.16	0.33	1.88	2.00
Al_2O_3	23.75	9.76	15.97	19.52
MnO	0.03	0.10	1.00	0.98
MgO	-	-	0.18	0.37
K_2O	5.43	0.37	2.81	3.52
P_2O_5	0.46	7.95	0.83	0.44
TiO_2	0.12	0.20	1.25	1.07
V_2O_5	0.08	0.04	0.16	0.18
	90.63	81.75	93.87	93.15

STAMFORD SLAG 700130 (Thin section)

	Fayalite Area A	Fayalite Area B	Wustite Area A	Wustite Area B	Glass Area A	Glass Area B
FeO	66.51	67.67	93.66	93.62	22.76	18.54
SiO_2	26.84	26.23	0.45	2.94	33.99	34.37
CaO	1.15	0.58	0.19	0.20	11.81	14.17
Al_2O_3	0.25	0.40	0.59	0.87	15.87	16.25
MnO	0.43	0.40	0.10	0.10	0.08	0.05
MgO	0.34	0.48	0.06	-	-	-
K_2O	0.32	0.02	0.04	0.02	5.60	6.49
P_2O_5	0.35	0.37	0.02	0.07	3.03	5.02
TiO_2	0.10	0.12	1.06	1.04	0.24	0.26
V_2O_5	0.04	0.04	0.48	0.42	0.06	0.06
S	n.d.	n.d.	n.d.	n.d.	n.d.	0.58
	96.33	96.31	96.75	99.28	93.44	95.79

	Iron Area A	Iron Area B
Fe	97.69	97.57
Si	0.06	0.19
Ca	0.06	0.07
Al	-	-
Mn	0.05	-
Mg	-	-
K	-	0.01
P	-	0.01
Ti	0.04	0.02
V	-	0.01
S	-	0.01
	97.90	97.89

RAMSBURY SLAG RAM5

	Fayalite Area A	Fayalite Area B	Fayalite Area C	Wüstite Area A	Wüstite Area B	Wüstite Area D
FeO	64.80	64.41	65.17	96.04	96.80	97.46
SiO_2	27.45	27.57	27.96	0.45	0.41	0.36
CaO	0.42	0.45	0.67	0.07	0.03	0.06
Al_2O_3	0.17	0.17	0.13	1.26	1.11	1.93
MnO	2.58	2.46	2.60	0.86	0.95	0.88
MgO	2.91	3.03	2.60	0.10	0.23	0.06
K_2O	0.01	0.01	0.03	-	0.09	0.01
P_2O_5	0.32	0.14	0.12	-	-	-
TiO_2	0.06	0.02	0.08	0.80	0.76	0.92
V_2O_5	0.02	-	0.04	0.44	0.40	0.48
	98.74	98.26	99.40	100.02	100.78	102.16

	Glass Area A	Glass Area B	Glass Area C	Hercynite Area B	Pale Ca-Phase
FeO	16.17	12.13	24.64	51.56	19.77
SiO_2	29.22	49.21	34.50	1.48	35.26
CaO	9.92	0.01	0.46	0.07	18.29
Al_2O_3	23.25	21.55	29.16	43.03	12.56
MnO	0.33	0.16	0.34	0.93	0.53
MgO	0.04	-	0.02	0.30	-
K_2O	9.10	14.26	9.87	0.01	0.99
P_2O_5	8.13	0.09	0.14	-	2.02
TiO_2	0.48	0.12	1.80	1.66	0.40
V_2O_5	0.06	0.04	0.35	0.51	-
	96.70	97.57	101.31	99.55	89.82

RAMSBURY SLAG RAM

	Fayalite	Wustite	Glass	Pale Ca-Phase
FeO	66.01	86.17	11.40	15.94
SiO_2	26.79	4.86	51.52	18.50
CaO	0.72	0.37	0.66	35.65
Al_2O_3	0.19	0.67	21.14	10.76
MnO	2.31	1.25	0.13	0.44
MgO	0.60	0.17	-	0.08
K_2O	0.04	0.06	11.82	1.01
P_2O_5	0.23	0.05	0.23	7.70
TiO_2	0.06	1.38	0.30	0.44
V_2O_5	0.04	0.26	0.06	-
	96.99	95.24	97.26	90.52

NORTHCHURCH SLAG NOR 1

	Fayalite Area A	Fayalite Area B	Fayalite Area C	Glass Area A	Glass Area B	Glass Area C
FeO	67.59	67.08	55.72	30.91	27.81	28.86
SiO_2	27.06	27.04	34.44	40.60	45.16	43.24
CaO	0.49	0.71	1.84	7.13	11.99	10.03
Al_2O_3	0.02	0.13	3.46	8.97	8.54	8.90
MnO	1.15	1.04	0.80	0.35	0.26	0.29
MgO	0.28	0.10	0.02	0.04	-	0.02
K_2O	0.01	0.02	1.79	4.31	1.86	2.73
P_2O_5	0.07	0.14	0.30	0.96	0.85	0.87
TiO_2	0.08	0.06	0.10	0.34	0.18	0.22
V_2O_5	-	-	0.02	0.08	-	-
	96.75	96.32	98.49	93.69	96.65	95.16

	Magnetite Area A	Magnetite Area B	Magnetite Area C
Fe_3O_4	90.74	87.88	79.84
SiO_2	0.94	2.53	4.73
CaO	0.09	0.42	0.40
Al_2O_3	4.31	3.51	3.31
MnO	0.21	0.19	0.19
MgO	0.02	-	-
K_2O	0.02	0.23	0.35
P_2O_5	0.02	0.05	0.09
TiO_2	3.19	2.83	2.11
V_2O_5	0.55	0.53	0.38
	100.09	98.17	97.32

CAERWENT SLAG 697096

	Fayalite Area A	Fayalite Area B	Fayalite Area C	Fayalite Area D	Glass Area B	Glass Area C
FeO	61.13	61.57	67.63	63.64	7.10	22.09
SiO_2	28.20	28.05	27.87	25.59	66.32	51.16
CaO	0.47	0.31	0.40	0.35	1.02	1.03
Al_2O_3	0.44	0.34	0.11	0.57	10.40	4.44
MnO	0.22	0.34	0.44	0.44	0.10	0.11
MgO	0.20	-	1.87	1.53	0.37	0.25
K_2O	0.02	0.01	-	-	0.28	0.85
P_2O_5	-	0.07	0.02	0.02	0.75	1.31
TiO_2	0.06	0.04	0.04	0.08	0.12	0.12
V_2O_5	-	-	0.02	0.02	0.02	0.02
	90.74	90.73	98.40	92.24	86.48	84.38

	Wüstite Area A	Wüstite Area B	Wüstite Area C	Wüstite Area D
FeO	96.19	95.60	96.42	96.00
SiO_2	0.34	0.29	0.43	0.32
CaO	0.04	0.04	0.04	0.04
Al_2O_3	0.54	0.48	0.43	0.69
MnO	0.13	0.15	0.27	0.13
MgO	0.13	0.10	0.21	0.06
K_2O	-	0.01	0.04	-
P_2O_5	-	-	-	-
TiO_2	0.28	0.28	0.32	0.26
V_2O_5	0.06	0.06	0.06	0.06
	97.71	97.11	98.22	97.56

BULWICK SLAG

	Fayalite Area 1	Fayalite Area 2	Fayalite Area 3	Fayalite Area 4	Wüstite Area 1	Wüstite Area 2	Wüstite Area 4
FeO	64.61	68.94	69.56	68.15	90.41	83.53	86.01
SiO_2	26.62	27.23	26.45	27.06	4.98	7.80	3.97
CaO	0.41	0.29	0.31	0.26	0.41	1.96	1.31
Al_2O_3	0.44	0.40	0.51	0.25	1.36	3.66	1.38
MnO	1.15	1.63	1.54	1.55	0.32	0.23	0.30
MgO	0.48	0.50	0.46	0.38	-	-	0.08
K_2O	0.02	0.01	0.01	-	0.34	0.98	0.44
P_2O_5	0.05	0.05	0.05	0.02	0.07	0.09	-
TiO_2	0.10	0.14	0.10	0.08	1.58	1.50	1.20
V_2O_5	0.04	0.02	0.04	0.02	0.18	0.18	0.10
	93.92	99.21	99.48	97.77	99.65	99.93	94.79

	Glass Area 2	Glass Area 3	Glass Area 4	Hercynite Area 5
FeO	27.43	26.93	32.23	53.33
SiO_2	33.92	34.17	44.03	0.50
CaO	10.32	10.84	8.26	0.04
Al_2O_3	15.56	13.97	13.92	43.27
MnO	0.25	0.25	0.31	0.57
MgO	-	-	-	0.11
K_2O	3.83	6.33	5.25	-
P_2O_5	0.66	0.73	0.55	-
TiO_2	0.76	0.74	0.70	1.30
V_2O_5	-	-	-	0.73
	92.73	93.96	105.25	98.85

SHAFT FURNACE RECONSTRUCTION - TAP SLAG GHR1

*Iron oxide figures are FeO for fayalite and glass and Fe_3O_4 for magnetite

	Fayalite Area A	Fayalite Area B	Fayalite Area D	Fayalite Area E	Magnetite Area A	Magnetite Area B	Magnetite Area C
FeO*	48.90	57.85	45.44	51.07	79.45	80.82	85.15
SiO_2	38.45	27.12	35.24	33.49	1.41	0.44	0.71
CaO	1.70	0.23	2.48	1.46	0.04	0.06	-
Al_2O_3	7.20	0.09	5.79	3.95	8.03	5.29	4.23
MnO	2.58	3.28	2.55	2.56	0.93	0.90	0.72
MgO	1.54	4.72	1.67	1.93	0.45	0.35	0.35
K_2O	1.02	0.01	0.83	0.86	-	0.01	0.01
P_2O_5	0.69	0.28	0.60	0.50	0.02	0.02	0.02
TiO_2	0.58	0.10	0.54	0.22	4.43	2.79	3.52
V_2O_5	0.08	0.02	0.06	0.02	0.85	0.50	0.57
	102.74	93.70	95.20	96.06	101.51	97.17	95.28

	Magnetite Area D	Magnetite Area E	Glass Area A	Glass Area B	Glass Area C	Glass Area D	Glass Area E
FeO*	91.15	85.11	34.83	27.87	22.75	21.85	22.12
SiO_2	0.34	2.53	38.84	44.90	45.15	48.02	46.08
CaO	0.06	0.22	4.23	4.84	6.80	6.22	6.46
Al_2O_3	4.82	3.75	8.29	11.99	14.83	13.12	12.43
MnO	0.84	0.92	1.38	1.81	1.42	1.33	1.53
MgO	0.47	0.33	0.23	0.30	0.26	0.26	0.23
K_2O	-	0.11	1.28	1.63	1.40	1.72	1.59
P_2O_5	-	0.02	0.78	0.85	1.05	1.01	1.01
TiO_2	1.79	3.21	0.84	0.68	1.45	1.01	0.16
V_2O_5	0.28	0.53	0.10	0.10	0.22	0.14	0.16
	99.75	96.73	90.80	94.97	95.33	94.68	92.80

SHAFT FURNACE RECONSTRUCTION - FURNACE SLAG GHR4

	Fayalite Area A	Fayalite Area B	Fayalite Area C	Fayalite Area D	Glass Area A	Glass Area C	Glass Area D
FeO	61.61	57.35	63.42	59.59	26.64	21.23	18.08
SiO_2	28.55	31.19	27.89	28.01	44.37	45.46	43.07
CaO	0.72	0.79	0.35	0.73	6.75	7.06	6.66
Al_2O_3	0.97	1.47	0.70	0.28	12.32	13.45	15.99
MnO	3.51	3.61	2.99	2.79	1.47	1.23	0.87
MgO	1.60	1.40	2.32	2.16	0.28	0.22	0.15
K_2O	0.15	0.31	0.04	0.15	2.05	2.79	2.64
P_2O_5	0.25	0.14	0.21	0.12	1.16	1.28	1.12
TiO_2	0.08	0.12	0.18	0.04	0.70	0.44	-
V_2O_5	0.00	0.02	0.04	0.08	0.10	0.06	0.20
	97.44	96.40	98.14	93.95	95.84	93.22	88.78

	Magnetite Area A	Magnetite Area B	Magnetite Area C	Magnetite Area D		Iron Area B	Iron
Fe_3O_4	87.06	82.43	83.96	91.53	Fe	99.98	99.11
SiO_2	1.95	9.31	2.09	-	Si	0.04	0.02
CaO	0.24	0.76	0.19	0.04	Ca	0.01	0.02
Al_2O_3	5.38	4.63	3.45	5.14	Al	-	-
MnO	0.87	0.95	0.95	0.62	Mn	-	-
MgO	0.33	0.14	0.06	0.19	Mg	-	-
K_2O	0.10	0.40	0.10	0.03	K	0.02	-
P_2O_5	0.02	0.09	0.07	-	P	0.26	0.47
TiO_2	4.22	2.73	6.23	3.70	Ti	0.13	-
V_2O_5	0.59	0.40	1.01	0.69	V	-	-
	100.76	101.84	98.11	101.94		100.44	99.62

BOWL FURNACE RECONSTRUCTION - SLAG RR1 a

	Fayalite Area A	Fayalite Area B	Fayalite Area C	Fayalite Area D	Spinel Area B	Spinel Area C
FeO	63.23	61.51	62.92	62.47	70.15	72.39
SiO_2	26.85	27.81	27.33	27.61	0.40	1.44
CaO	1.44	1.16	1.75	1.02	0.15	0.33
Al_2O_3	0.08	0.06	0.13	0.04	12.75	12.31
MnO	3.33	3.60	3.40	3.81	1.15	0.94
MgO	0.66	2.81	0.98	2.42	0.18	0.12
K_2O	0.04	0.02	0.01	0.04	0.01	0.02
P_2O_5	0.25	0.16	0.23	0.30	-	-
TiO_2	0.16	0.10	-	0.10	11.11	10.80
V_2O_5	0.06	-	-	-	2.18	1.67
	96.10	97.23	96.75	97.81	98.08	99.08

	Leucite Area C *	Leucite Area D *	Glass Area A	Glass Area B	Glass Area C	Glass Area D
FeO	0.97	1.43	21.27	20.15	20.28	21.02
SiO_2	39.79	61.07	35.09	39.87	35.58	38.27
CaO	0.06	0.06	16.07	13.56	14.80	13.27
Al_2O_3	40.12	24.74	16.61	15.09	16.80	16.49
MnO	0.03	0.03	1.12	1.03	0.95	1.11
MgO	-	-	0.06	0.04	-	0.02
K_2O	5.40	9.19	1.17	3.16	1.97	2.64
P_2O_5	0.05	-	2.52	1.97	2.27	2.17
TiO_2	-	0.04	1.36	0.90	1.64	1.16
V_2O_5	0.04	-	0.20	0.12	0.24	0.14
	86.46	96.56	95.47	95.89	94.53	96.29

BOWL FURNACE RECONSTRUCTION - SLAG RR1 a

	Grey Lath, C	Grey Lath, D		Iron Area A	Iron Area A
FeO	41.10	41.48	Fe	99.83	99.00
SiO_2	23.73	23.81	Si	0.02	-
CaO	12.08	11.77	Ca	0.02	0.02
Al_2O_3	11.93	13.23	Al	-	-
MnO	0.90	0.88	Mn	-	-
MgO	0.20	0.23	Mg	0.03	0.01
K_2O	0.14	0.04	K	0.01	-
P_2O_5	0.28	0.34	P	0.09	0.07
TiO_2	4.21	6.27	Ti	0.02	-
V_2O_5	0.61	0.91	V	-	-
	95.18	98.96		100.02	99.10

BOWL FURNACE RECONSTRUCTION - SLAG RR2

	Fayalite Area A	Fayalite Area B	Fayalite Area C	Spinel Area B	Spinel Area C	Leucite Area C*	Leucite Area C*
FeO	58.03	64.39	64.75	72.52	66.10	1.52	1.51
SiO_2	28.29	26.98	27.78	1.00	2.68	62.11	63.12
CaO	1.29	0.60	0.56	0.17	0.39	0.11	0.11
Al_2O_3	0.19	0.21	0.15	11.80	17.82	25.97	20.37
MnO	4.63	3.82	3.89	1.26	1.26	0.06	0.03
MgO	4.40	0.22	1.21	0.22	0.12	-	-
K_2O	-	0.03	0.02	0.07	0.11	8.87	9.84
P_2O_5	0.48	0.30	0.18	0.02	0.21	0.05	0.05
TiO_2	0.10	0.26	0.24	11.50	11.10	0.12	0.08
V_2O_5	-	0.04	0.04	1.76	1.69	0.02	-
	97.41	96.85	98.82	100.32	101.48	98.83	95.11

	Glass Area A	Glass Area B	Glass Area C		Iron Area A	Iron Area B	Iron Area C
FeO	17.70	18.50	23.50	Fe	98.80	99.99	99.99
SiO_2	42.29	42.96	43.41	Si	0.13	-	0.01
CaO	10.69	7.84	9.94	Ca	0.08	0.01	0.04
Al_2O_3	16.52	17.87	16.59	Al	-	-	-
MnO	1.35	1.03	1.00	Mn	0.05	-	-
MgO	0.13	-	0.04	Mg	-	0.28	0.01
K_2O	3.60	3.07	3.33	K	-	-	0.01
P_2O_5	1.77	1.54	1.83	P	-	-	0.01
TiO_2	1.65	1.37	1.06	Ti	0.11	0.04	0.06
V_2O_5	0.20	0.16	0.22	V	0.02	-	0.01
	95.90	94.34	100.92		99.19	100.32	100.14

APPENDIX C

X-ray fluorescence analyses

Analyses of slags and excavated ironstones are listed according to archaeological site. Other ironstones are listed according to geographical area and some published analyses are included for comparison. The proportions of FeO and Fe_2O_3 in the slags were determined by wet chemical analysis; iron in the ores is calculated as Fe_2O_3. For samples 1-34, MgO content was determined by Atomic Absorption Spectrophotometry because the calibration curve was found to be poor, but good results were obtained for the remainder of the samples.

-	not determined
LOI	loss on ignition

Table C1

Wakerley, Northants, slags, ores and locally-available ironstones

	Furnace slag WK-AV	Furnace slag WK K4	Furnace slag WAK 48A	Tap slag WGW	Roasted ore WAK 01	Roasted ore WAK 132	Ironstone WAK 03	Junction-Band(field-brash)			Northampton Sand Iron-stone WAK NSI	Boulder Clay nodule WAK BC	Boulder Clay nodule WAK 010
								WAK 04	WAK 05	WAK 06			
FeO	64.04	50.31	57.40	59.59	-	-	-	-	-	-	-	-	-
Fe_2O_3	9.06	15.78	14.88	4.92	88.7	77.7	56.8	69.4	75.2	75.7	69.9	52.9	48.4
SiO_2	17.0	22.0	14.9	23.3	4.5	15.5	30.8	11.1	6.3	7.9	8.1	18.6	22.4
Al_2O_3	5.22	4.86	6.99	7.50	2.66	2.60	2.30	6.61	3.87	3.76	4.56	4.74	5.34
CaO	1.20	1.86	4.75	1.15	0.53	0.62	0.13	0.20	2.83	0.19	2.34	6.70	7.00
MnO	0.40	0.28	0.98	0.65	0.62	0.27	0.11	0.34	0.63	0.09	0.20	0.38	0.27
MgO	0.32	0.26	0.44	0.34	0.10	0.02	0.06	0.11	0.10	0.05	0.32	0.34	0.47
TiO_2	0.41	0.59	0.50	0.64	0.27	0.20	0.69	0.30	0.19	0.36	0.21	0.27	0.33
V_2O_5	0.11	0.09	0.09	0.08	0.04	0.03	0.05	0.08	0.08	0.05	0.11	0.05	0.06
P_2O_5	1.25	1.20	0.34	0.18	0.42	0.43	0.05	0.03	0.03	0.06	1.85	2.49	2.57
K_2O	0.50	0.65	0.45	0.63	0.06	0.09	0.19	0.14	0.07	0.12	0.32	0.63	0.75
L.O.I.	-	-	-	-	2.42	3.15	9.31	15.22	13.51	12.88	14.49	13.71	13.41
Total	99.51	97.88	101.72	98.98	100.32	100.61	100.49	103.53	102.81	101.16	102.40	100.81	101.00

* Total Fe calculated as Fe_2O_3

Table C2

Great Oakley, Northants, slags and possible ores

	Furnace slag G04	Furnace slag, bulk G07	Ironstone, found on site G06+	Boulder Clay nodule G01+	Boulder Clay nodule G02+1	Boulder Clay nodules, bulk G05+
FeO	59.13	59.94	-	-	-	-
Fe_2O_3	9.29	9.31	76.4	55.4	31.3	55.6
SiO_2	22.30	21.9	6.4	28.8	11.2	13.1
Al_2O_3	4.16	4.05	3.07	3.80	4.04	3.33
CaO	0.78	1.14	1.41	0.15	23.00	5.35
MnO	0.47	0.53	0.81	0.04	0.30	0.35
MgO	0.25	0.37	0.21	0.04	0.56	1.69
TiO_2	0.27	0.34	0.24	0.15	0.16	0.18
V_2O_5	0.05	0.05	0.04	0.08	0.02	0.05
P_2O_5	0.65	0.31	0.03	0.17	0.40	1.22
K_2O	0.42	0.42	0.06	0.47	0.57	0.46
LOI	-	-	13.48	13.04	12.91	19.47
Total	97.77	98.37	102.15	102.14	84.46	100.80

+ Total Fe calculated as Fe_2O_3
1 Loss on ignition incomplete

Table C3

Other Northamptonshire slags, ores and possible ores

	Stamford				South Witham	Blind Eye Quarry		Bulwick	Brigstock	Brookfield Cottage Pit		Beeby's Sand Pit
	Tap slag 700130	Tap slag 630532	Roasted ore, bulk	Raw ore, bulk	Tap slag 753058*	Tap slag BEQ 1	Tap slag BEQ 2	Tap slag	Furnace slag	sandy lithology BC4 (2)+	clayey nodule BC5+	Boulder Clay nodule+
FeO	57.85	60.81	-	-	58.4	61.66	63.00	59.92	52.70	-	-	-
Fe_2O_3	6.58	5.76	68.6	70.6	-	7.13	5.48	4.25	15.28	59.5	21.9	42.6
SiO_2	22.8	22.8	17.4	10.5	21.1	23.8	23.0	25.1	15.8	20.8	29.8	8.5
Al_2O_3	6.57	6.20	4.20	3.65	7.72	3.84	4.35	6.49	6.81	4.16	8.75	3.27
CaO	2.23	1.34	0.73	0.88	4.89	0.79	1.00	1.07	2.56	1.60	13.35	11.0
MnO	0.27	0.24	0.35	0.20	0.58	0.56	0.62	1.06	0.27	0.39	0.03	0.42
MgO	0.30	0.17	0.17	0.15	1.73	0.17	0.20	0.30	0.35	0.46	0.78	3.72
TiO_2	0.33	0.35	0.22	0.20	0.34	0.41	0.42	0.46	0.33	0.27	0.39	0.13
V_2O_5	0.11	0.10	0.07	0.08	0.14	0.04	0.04	0.07	0.13	0.03	0.03	0.04
P_2O_5	0.70	0.71	1.00	1.55	2.43	0.22	0.29	0.09	2.27	0.33	0.07	0.55
K_2O	1.03	0.84	0.62	0.44	1.64	0.37	0.44	0.49	0.51	0.70	1.41	0.41
LOI	-	-	7.71	13.36	-	-	-	-	-	12.79	14.71[2]	29.67
Total	98.77	99.32	101.07	101.61	98.97	98.99	98.84	99.30	97.01	101.03	91.22	100.31

* total Fe calculated as FeO

\+ total Fe calculated as Fe_2O_3

[2] probably incomplete ignition

Table C4

Ironstone nodules from Ironstone Junction-Band*

	Cowthick Pit	Brookfield Cottage Pit BC1+2	Adamix Refractories, King's Cliffe	Woodside Qy, Wansford Y1+2	Southorpe Quarry S1+2	Ketton Quarry K1	Ketton Quarry K2	Ketton Quarry K3	Ketton Quarry K4	Castor CAS3	Clipsham New Quarry, poor	Clipsham New Quarry, rich	Creeton Quarry
FeO^+	-	-	-	-	-	-	-	-	-	-	-	-	-
Fe_2O_3	75.7	71.3	84.1	75.0	66.0	87.8	59.7	83.6	67.2	40.5	63.2	83.2	75.9
SiO_2	4.0	14.4	3.6	10.8	19.4	3.2	19.2	0.5	6.9	45.8	16.2	4.3	8.0
Al_2O_3	1.44	2.66	1.50	2.24	3.75	0.90	7.63	1.36	2.13	3.10	6.22	2.14	4.08
CaO	5.19	0.23	0.55	0.41	0.46	0.63	0.23	0.38	7.1	0.17	0.81	1.16	0.16
MnO	1.48	0.47	0.80	0.71	0.58	0.68	0.03	0.44	0.35	0.26	0.55	1.64	0.20
MgO	0.17	0.06	0.09	0.19	0.08	0.15	0.15	0.12	0.20	0.22	0.15	0.18	0.02
TiO_2	0.09	0.17	0.12	0.41	0.48	0.06	0.24	0.10	0.11	0.36	0.50	0.12	0.33
V_2O_5	0.03	0.03	0.02	0.04	0.03	0.03	0.09	0.03	0.03	0.03	0.05	0.03	0.04
P_2O_5	0.04	0.07	0.03	0.02	0.04	0.03	0.06	0.04	0.10	0.03	0.05	0.03	0.07
K_2O	0.10	0.08	0.06	0.10	0.09	0.03	0.12	0.04	0.11	0.57	0.14	0.06	0.10
LOI	14.09	11.34	11.91	12.48	11.81	9.37	14.99	10.81	11.45	8.02	13.37	10.73	12.57
Total	102.33	100.81	102.78	102.40	102.72	102.88	102.44	97.42	95.68	99.06	101.24	103.58	101.17

* see also Table C1

\+ Total Fe calculated as Fe_2O_3

Table C5

Northampton Sand Ironstone, Brookfield Cottage Pit

	BC6 box wall	BC6, core to boxstone	BC7	BC8 box wall	BC8, core to boxstone	BC9	BC10	BC11
FeO*	-	-	-	-	-	-	-	-
Fe_2O_3	64.4	55.9	49.1	59.8	50.0	49.3	51.6	51.9
SiO_2	7.8	7.4	8.1	13.1	10.3	11.3	9.9	10.4
Al_2O_3	5.02	5.07	5.21	9.00	7.60	8.20	5.40	5.54
CaO	5.38	4.98	6.27	0.82	2.51	2.33	4.46	4.76
MnO	0.15	0.16	0.19	0.20	0.21	0.17	0.16	0.13
MgO	0.73	2.12	3.08	0.28	1.30	2.04	2.89	2.55
TiO_2	0.23	0.23	0.28	0.39	0.34	0.37	0.25	0.28
V_2O_5	0.11	0.11	0.11	0.20	0.15	0.17	0.12	0.12
P_2O_5	1.43	1.26	1.43	2.05	1.95	1.29	0.80	1.04
K_2O	0.38	0.33	0.40	0.52	0.44	0.40	0.31	0.31
LOI	16.24	23.20	26.82	14.36	25.52	24.39	26.43	25.32
Total	101.87	100.76	100.99	100.72	100.32	99.96	102.32	102.35

* Total Fe calculated as Fe_2O_3

Table C6

Northampton Sand Ironstone, published analyses^x

	Stanion	Lane				Rockingham
	1	2	3	4	5	
FeO	-	-	-	-	-	-
Fe_2O_3*	54.60	59.73	42.75	36.17	66.05	42.83
SiO_2	20.35	7.30	10.14	8.23	13.47	8.53
Al_2O_3	5.46	6.10	7.50	4.75	3.21	6.29
CuO	3.25	6.55	10.21	17.10	1.10	13.60
MnO	0.27	0.14	0.10	0.10	0.51	0.14
MgO	1.19	0.93	3.25	2.90	0.50	1.64
TiO_2	0.20	0.22	0.24	0.15	0.12	0.22
V_2O_5	0.05	0.08	0.14	0.11	0.05	0.05
P_2O_5	1.01	1.84	1.70	1.13	0.47	1.73
K_2O	0.05	0.06	0.02	0.05	0.01	0.02
LOI	-	-	-	-	-	-

x From Riley, R.V. 1973
* Total Fe calculated as Fe_2O_3
1 Figures are for K_2O + Na_2O

Table C7

Slags and ores from Garden Hill, Sussex

	in situ furnace slag GH1	tap slag GH2	in situ furnace slag GH 671[1]	furnace slag GH 631[1]	furnace slag GH 653[1]	'boxwall' raw GH5	'boxwall' roasted GH6	boxstone (wall+core) roasted GH 673[3]	?spherulitic ironstone raw GH7
FeO	62.92	57.67	62.1	60.7	63.17	-	-	-	-
Fe_2O_3	10.37	9.62	-	-	-	40.1	50.8	84.8	47.9
SiO_2	18.5	20.4	24.3	23.4	22.8	42.8	31.6	8.0	23.8
Al_2O_3	3.32	2.95	4.66	9.32	4.24	7.08	10.0	3.12	12.00
CaO	1.56	3.93	1.88	1.22	3.90	0.05	0.03	1.68	0.28
MnO	0.81	1.58	3.09	2.50	2.40	0.37	0.40	2.11	0.07
MgO	0.35	0.72	0.81	1.06	1.03	0.31	0.56	1.38	0.04
TiO_2	0.29	0.27	0.34	0.50	0.29	0.55	0.65	0.13	0.19
V_2O_5	0.02	0.02	0.03	0.03	0.02	0.03	0.04	0.02	0.06
P_2O_5	0.26	0.40	0.73	0.66	0.60	0.51	0.58	0.67	1.69
K_2O	0.37	0.45	0.85	0.70	1.03	1.04	1.70	0.43	0.16
LOI	-	-	-	-	-	9.24	3.22	-	13.40
Total	98.67	98.01	98.79	100.09	99.48	102.08	99.58	102.34	99.59

[1] Total Fe calculated as FeO

[2] Total Fe calculated as Fe_2O_3

[3] Analysis of material after ignition (loss on ignition was 18.89%)

Table C8

Millbrook slags and limonite nodule

	Furnace slag, bulk	Furnace slag, E^+	Furnace slag, D^+	Limonite nodule*
FeO	50.70	74.2	45.0	-
Fe_2O_3	14.00	-	-	83.0
SiO_2	20.9	12.5	29.8	3.0
Al_2O_3	3.90	0.81	5.56	1.54
CaO	3.34	1.24	9.65	0.03
MnO	1.60	1.06	3.76	0.13
MgO	0.77	0.19	1.84	0.02
TiO_2	0.25	0.21	0.42	0.06
V_2O_5	0.02	0.05	0.02	0.02
P_2O_5	0.81	1.55	0.72	0.32
K_2O	0.66	0.15	0.93	0.08
LOI	-	-	-	14.72
Total	96.95	91.96	97.70	102.92

+ Total Fe calculated as FeO

* Total Fe calculated as Fe_2O_3

Table C9

Slags from furnace reconstructions

	Tap slag, 30 cm diam. slag-tapping shaft furnace GHR1*	Furnace slag, 30 cm diam. slag-tapping shaft furnace GHR4*[1]	Furnace slag, 23 cm diam. slag-tapping shaft furnace GHR10*	Furnace slag, 45 cm diam. non-slag-tapping domed furnace GHR11*	Furnace slag, non-slag-tapping bowl furnace RR1^{+}	Furnace slag non-slag-tapping bowl furnace RR2^{+}
FeO	38.22	44.62	49.30	41.35	42.31	47.17
Fe_2O_3	12.15	5.73	0.92	4.99	2.17	2.50
SiO_2	34.0	33.6	32.0	35.9	32.9	31.5
Al_2O_3	6.52	6.26	5.70	5.15	7.15	7.28
CaO	2.25	2.78	3.62	3.20	5.75	3.77
MnO	2.13	2.38	2.62	2.47	2.34	2.53
MgO	1.34	1.63	2.54	2.18	1.12	0.82
TiO_2	0.69	0.69	0.57	0.59	0.65	0.67
V_2O_5	0.03	0.03	0.01	0.02	0.03	0.02
P_2O_5	0.62	0.63	0.60	0.56	0.96	0.86
K_2O	0.87	1.18	1.08	1.07	2.27	1.93
LOI	-	-	-	-	-	-
Total	98.82	99.53	98.96	97.48	97.63	99.05

[1] same smelt as GHR1

* built and run by R.J. Adams

\+ built and run by R. Clough

Table C10

Ores smelted in furnace reconstructions

	Sideritic ironstone, West Hoathly partially roasted GHR2	Sideritic ironstone, West Hoathly GHR3	Sideritic ironstone, West Hoathly boxwall GHR3	Sideritic ironstone, West Hoathly core to box-stone GHR3	Sideritic ironstone, West Hoathly Batch 2 (core of boxstone) WH3	Sideritic ironstone, Hurstmon-ceaux
FeO[1]	-	-	-	-	-	-
Fe_2O_3	57.1	53.9	64.1	45.6	44.4	53.7
SiO_2	17.9	15.3	15.8	15.1	17.3	6.4
Al_2O_3	4.45	3.76	3.87	3.77	4.04	2.25
CaO	1.67	1.75	0.40	2.72	2.57	4.02
MnO	2.44	2.51	2.46	2.73	2.45	1.85
MgO	0.89	0.66	0.33	0.98	1.05	2.33
TiO_2	0.45	0.40	0.39	0.43	0.47	0.23
V_2O_5	0.03	0.03	0.03	0.02	0.03	0.03
P_2O_5	0.72	0.78	0.89	0.66	0.60	0.29
K_2O	0.65	0.59	0.62	0.61	0.64	0.35
LOI	14.57	20.79	13.01	26.73	25.95	30.01
Total	100.87	100.47	101.80	99.35	99.50	101.46

[1] total Fe calculated as Fe_2O_3

Table C11

Wealden Ironstones, published analyses*

	Wadhurst Clay Ironstone							
	1 Giffords Farm, nr Ashburnham	2 nr s. end of Crowhurst Park	3 Rackwell Wood Quarry, Crowhurst	4 Sharpthorne Brick-works, nr West Hoathly	Ashdown Beds Ironstone, Snape Wood	U. Tunbridge Wells Sand Ironstone, nr Crawley	Iron pan, on Weald Clay Ironstone outcrop	'Ragstone' on Wadhurst Clay or Ashdown Beds
FeO	42.08	48.09	39.52	25.4	30.42	37.10	n.d.	n.d.
Fe_2O_3	6.85	5.41	2.49	28.1	10.10	1.52	39.73	17.18
SiO_2	6.46	4.13	9.49	10.3	26.10	22.43	23.96	60.75
Al_2O_3	2.64	4.67	6.90	1.1	8.24	4.64	9.56	12.07
CaO	3.87	3.80	5.20	3.3	0.86	1.38	0.30	0.47
MnO	2.32	0.46	0.71	1.6	1.29	1.86	5.88	3.30
MgO	1.76	0.19	0.25	2.0	0.25	1.13	0.52	0.10
TiO_2	0.21	0.10	0.23	0.2	0.60	0.36	0.55	0.62
V_2O_5	-	-	-	-	-	tr.	0.01	-
P_2O_5	0.65	n.d.	n.d.	1.0	0.49	0.23	0.48	0.15
K_2O	-	-	-	-	-	0.71	1.16	-
LOI	33.05	31.39	34.35	27.0	21.54	28.23	15.87	5.36
Total	99.89	98.23	99.14	100.00	99.89	99.68	98.02	100.00

* from Worssam, B.C. and Gibson-Hill, J. 1976 n.d. = not detected

Table C12

Berkhamsted area (Herts.) slags and possible ores

	?Raked slag NOR	Tap slag NOR2	Tap slag BCR1[1]	Tap slag BBS[1]	Tap slag bulk[1]	Lower Greensand Ironstone LBA*	Lower Greensand Ironstone LBB*	Excavated marcasite modules*
FeO	55.6	63.90	65.2	64.4	67.1	-	-	-
Fe_2O_3	4.56	6.01	-	-	-	81.9	69.2	98.1
SiO_2	32.5	24.6	21.6	26.0	26.4	17.2	29.7	1.5
Al_2O_3	2.04	1.74	3.88	3.08	3.32	1.41	1.76	0.22
CaO	1.65	1.01	1.20	0.80	0.92	0.31	0.27	0.45
MnO	0.84	0.69	5.90	2.54	1.14	0.11	0.18	0.01
MgO	0.37	0.52	0.49	0.34	0.25	0.17	0.09	0.04
TiO_2	0.15	0.14	0.15	0.14	0.15	0.11	0.06	0.00
V_2O_5	0.02	0.03	0.02	0.03	0.03	0.06	0.06	0.02
P_2O_5	0.20	0.16	0.99	0.65	0.42	0.36	0.43	0.29
K_2O	0.76	0.46	0.93	0.60	0.56	0.24	0.35	0.11
LOI*	-	-	-	-	-	-	-	-
Total	98.69	99.26	100.31	100.58	100.29	100.87	102.10	100.74

[1] total Fe calculated as FeO

* Analyses were carried out after ignition. Loss on ignition was 10.05%, 13.44% and 25.06% respectively.

Table C13

Slags and ore from Ramsbury, Wilts.

	Furnace slag RAM 5	Tap slag RAM 6$^+$	Roasted ore, bulk sample RAM 1*	Raw ore, bulk sample RAM 2*	Box wall of boxstone RAM 3*	Siderite core to boxstone RAM 4*
FeC	55.31	67.04	-	-	-	-
Fe_2O_3	3.76	-	89.2	68.2	79.9	64.0
SiO_2	26.0	20.9	5.6	5.9	0.5	3.3
Al_2O_3	5.51	6.40	2.01	2.12	1.75	1.36
CaO	2.23	0.68	1.13	0.95	0.46	0.48
MnO	1.58	1.83	0.73	0.54	0.60	0.50
MgO	1.08	0.88	0.35	0.18	0.22	0.45
TiO_2	0.30	0.28	0.14	0.16	0.11	0.18
V_2O_5	0.06	0.05	0.02	0.04	0.04	0.02
P_2O_5	0.95	0.77	0.58	0.76	0.74	0.19
K_2O	1.74	1.10	0.26	0.27	0.22	0.20
LOI	-	-	1.32	22.95	13.90	30.70
Total	98.52	99.93	101.34	102.07	98.44	101.38

$^+$ total Fe calculated as FeO

* total Fe calculated as Fe_2O_3

Table C14

Caerwent slag and possible ore sources[x]

	Tap slag 697096	Forest of Dean hematite			Bristol District haematite Red House dump, Winford iron ore and Redding Co.		
		Robin Hood mine, bulk	Robin Hood mine, brush ore (bulk)	Bixslade (as received)	1	2	3
FeO	60.48	0.13	0.39	0.39	0.77	1.26	0.55
Fe_2O_3	15.60	72.14	66.79	80.77	37.64	35.59	38.82
SiO_2	16.50	3.30	5.80	3.96	44.01	35.60	39.25
Al_2O_3	2.46	1.41	2.32	0.85	1.27	1.82	0.75
CaO	0.45	5.50	5.60	2.90	0.28	0.38	0.65
MnO	0.15	0.08	0.09	0.06	0.03	0.14	0.03
MgO	0.50	3.19	3.38	0.32	0.22	0.33	0.24
TiO_2	0.15	0.05	0.07	0.05	tr.	0.00	0.01
V_2O_5	0.02	-	-	-	-	-	-
P_2O_5	0.18	0.05	0.07	0.04	0.02	0.05	0.02
K_2O	0.42	0.02	0.02	-	0.02	-	tr.
LOI	-	14.05	15.40	10.60	0.80	1.25	0.70
Total	96.91	99.92	99.93	99.94	85.06[+]	76.42[+]	81.02[+]

x ore analyses from Groves, A.W. 1952

+ these ores also contain high BaO (9.53, 14.98 and 12.34 wt % respective